REDUCTIVE DECHLORINATION OF CHLORINATED ALIPHATIC

HYDROCARBONS BY Fe(II)

IN DEGRADATIVE SOLIDIFICATION/STABILIZATION

A Dissertation

by

BAHNG MI JUNG

Submitted to the Office of Graduate Studies of
Texas A&M University
in partial fulfillment of the requirements for the degree of

DOCTOR OF PHILOSOPHY

December 2005

Major Subject: Civil Engineering

REDUCTIVE DECHLORINATION OF CHLORINATED ALIPHATIC

HYDROCARBONS BY Fe(II)

IN DEGRADATIVE SOLIDIFICATION/STABILIZATION

A Dissertation

by

BAHNG MI JUNG

Submitted to the Office of Graduate Studies of
Texas A&M University
in partial fulfillment of the requirements for the degree of

DOCTOR OF PHILOSOPHY

Approved by:
Chair of Committee,   Bill Batchelor
Committee Members,   Timothy A. Kramer
                     Bruce E. Herbert
                     Jennifer T. McGuire
Head of Department,   David V. Rosowsky

December 2005

Major Subject: Civil Engineering

ABSTRACT

Reductive Dechlorination of Chlorinated Aliphatic Hydrocarbons by Fe(II)

in Degradative Solidification/Stabilization. (December 2005)

Bahng Mi Jung, B.S., Chung-Ang University;

M.S., Chung-Ang University

Chair of Advisory Committee: Dr. Bill Batchelor

This dissertation examines the applicability of the iron-based degradative solidification/stabilization (DS/S-Fe(II)) to various chlorinated aliphatic hydrocarbons (CAHs) that are common chemicals of concern at contaminated sites. The research focuses on the transformation of 1,1,1-trichloroethane (1,1,1-TCA), 1,1,2,2-tetrachloro-ethane (1,1,2,2-TetCA) and 1,2-dichloroehtane (1,2-DCA) by Fe(II) in cement slurries. It also investigates the degradation of 1,1,1-TCA by a mixture of Fe(II), cement and three iron-bearing phyllosilicates.

Transformation of 1,1,1-TCA and 1,1,2,2-TetCA by Fe(II) in 10% cement slurries was characterized using batch reactors. Dechlorination kinetics of 1,1,1-TCA and TCE[*] (TCE that was produced by transformation of 1,1,2,2-TetCA) was strongly dependent on Fe(II) dose, pH and initial target organic concentration. Degradation of target organics in DS/S-Fe(II) process was generally described by a pseudo-first-order rate law. However, saturation relationships between the rate constants and Fe(II) dose or between the initial degradation rates and target organic concentration were observed.

These behaviors were properly described by a modified Langmuir-Hinshelwood kinetic model. This supports the working hypothesis of this research that reductive dechlorination of chlorinated ethanes occurs on the surface of active solids formed in mixtures of Fe(II) and cement. Transformation products for 1,1,1-TCA and 1,1,2,2-TetCA in mixtures of Fe(II) and cement were identified. The major product of the degradation of 1,1,1-TCA was 1,1-DCA, which indicates that the reaction followed a hydrogenolysis pathway. However, a small amount of ethane was also observed. TCE[*] was rapidly produced by degradation of 1,1,2,2-TetCA and is expected to undergo β-elimination to produce acetylene.

Dechlorination of 1,1,1-TCA in suspension of Fe(II), cement and three soil minerals (biotite, vermiculite, montmorillonite) was characterized using batch reactors. A first-order rate model was generally used to describe the dechlorination kinetics of 1,1,1-TCA in this heterogeneous system. The rate constants for 1,1,1-TCA in mixtures of Fe(II), cement and soil minerals were influenced by soil mineral types, Fe(II) dose and the mass ratio of cement to soil mineral. It was demonstrated that structural Fe(II) and surface-bound Fe(II) in the soil minerals affect dechlorination kinetics and the effects vary with mineral types. Furthermore, it suggests that the reductant formed from Fe(II) and cement hydration components is also effective in systems that include soil minerals.

DEDICATION

To my parents

ACKNOWLEDGMENTS

I am glad to have come upon many people who contributed to this research in various ways. First of all, I express my gratitude to my academic advisor, Dr. Bill Batchelor, for his support and advice throughout this research. His thoroughness and passion for research as well as consideration for students inspired me greatly and I believe that is the path I should follow as a researcher and engineer throughout my whole life. I would also like to sincerely thank my committee members, Dr. Timothy Kramer, Dr. Bruce Herbert and Dr. Jennifer McGuire, for their constructive comments and interest in this research. Furthermore, I wish to show my appreciation to Dr. SooSam Kim, my academic advisor during my Masters program in Korea, for his continued concern and encouragement.

I would also like to thank Dr. Saebom Ko and Dr. Jeongyun Choi for their help and advice in this study. Furthermore, I wish to thank all my colleagues, Jinkun Song, Sihyun Do, Eunjung Kim, Sunhee Yoon, and Dongsuk Han, for their kind friendship at the office and laboratory. I am also grateful to my friends, Youngjoo, Hyejung, Minna, Yeonkyong, and Jeehee, for their love and encouragement. I sincerely thank my friends, Hyunjung, Hyejin, Rachel, Christine, Jennifer, Tara, and Lisa, who have shared with me both my gladness and my sadness in America. Finally, I am sincerely grateful to my parents, sister, brother and sister-in-law. Their unwavering belief and support was enough of a reason for me to do my best to succeed in life. In particular, I would like to share the happiness of completing this work with my lovely sister, Hyunjung.

TABLE OF CONTENTS

LIST OF FIGURES

LIST OF TABLES

CHAPTER I

INTRODUCTION

Chlorinated aliphatic hydrocarbons (CAHs) are a group of contaminants that are frequently found in soils and groundwater at superfund and hazardous waste sites (1). These chlorinated solvents have been produced for degreasing of aircraft engines and automobile parts, for semiconductor manufacture, and for dry cleaning operations (2). Chlorinated solvents commonly used in industrial and commercial processes have contaminated many sites, including 65% of the sites on the National Priorities List (NPL) (3). The most commonly found chlorinated aliphatic compounds in soils and sediments at DOE sites are (in order of frequency of occurrence); trichloroethylene (TCE), 1,1,1-trichloroethane (1,1,1-TCA), tetrachloroethylene (PCE), carbon tetrachloride (CT), chloroform (CF) 1,2-dichloroethane (1,2-DCA), and 1,1,2,2-tetrachloroethane (1,1,2,2-TeCA) (4). 1,1,1-trichloroethane has been reported as a contaminant at 696 of the 1430 NPL sites identified by the Environmental Protection Agency (EPA) in 1996 (5). 1,1,2,2-tetrachloroethane has been found in at least 273 of the 1430 NPL sites on the list in 1997 and 1,2-dichloroethane was found at 570 of the 1586 NPL sites on the list in 2001 (6, 7). The impacts of these CAHs on the environment will be determined by their toxicity and persistence (8). Many CAHs are known human carcinogens (e.g. VC) or probable human carcinogens (e.g. CF, 1,2-DCA) (9).

_____

This thesis follows the style of *Environmental Science and Technology*.

Many technologies have been developed to remediate groundwater or soils/sediments contaminated with chlorinated organics (3). Many remedial actions have been applied to contaminated sites with CAHs, including pump and treat, soil washing, bioremediation, soil vapor extraction, and incineration. These remedial technologies, except incineration, are largely applicable only when the site has high permeability soils (10). Pump and treat is greatly affected by geological conditions and often displays limitations such as the rebound effect when dense nonaqueous phase liquids (DNAPL) are present (10). Soil washing has been applied to various target contaminants, but for complex waste mixtures of metals and organics it may be difficult to find a proper washing solution to simultaneously remove all of the contaminants (11). Bioremediation is limited by long remediation times and toxicity caused by high concentrations of contaminants or the presence of highly chlorinated organics (10). Soil vapor extraction volatilizes contaminants, but is ineffective when a site has low concentrations of contaminants, high moisture content, or high humic content (10, 12). Incineration can be applied to soils contaminated with chlorinated hydrocarbons, PCBs, and dioxins, but its cost can be as high as $200/ton to $1000/ton (13). These high costs will limit public acceptance of incineration.

Conventional solidification/stabilization (s/s) is another remediation technology to treat sources of contaminants. Conventional s/s has been used to immobilize inorganic contaminants at high pH using binders such as Portland cement, fly ash and lime (10). S/S can achieve the goals of reduction in waste toxicity, solubility, and mobility as well as high structural integrity (10). The major advantages of s/s are that it can be applied to

waste mixtures of organics and inorganics and that it is very cost effective with costs as low as \$30 per ton (14, 15). However, traditional s/s would not destroy organic contaminants so that the potential for future contamination would remain. Degradative solidification/stabilization technology (DS/S) is an attractive treatment method that overcomes these limitations of s/s by combining a chemical degradation process with conventional s/s. An example of ds/s is iron-based degradative solidification /stabilization. DS/S-Fe(II) is a treatment process that combines reductive dechlorination by iron compounds with immobilization by the hydration reactions of Portland cement. Reductive dechlorination will be achieved by a reactive agent formed by reaction of ferrous iron with components of Portland cement.

Reductive dechlorination is an important mechanism for transformation of CAHs in natural anaerobic environments produced by depletion of oxygen caused by microbial activities. It has been reported that CAHs are biologically treatable under an aerobic or anaerobic condition (16). During metabolic degradation under anaerobic conditions, CAHs act as electron acceptors and dissolved hydrogen formed from fermentation acts as the electron donor. Similar to its role in metabolic processes, CAHs act as electron acceptors during abiotic dechlorination in DS/S-Fe(II). Fe(II), possibly present in Fe(II)-Fe(III) hydroxides will provide electrons. Other reduced iron or sulfur compounds could be electron donors for abiotic reductive dechlorination. These include zero valent iron (17-19), ferrous iron (20), iron-oxides (e.g., goethite, hematite, magnetite) (21-29), iron hydroxides (green rust) (30-33), iron sulfide (FeS) (34-36), pyrite (FeS_2) (24, 37), sulfides (20, 38, 39), and iron-phyllosilicates (38, 40-46). Reductive dechlorination of

various CAHs such as PCE, TCE, 1,1,1-TCA and CT using these natural or synthesized reductants has been evaluated. Recent research has demonstrated that DS/S-Fe(II) can reductively dechlorinate tetrachloroethylene, carbon tetrachloride, chloroform, and polychlorinated biphenyls (47-49).

1.1 Research Objectives and Dissertation Overview

The overall goal of this research is to extend the application of the DS/S-Fe(II) process to various chlorinated aliphatic hydrocarbons that can exist in contaminated soils and sediments. Chlorinated aliphatic hydrocarbons chosen for this research are chlorinated ethanes that include 1,1,1-trichloroethane, 1,1,2,2-tetrachloroethane and 1,2-dichloroethane. To achieve this goal, two subordinate objectives were conducted in different environments. First, reductive dechlorination of three target organic contaminants (1,1,1-TCA, 1,1,2,2-TetCA, 1,2-DCA) by Fe(II) in cement slurries was characterized. Second, reductive dechlorination of 1,1,1-trichloroethane in the presence of soil minerals in iron-based degradative solidification/stabilization was characterized.

The hypotheses of this study were that: (1) DS/S-Fe(II) process will be effective in degrading various CAHs; (2) transformation rates of CAHs will be related to Fe(II) dose, target organic concentration, pH, mineral types, and mass ratio of soil mineral to cement; (3) the reducing agent for CAHs will be Fe(II)Fe(III)-hydroxides formed by reactions among ferrous iron and the components of Portland cement; and (4) transformations of CAHs will occur on the surfaces of reactive solids. These hypotheses were tested using the results of batch reduction experiments that are presented in Chapter

IV and Chapter V. This dissertation is organized into seven Chapters as shown in Figure 1.1. Chapter I describes established remediation technologies applied to contaminated soils and their limitations and introduces the DS/S-Fe(II) process and its advantages. And the objectives and organization of this study are described. Chapter II describes cement chemistry and soil mineralogy as well as transformation mechanisms of CAHs. An understanding of cement hydration reactions, structural mineralogy, and reductive transformation mechanism will be helpful in developing the fundamental knowledge needed to apply DS/S-Fe(II) processes to degrade various CAHs in contaminated soils and sediments. Chapter III explains the experimental and analytical procedures used in this study. Chapter VI presents the results of batch kinetic experiments in cement slurries. Factors that influence degradation kinetics such as Fe(II) dose, pH, and target organic contaminant concentration were investigated and degradation products were identified. Chapter V presents the results of experiments on the reductive transformation of 1,1,1,-trichloroethane by Fe(II) in cement slurries containing iron-bearing phyllosilicates such as biotite, vermiculite, and montmorillonite. Chapter V evaluates sorption of target organic onto the soil and the effects of mineral type, Fe(II) dose, and the mass ratio of cement to soil on degradation of CAHs. Chapter VI is concerned with systems that are mixtures of Fe(II), cement and iron-bearing phyllosilicates. The chapter discusses the reaction mechanism, reaction pathway, the effect of chemical structure on reduction kinetics, and correlation analysis of rate constants. Chapter VII summarizes the results from this research.

Chapter I
Introduction

Chapter II
Background

- Cement chemistry
- Clay chemistry
- Transformation mechanism for CAHs

Literature Review
- DS/S-Fe(II)
- Various reductants with iron

Chapter III
Experimental Works

Chapter IV
Experimental Results

Batch experiments in cement slurries
Influencing factors
- Fe(II) dose
- pH
- Initial conc.

Chapter V
Experimental Results

Batch experiments in soil minerals
Influencing factors
- Soil mineral type
- Fe(II) dose
- Cement/Soil ratio

Chapter VI
Discussion

- Reaction mechanism
- Reaction pathway
- Effect of chemical structure
- Correlation analysis of rate constants

Chapter VII
Concluding Remarks

Figure 1.1 Organization of this study.

CHAPTER II

BACKGROUND

2.1   Degradative Solidification/Stabilization

Solidification/Stabilization has been applied to wastes containing mixtures of inorganic and organic contaminants as well as to low level of radioactive wastes (10, 50). Stabilization is the process of altering contaminants in wastes to more stable forms that are less mobile, soluble, and toxic. Solidification is the process of physically altering a waste to forms that are solids with higher strength. S/S has been supported as a promising technology to satisfy environmental regulations. Two major federal laws and their amendments have been applied to cleanup and disposal of hazardous wastes (50). The Resource Conservation and Recovery Act (RCRA) of 1976 and the Hazardous and Solid Waste Amendments (HSWA) of 1984 gave EPA the authority to regulate the disposal of hazardous wastes and establish treatment standards based on Best Demonstrated Available Technology (BDAT). S/S has been accepted as the BDAT for treating various RCRA-listed wastes, including most of the wastes that contain metal contaminants. The Comprehensive Environmental Response, Compensation, and Liability Act (CERCLA) of 1980 and the Superfund Amendments and Reauthorization Act (SARA) of 1986 regulate the cleanup sites contaminated with hazardous materials (50). S/S has been applied in both in-situ and ex-situ applications at approximately 24% of superfund sites for which remedial actions were proposed between 1982 and 2002 (51). Analysis of the Records of Decision (ROD) at Superfund sites shows that s/s could

treat wastes containing volatile organic compounds (VOCs), when the VOCs were not major contaminants (50). When low concentrations of VOCs exist with inorganic contaminants, in-situ s/s can effectively treat wastes while minimizing volatilization of VOCs. However, the risk of release of organics from the wastes treated by s/s remains for a long time because the organic contaminants are contained but not destroyed. This disadvantage is overcome by ds/s, which combines a chemical process for degradation with immobilization. DS/S can destroy chlorinated organic contaminants by reductive dechlorination in a reducing environment. Fe(II) was selected as the chemical reagent to provide a reducing environment for the DS/S process in this research.

As the result of batch screening experiments with cement slurries containing five electron donors (sulfide, polysulfide, dithionite, pyrite, ferrous iron), ferrous iron (Fe(II)) was chosen as the most effective reductant for tetrachloroethylene (PCE) (47). Furthermore, Fe(II) has been commonly used as a reductant in s/s and is cost competitive to other chemical reagents (47, 52).

2.2   Cement Chemistry

2.2.1   Portland Cement

Portland cement is the most common binder used in s/s technology. Portland cement is manufactured with fly ash, lime, soluble silicates, clay and other materials (53). The four major chemical elements of Portland cement are calcium, silicon, aluminum and iron. The mixture of raw materials is fed to a rotary kiln of 1450 ºC. The kiln produces what is called clinker. A clinker is finely ground with the addition of 4%~7%

of calcium sulfate (gypsum) to produce Portland cement (53, 54). The four principal compounds in clinker and their percentages by weight are: tricalcium silicate $((CaO)_3SiO_2,$ 50~70%), dicalcium silicate $((CaO)_2SiO_2,$ 15~30%), tricalcium aluminate $((CaO)_3Al_2O_3,$ 5~10%) and tetracalcium aluminoferrite $((CaO)_4Al_2O_3Fe_2O_3,$ 5~15%) (54). Table 2.1 shows the chemical and compound composition of typical cements.

Table 2.1 Composition of typical cements (53, 55).

Type of Portland Cement	Chemical composition, %						Compound composition, %			
	SiO_2	Al_2O_3	Fe_2O_3	CaO	MgO	SO_3	C_3S	C_2S	C_3A	C_4AF
Type I	20.9	5.2	2.3	64.4	2.8	2.9	55	19	10	7
Type II	21.7	4.7	3.6	63.6	2.9	2.4	51	24	6	11
Type III	21.3	5.1	2.3	64.9	3.0	3.1	56	19	10	7
Type IV	24.3	4.3	4.1	62.3	1.8	1.9	28	49	4	12
Type V	25.0	3.4	2.8	64.4	1.9	1.6	38	43	4	9

The chemical formulas for the compound described by abbreviations are as follows: $C_3S=(CaO)_3SiO_2,$ $C_2S=(CaO)_2SiO_2,$ $C_3A=(CaO)_3Al_2O_3,$ $C_4AF=(CaO)_4Al_2O_3Fe_2O_3,$ Here, $C=CaO,$ $S=SiO_2,$ $A=Al_2O_3,$ and $F=Fe_2O_3.$

C_3S in clinkers is impure and typically contain a few percent of oxides like MgO and Fe_2O_3 (54). Alite is the mineral name for tricalcium silicate (C_3S) and its crystal structure is shown in Figure 2.1(a). The structure consists of SiO_4-tetrahedra that connect to calcium ions. Calcium is coordinated by eight oxygens (56).

Pure C_2S contains 34.9% SiO_2 and 65.1% of CaO. C_2S clinker includes 4~6% oxides of which the main ones are Al_2O_3 and Fe_2O_3. The crystal structure of dicalcium silicate shows polyhedral links between SiO_4-tetrahedral and calcium, as shown in Figure 2.1(b).

Pure C_3A contain 62.3% CaO and 37.7% Al_2O_3. Substantial amounts of Ca and Al can be substituted so that typically the total content of oxides reaches 33% (54). The typical composition of C_4AF is 46.1% CaO, 21.0% Al_2O_3, and 32.9% Fe_2O_3 (54).

The crystal structure of tricalcium aluminate is cubic as shown in Figure 2.1(c). The structure of tetracalcium aluminate ferrite consists of layers of (Al, Fe)O_6-octahedral and (Al, Fe)O_4-tetrahedral with Ca^{2+} being located in open space between layers, as shown in a Figure 2.1(d) (56). Iron is mainly located in the calcium aluminate ferrite phase. Tetracalcium aluminoferrite provides most of the iron oxide in cement, which ranges to a few percent. This Fe(III) may provide sites to react with Fe(II) in solution.
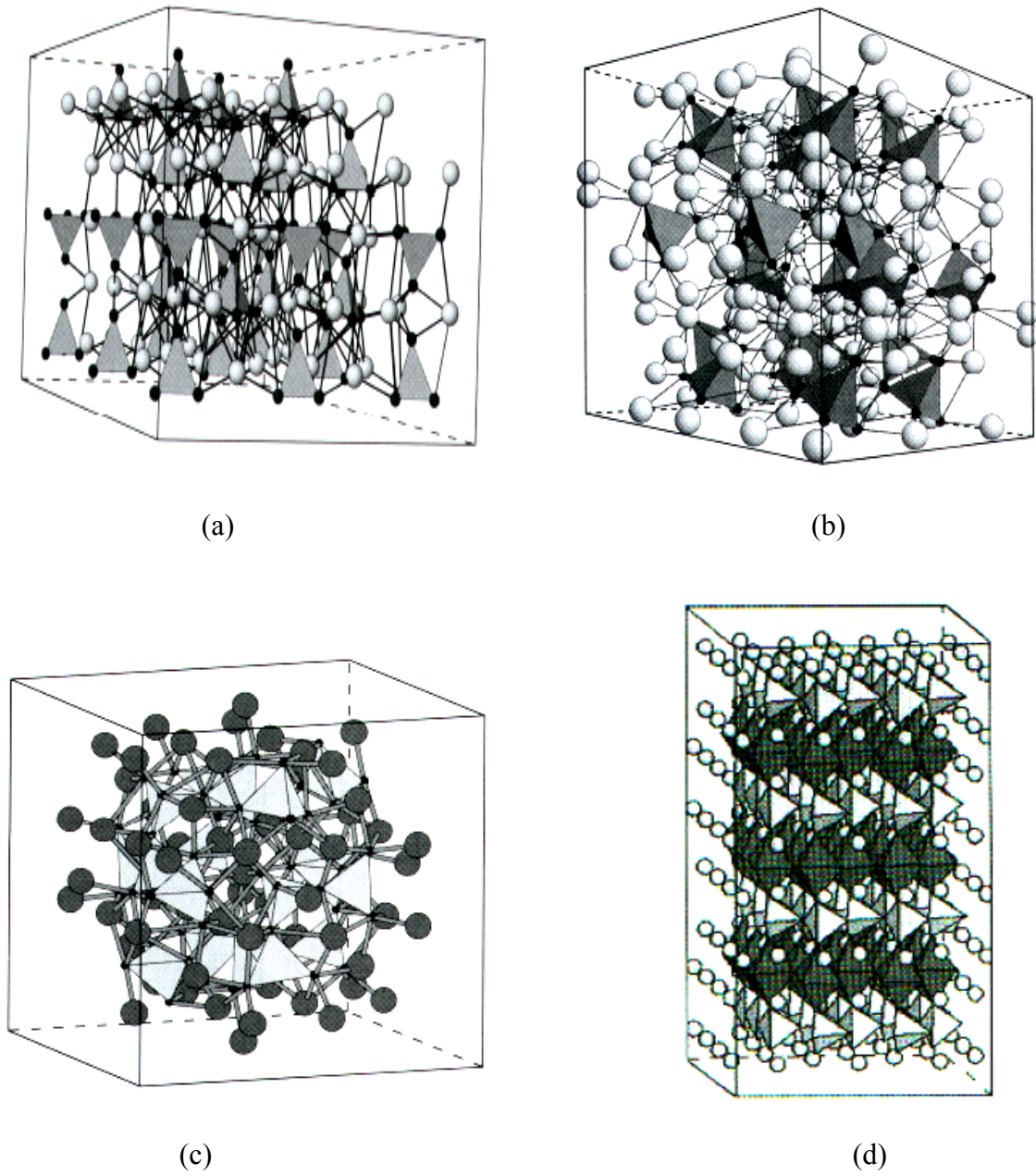
Figure 2.1 Crystal structure of tricalcium silicate (C_3S) (a), dicalcium silicate (C_2S) (b), tricalcium aluminate (C_3A) (c), and tetracalcium aluminate ferrite (C_4AF) (d) (56).

2.2.2   Cement Hydration

The mechanism of cement hydration can be described in two ways, 'through solution' and 'solid state reactions' (57). In the 'through solution' mechanism, reactants dissolve into solution from cement particles and the ions precipitate from solution to form hydration products. In the 'solid state reaction' mechanism, the hydration reactions occur at the surface of the solid without the constituents dissolving into the solution. It seems that the through-solution mechanism controls in the early stages of hydration whereas the second mechanism will occur during the later stages (57).

Table 2.2 summarizes some of the cement hydration reactions. Tricalcium silicate hydration can be described by reaction (Equation 2-1) in Table 2.2. The calcium silicate hydrate (C-S-H) formed is an amorphous phase and is called tobomorite gel (53). Hydration of dicalcium silicate can be described by reaction (Equation 2-2). The calcium silicates hydrates formed by hydration of C_3S and C_2S make up about 75% of the weight of cement (53). The presence of $Ca(OH)_2$ makes the cement solution highly alkaline with pH near 12.5 (57). Tricalcium aluminate (C_3A) is the most reactive compound in Portland cement (56). The hydration of $(CaO)_3(Al_2O_3)$ produces hexagonal plate crystals such as $(CaO)_4(Al_2O_3) \cdot 19(H_2O)$ or $(CaO)_2(Al_2O_3) \cdot 8(H_2O)$. These hydrates are metastable so that they transform into more stable forms such as $(CaO)_3(Al_2O_3) \cdot 6(H_2O)$ (57). The products of C_3A hydration depend on the presence of gypsum ($CaSO_4 \cdot 2H_2O$). In the absence of sulfate, tricalcium aluminate hydrates and tetracalcium aluminate hydrates will be formed by reactions (Equation 2-4) and (Equation 2-7). In the presence of sulfate, the reactions are given by (Equation 2-5) and (Equation 2-8). Ettringite is the first stable

hydration product. If sufficient sulfate is not present, ettringite will form a tetracalcium monosulfoaluminate hydrate ("monosulfate") as the stable hydration product by reaction (Equation 2-6). The ferrite phase reacts with gypsum and $Ca(OH)_2$ and form a sulfoferrite of needle-like crystals as described by reaction (Equation 2-8) (54, 57).

The hydration products of aluminate and ferrite can be divided into AFt (aluminate-ferrite-trisubstituted), AFm (aluminate-ferrite-monosubstituted), and hydro-garnet phases. AFt, AFm, and hydrogarnet represent respectively crystal structures of needles, plates and spheres. AFt phases have the formula $[Ca_3(Al,Fe)(OH)_6^-$ $\cdot 12H_2O]_2 \cdot X_3 \cdot xH_2O$ and AFm phases have the formula $[Ca_2(Al,Fe)(OH)_6] \cdot X \cdot xH_2O$, where X denotes a single charged anion (OH^-) or half of a doubly charged anion (SO_4^{2-} or CO_3^{2-}) (54, 58). Ettringite (trisulfate) and monosulfate are each considered to be AFt and AFm phases, respectively. In particular, Friedel's salt $(Ca_2Al(OH)_6(Cl,OH) \cdot 2H_2O)$ is an AFm phase that is structurally similar to layered double hydroxides (LDH) (58, 59).

LDH are also called anionic clays and they consist of positively charged mixed metal hydroxide layers with anions and water in the interlayer. The formula of LDH is described by $[M^{2+}_{1-x}M^{3+}_x(OH)_2]A^{n-}_{x/n} \cdot mH_2O$, where M^{2+} and M^{3+} are divalent and trivalent cations, x is equal to the ratio of $M^{3+}/(M^{2+} + M^{3+})$ and A is an anion (60). M^{2+} and M^{3+} can be Mg^{2+}, Fe^{2+}, Mn^{2+} or Zn^{2+} and Al^{3+}, Cr^{3+}, or Fe^{3+}, respectively. A^{n-} can be Cl^-, NO_3^-, or CO_3^{2-}. The LDH formed with Fe(II) and Fe(III) is called green rust and has been proposed as an active reducing agent for this study. The anion exchange properties of LDH for monovalent ions is in the order $OH^- > F^- > Cl^- > Br^- > NO_3^-$ and divalent ions (SO_4^{2-} and CO_3^{2-}) are preferred over monovalent anions (60). LDH can

exist in a three-layer structure (Pyroaurite) and a two-layer structure (Sjogrenite), depending on the arrangement of the hydroxide layers (60, 61). Figure 2.2 represents the structure of layered double hydroxides (LDH).
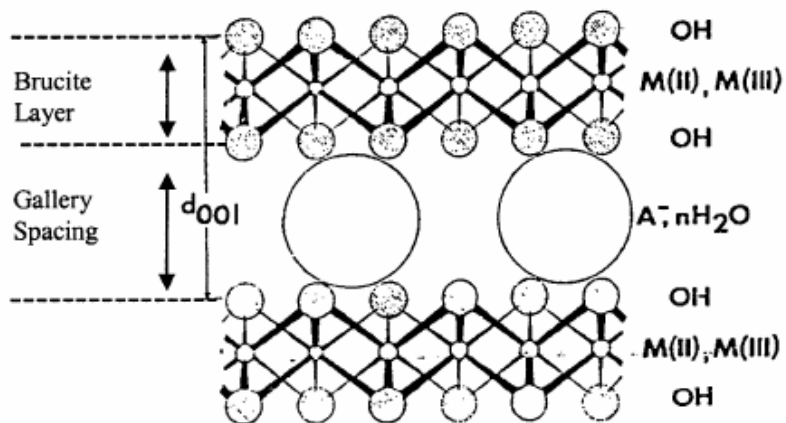
Figure 2.2 Schematic representation of a LDH structure (62).

Table 2.2 Portland cement compound transformation (53, 54, 57, 58).

C_3S	$2(3CaO \cdot SiO_2) + 6H_2O \rightarrow 3CaO \cdot 2SiO_2 \cdot 3H_2O + 3Ca(OH)_2$ (tricalcium silicate + water $\rightarrow$ C-S-H + calcium hydroxide)	(2-1)
C_2S	$2(2CaO \cdot SiO_2) + 4H_2O \rightarrow 3CaO \cdot 2SiO_2 \cdot 3H_2O + Ca(OH)_2$ (dicalcium silicate + water $\rightarrow$ C-S-H + calcium hydroxide)	(2-2)
C_3A	$3CaO \cdot Al_2O_3 + 6H_2O \rightarrow 3CaO \cdot Al_2O_3 \cdot 6H_2O$ (tricalcium aluminate + water $\rightarrow$ tricalcium aluminate hydrate)	(2-3)
C_3A	$3CaO \cdot Al_2O_3 + 12H_2O + Ca(OH)_2 \rightarrow 3CaO \cdot Al_2O_3 \cdot Ca(OH)_2 \cdot 12H_2O$ (tricalcium aluminate + water + calcium hydroxide $\rightarrow$ tetracalcium aluminate hydrate)	(2-4)
C_3A	$3(CaO) \cdot Al_2O_3 + 3CaSO_4 \cdot 2H_2O + 26H_2O \rightarrow (CaO)_3Al_2O_3(CaSO_4)_3 \cdot 32H_2O$ (tricalcium aluminate + gypsum + water $\rightarrow$ ettringite)	(2-5)
C_3A	$(CaO)_3(Al_2O_3)(CaSO_4)_3 \cdot 32H_2O + 2(CaO)_3(Al_2O_3) + 4H_2O \rightarrow$ $3(CaO)_3(Al_2O_3)(CaSO_4) \cdot 12H_2O$ (ettringite + tricalcium aluminate + water $\rightarrow$ calcium monosulfoaluminate hydrate)	(2-6)
C_4AF	$4CaO \cdot Al_2O_3 \cdot Fe_2O_3 + 10H_2O + 2Ca(OH)_2 \rightarrow 6CaO \cdot Al_2O_3 \cdot Fe_2O_3 \cdot 12H_2O$ (tetracalcium aluminoferrite + water + calcium hydroxide $\rightarrow$ calcium aluminoferrite hydrate)	(2-7)
C_4AF	$4CaO \cdot Al_2O_3 \cdot Fe_2O_3 + CaSO_4 \cdot 2H_2O + Ca(OH)_2 \rightarrow 3CaO(Al_2O_3, Fe_2O_3) \cdot 3CaSO_4 \cdot aq$ (tetracalcium aluminoferrite + gypsum + calcium hydroxide $\rightarrow$ sulfoaluminate and sulfoferrite)	(2-8)

2.3 Clay Minerals

Soil consists of three phases: fluid, solid and gas. The solid phase of soil can be separated into organic and inorganic components. Inorganic components can be

structurally classified as non-crystalline or crystalline minerals. The inorganic elements in the order of decreasing abundance are: O, Si, Al, Fe, C, Ca, K, Na, and Mg (63). The crystalline minerals include primary minerals; secondary minerals; oxides and hydrous oxides of iron, aluminum, and silicon; and carbonates, sulfates, phosphates, and sulfides (63). Ferrous iron (Fe(II)) commonly occurs as a component in minerals and is an important reductant present in subsurface environments under anoxic conditions. Fe(II) may be present as various species such as dissolved iron, iron sorbed onto or within the iron-bearing (hydro) oxides, phyllosilicates and sulfides. Table 2.3 shows the oxides, hydroxides, and oxyhydroxides of ferrous and ferric iron.

Table 2.3 The oxides, hydroxides, and oxyhydroxides of Fe (adapted from 64, 65).

Oxides
Hematite (α-F_2O_3)
Maghemite (γ-Fe_2O_3)
Magnetite (Fe_3O_4)
Hydroxides
Ferrihydrite ($Fe_{10}O_{15} \cdot 9H_2O$)
Green Rust ($[Fe^{II}_{6-x}Fe^{III}_x(OH)_{12)}]^{x+}[(A)_{x/n} \cdot yH_2O]^{x-}$)
Oxyhydroxides
Goethite (α-FeOOH)
Lepidocrocite (γ-FeOOH)
Feroxyhyte (δ-FeOOH)
Akaganeite (β-FeOOH)

2.3.1   Iron-Bearing Phyllosilicates

Phyllosilicates are divided into two groups on the basis of the number of tetrahedral and octahedral sheets in the layer structure. The 1:1 layer structure consists of one octahedral and one tetrahedral sheet. Kaolinite and halloysite are included in the 1:1 mineral groups. The 2:1 layer structure consists of two tetrahedral sheets with one octahedral sheet (63, 66). These 2:1 minerals include pyrophyllite-talc, smectite-saponite, vermiculite, illite, and mica groups. It is known that the oxidation state of structural Fe in clay minerals has an effect on the rate of transformation of chlorinated aliphatic compounds by dehydrochlorination and reductive dechlorination (42). Therefore, understanding the structural factors of a mineral affecting the fate of contaminants will be helpful to assess the DS/S-Fe(II) as an in-situ remediation technology for chlorinated aliphatic hydrocarbons (43).

2.4   Transformation of Chlorinated Aliphatic Hydrocarbons

There are two prospective reactions for chlorinated aliphatic hydrocarbons in the DS/S system. The first one is a non-reductive process, which does not involve external electron transfer and the other is a reductive process requiring electron transfer.

2.4.1   Non-Reductive Transformation of Chlorinated Aliphatic Hydrocarbons

Nucleophilic substitution (hydrolysis) and dehydrochlorination (elimination) are non-reductive transformations. In a nucleophilic substitution, water or the hydroxide ion will act as the nucleophile and substitute for chloride. Chlorinated alkanes are known to be more susceptible to nucleophilic substitution than chlorinated alkenes and aromatics

(67). The hydrolysis of 1,1,1-trichloroethane (1,1,1-TCA) can be described by equation 2-9.

$$CH_3CCl_3 + 2H_2O \rightarrow CH_3COOH + 3HCl \qquad (2\text{-}9)$$
$$(1,1,1-TCA) \qquad\qquad (HAc)$$
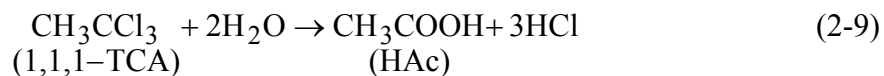
The half-life for 1,1,1-TCA being degraded by abiotic hydrolysis to acetic acid (HAc) is reported as 0.5 to 1.7 years (67). The half-life of 1,1,2,2-TetCA and 1,2-DCA degraded by hydrolysis are reported as 0.8 to 1.1 years and 50 to 72 years, respectively (67, 68). Chlorinated aliphatic hydrocarbons in water can undergo an elimination reaction (dehydrochlorination), which produces a double bond by removing hydrogen and chloride. The dehydrochlorination of 1,1,1-TCA and 1,1,2,2-TeCA to 1,1-DCE and TCE can be described by equations 2-10 and 2-11.

$$CH_3CCl_3 \rightarrow CH_2=CCl_2 + H^+ + Cl^- \qquad (2\text{-}10)$$
$$(1,1,1-TCA) \quad (1,1-DCE)$$

$$C_2H_2Cl_4 \rightarrow CHCl=CCl_2 + H^+ + Cl^- \qquad (2\text{-}11)$$
$$(1,1,2,2-TetCA) \qquad (TCE)$$
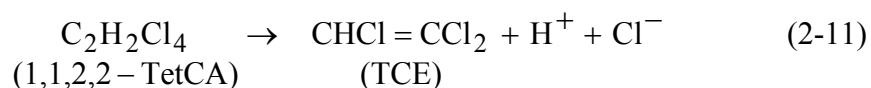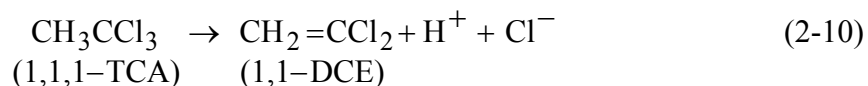
It is known that polychlorinated alkanes undergo dehydrochlorination under extreme basic conditions and at neutral pH (67).

2.4.2   Reductive Transformation of Chlorinated Aliphatic Hydrocarbons

Reductive transformation requires electron acceptors and electron donors. CAHs behave as electron acceptors and are reduced in the process. Three kinds of reductive degradation are possible: 1) hydrogenolysis, in which a hydrogen atom replaces a chloride substituent, 2) β-elimination, in which two chlorides are removed from different carbons that are next to each other in the molecule; and 3) coupling, in which two alkyl groups connect to one another (67). Various reduced iron or sulfur compounds play the role of electron donors. Transformation of chlorinated aliphatic hydrocarbons by various reducing agents is summarized in Table 2.4.

Reductive dechlorination is a major mechanism in degradative solidification/ stabilization. Recent research has demonstrated that DS/S-Fe(II) can reductively dechlorinate tetrachloroethylene, trichloroethylene, 1,1-dichloroethylene, vinyl chloride, carbon tetrachloride, chloroform, and polychlorinated biphenyls (47-49, 69). It showed that PCE was completely degraded to non-chlorinated products with a half-life as low as 4.1 days at pH 12.1, when $[PCE]_0$ was 0.245 mM, and $[Fe(II)]_0$ was 39.2 mM (70). Kinetics of CT and CF transformation in cement slurries containing Fe(II) were generally very rapid. A half-life of CT at pH 12.6 as short as 0.32 min was obtained when $[CT]_0$ was 0.26 mM and $[Fe(II)]_0$ was 41.6 mM (49). The pseudo-first-order rate constant of 2,2',3,3',4,4'-Hexachlorobiphenyl degradation in 10% cement slurries was 1.2 (1/day) at pH 12.3 when $[HCB]_0=0.0277$ mM and $[Fe(II)]_0=50$ mM (48). These previous studies demonstrate the promise of expanding the DS/S-Fe(II) process to various target organic contaminants.

Table 2.4 Transformation of chlorinated aliphatic hydrocarbons by various reducing agents.[a]

Reductant	Target contaminants	Reference
Fe(0)	1,1,1-TCA	Fennelly, J.P. 1998, (17)
	CT and PCE	Doong, Ruey-An. 2003, (18)
	1,1,1-TCA	Lookman, Richard. 2004, (19)
Fe(II) (aq)	CT, 1,1,1-TCA, PCE.	Doong, Ruey-An. 1992, (20)
Green Rust ($Fe^{2+}Fe^{3+}$hydroxides)	CT	Erbs, Marianne. 1999, (30)
	PCE, TCE, DCE, VC	Lee, Woojin. 2002, (31)
	CT	O'loughlin, E.J. 2003, (32)
	Chlorinated Ethanes	O'Loughlin, E.J. 2004, (33)
Pyrite (FeS_2)	CT	Kriegman-King, M.R. 1994, (37)
	PCE, TCE, DCE, VC	Lee, Woojin. 2002, (24)
Iron sulfide (FeS)	PCE and TCE	Butler, E.C. 1999, (36)
	Chlorinated Ethanes	Butler, E.C. 2000, (35)
	1,1,1-TCA	Gander, J.W. 2002, (34)
Iron oxides	CT, 1,1,1-TCA.	Klecka, C.M. 1984, (21)
	TCE.	Charlet, L. 1998, (22)
	PCE, TCE, DCE, VC	Lee, Woojin. 2002, (24)
	CT	Danielsen, K.M. 2004, (26)
	CT	McCormick, M.L. 2004, (27)
	CT	Maithreepala, R.A. 2004, (29)
Iron-bearing phyllosilicates	CT	Kriegman-King, M.R. 1992, (38)
	CT and TCE	Amonette, J.E. 1999, (40)
	CT	Amonette, J.E. 2000, (41)
	PCA	Cervini-Silva, J. 2002, (44)
	Polychlorinated Ethane.	Cervini-Silva, J. 2003, (45)
	PCE, TCE, DCE, VC	Lee, Woojin. 2004, (46)

[a]see references for specific reaction conditions.

2.4.2.1   1,1,1-Trichloroethane

1,1,1-TCA is one of the most common chlorinated solvents. The maximum contaminant level for drinking water is 0.2 mg/L (34). Many studies have investigated the transformation of 1,1,1-TCA by Fe(0), Fe(II), iron oxides, iron-bearing phyllosilicates, iron sulfide, green rust, pyrite (Table 2.4). Figure 2.3 shows the potential scheme that could explain the transformation products of 1,1,1-TCA by Fe(0) or other reducing agent reported in the literature. 1,1,1-TCA obtains one electron from electron donors and forms the 1,1-dichloroethyl radical (17):

$$CH_3CCl_3 + e^- \rightarrow [CH_3CCl_3]^{\bullet-} \rightarrow [CH_3\overset{\bullet}{C}Cl_2] + Cl^- \qquad (2\text{-}12)$$
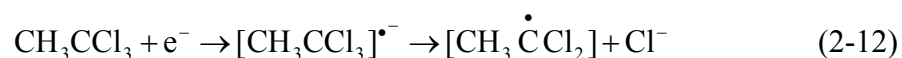
This radical can couple with other dichloroethyl radicals to form 2-butyne via 2,2,3,3-tetrachlorobutane. Also, the dichloroethyl radical can go to ethane through elimination and protonation steps. Transformation products of 1,1,1-TCA by Fe(0) were observed to include 1,1-DCA, ethane, cis-2-butene, ethylene, and a trace of 2-butyne. The observation that the major reaction products for degradation of 1,1,1-TCA were 1,1-DCA and ethane is consistent with hydrogenolysis pathway.
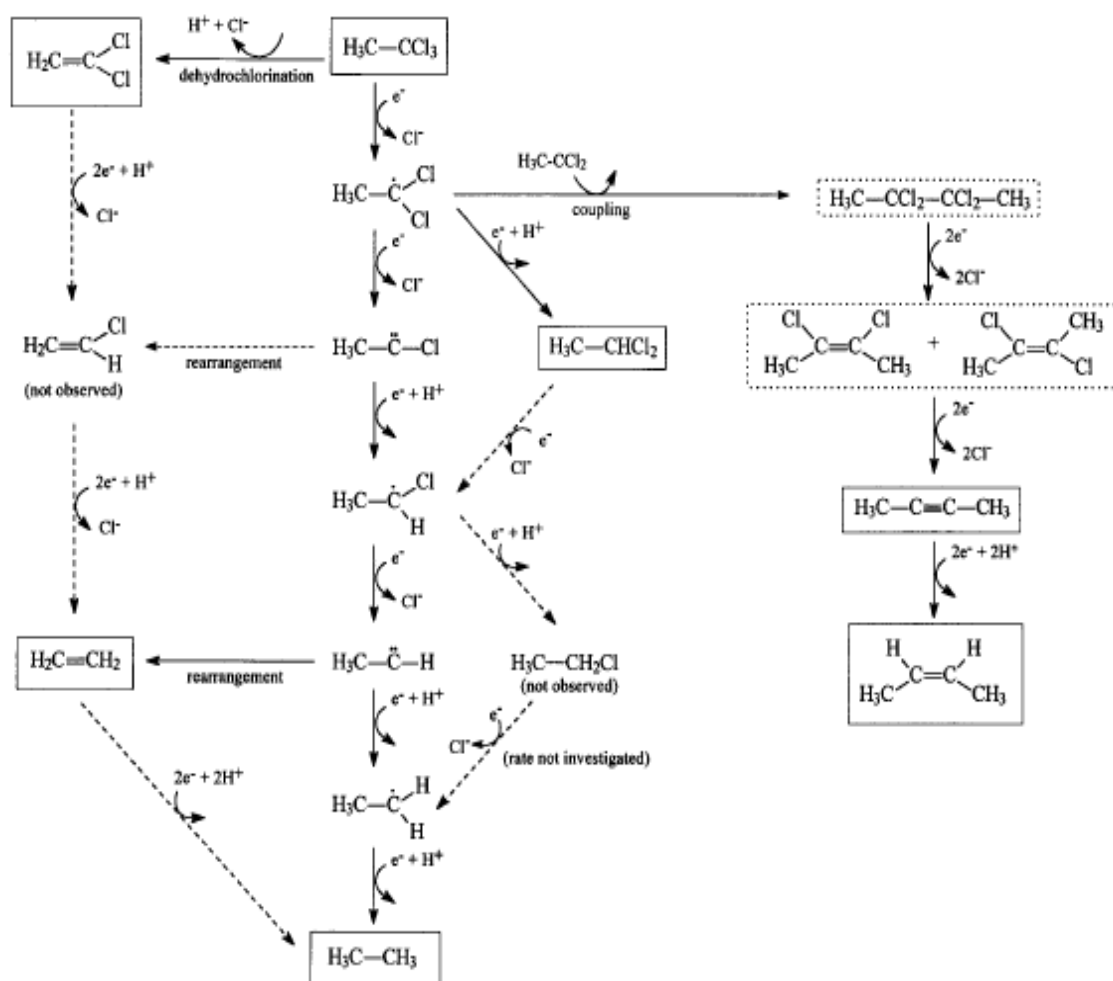
Figure 2.3 Proposed scheme for reaction of 1,1,1-TCA with Fe(0) (17). Boxes indicate reaction products identified in the referenced study: dashed boxes indicate products previously reported in the literature. Dashed arrows reflect potential pathways that are too slow to explain the observed distribution of reaction products as shown by the referenced study or by unpublished data from their laboratory (17).

2.4.2.2 1,1,2,2-Tetrachloroethane

It is known that 1,1,2,2-tetrachloroethane will rapidly transform to trichloroethylene (TCE) by dehydrochlorination (33). 1,1,2,2-TetCA can be degraded in various ways, such as hydrogenolysis, β-elimination, coupling, and dehydrochlorination. 1,1,2,2-TetCA can transform to c-DCE and t-DCE by β-elimination. Also c-DCE, t-DCE and 1,1-DCE can be produced from TCE by hydrogenolysis and then they can be transformed to ethylene via VC by hydrogenolysis. TCE can be converted to chloroacetylene by β-elimination and then to acetylene by hydrogenolysis. Both c-DCE and t-DCE can follow the β-elimination pathway, resulting in acetylene.

The major products of TCE reduction by Zn(0) were c-DCE, t-DCE and acetylene. Acetylene was observed to be produced simultaneously with DCEs during TCE reduction, so it was suggested that acetylene can be produced via a pathway that operates simultaneously with hydrogenolysis of TCE to DCEs (71). In addition, the reaction of chloroacetylene with Zn(0) proceeded very rapidly and produced acetylene and VC (71). Acetylene was the dominant product of reduction of PCE by Fe(II) in cement slurries, where it represented 82.8% of the total carbon 6 days after complete removal of PCE (47). The products of TCE degradation by GR_{SO4} were ethylene and acetylene (72). Figure 2.4 presents the proposed pathways for reduction of chlorinated ethanes in green rust suspension.
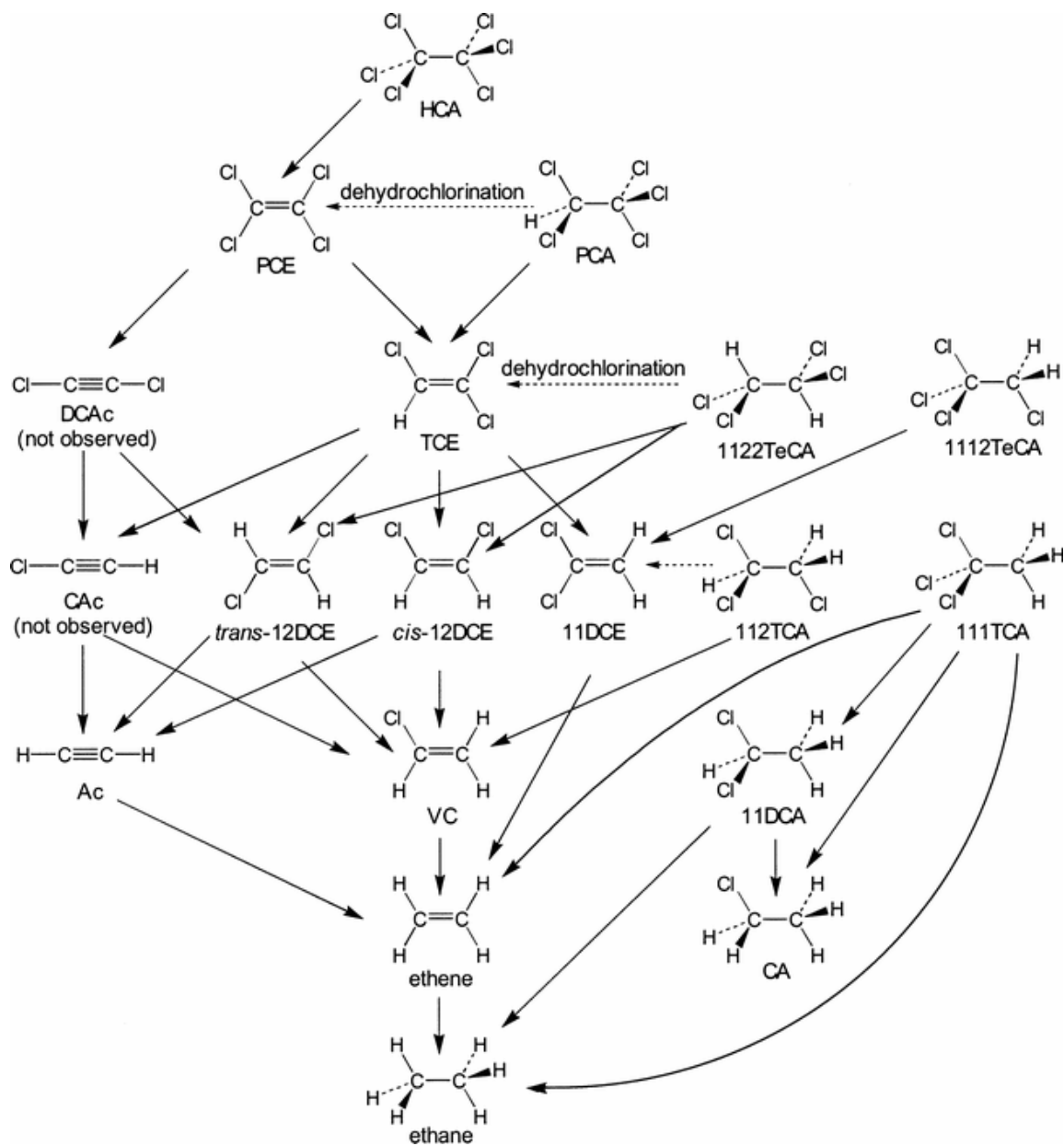
Figure 2.4 Proposed pathways for the reduction of chlorinated ethanes in aqueous green rust suspensions and in green rust suspensions spiked with Ag^I or Cu^{II} (33).

2.4.2.3 1,2-Dichloroethane

1,2-DCA is one of the contaminants that is frequently found at hazardous waste sites. 1,2-DCA can transform to ethylene by β-elimination or to ethane via chloroethane by hydrogenolysis (67). However, several studies have demonstrated that 1,2-DCA is not reactive with Pd/Fe bimetallic nanoparticles or with green rust, green rust modified with silver or with copper (33, 73).

2.4.3 Reductive Transformation of Chlorinated Aliphatic Hydrocarbons in the Presence of Soil Minerals

Many studies have been conducted to characterize the transformation of chlorinated compounds by iron-bearing phyllosilicates. The effect of mineral surfaces on the reduction rates of carbon tetrachloride (CT) reacting with sulfide was investigated by Kriegman-King et al. (38, 74). They found that the disappearance of CT could be described by a first-order reaction rate. The presence of mineral surfaces increased the transformation rates and biotite had a greater effect than vermiculite (38). Also, the presence of biotite and vermiculite enhanced the transformation rate of hexachloroethane (HCA) and the addition of hydrogen sulfide (HS^-) resulted in much faster rates of HCA degradation (74). Reductive dechlorination of PCE, TCE, c-DCE, and VC by iron-bearing phyllosilicates (biotite, vermiculite, and montmorillonite) alone or with the addition of Fe(II) was characterized (72). Biotite had the greatest rate constant among the three minerals and the rate constants increased by a factor of 1.4 to 2.5 by addition of

Fe(II). Based on this observation, it was proposed that Fe(II) surface complex groups on biotite surfaces may be effective reductants (72).

Recent studies have demonstrated that the oxidation state of structural Fe in clays could influence the surface chemistry of clay. Every smectite groups contain some iron in the octahedral sheet (75). The reduction of octahedral Fe^{3+} by biotic or abiotic processes changed surface chemistry of clays including the surface charge density, swelling properties, cation exchange capacity, and specific surface area. The reduction of structural Fe^{3+} to Fe^{2+} in smectites increased total net negative clay layer charge so that free-swelling is decreased and inter surface area is reduced (75).

The oxidation state of Fe is important to understanding the redox reactions with organic contaminants as well as the changes in the chemical properties or physical behavior of clays. Ferrous iron present within the clay structure or at the mineral surface can be described as being one of three types as shown in Figure 2.5: (1) Structural Fe(II), (2) Fe(II) complexed by surface hydroxyl groups at edge surfaces, and (3) Fe(II) bound by ion exchange at basal siloxane surfaces (42). It was found that structural Fe(II) and Fe(II) complexed by surface hydroxyl groups of nontronite reduced nitroaromatic compounds (NAC) to anilines. Fe(II) bound by ion exchange was not effective in reducing NACs (42). In addition, it was suggested that reactive Fe(II) sites of reduced nontronite and exchanged Fe(II) were located at the edge of surfaces of the clays (42). The interaction between the basal surface of the clay and pentachloroethane (PCA) in the surface of reduced smectite is shown in Figure 2.6 (76). The surface of reduced smectite

behaves as a Bronsted base, which can combine with an H^+ and will transform PCA to PCE by dehydrochlorination.
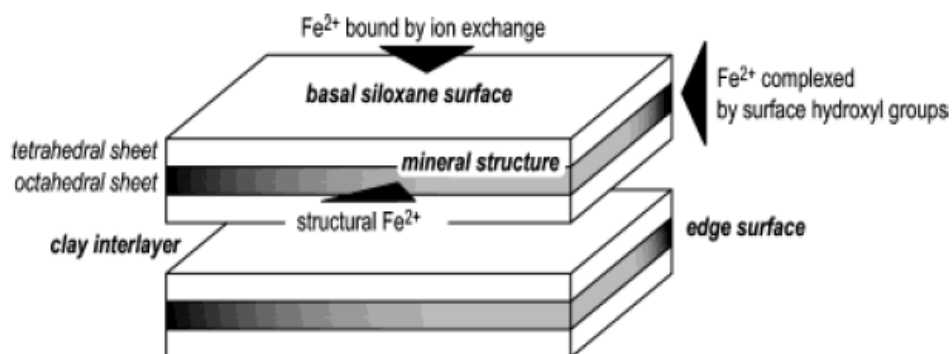
Figure 2.5 Schematic representation of iron within the clay structure (42).
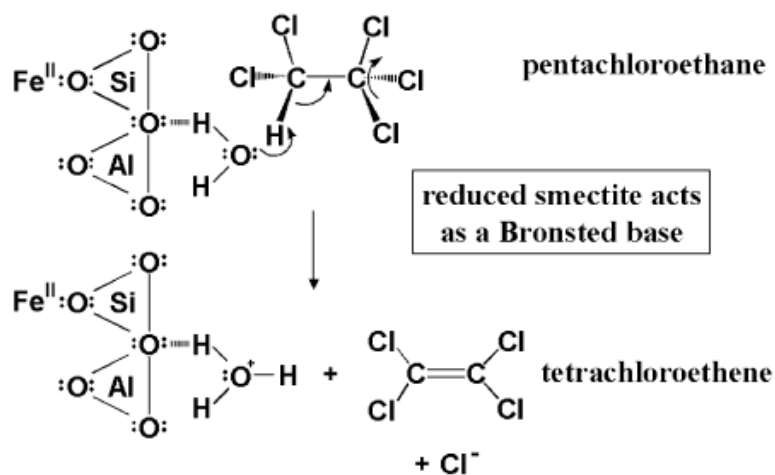
Figure 2.6 Possible Bronsted base-catalyzed reaction mechanism between reduced smectite surface and pentachloroethane (76).

The effect of surface bound Fe(II) on redox reactions was also observed in various Fe(III) oxides other than iron-bearing phyllosilicates (23, 24). The enhanced reactivity of surface-bound Fe(II) can be explained within the framework of a surface complexation theory. The formation of a surface complex upon adsorption of Fe(II) to iron oxides was represented by two types of surface species: $\equiv$Fe(III)-O-Fe(II)-OH or $\equiv$Fe(III)-O-Fe$^+$ (77). The formation of these surface species is shown in equations 2-13 and 2-14 (78).

$$-H^+ + \equiv FeOH + Fe^{2+} \leftrightarrow \equiv FeOFe^+ \tag{2-13}$$

$$-2H^+ + \equiv FeOH + Fe^{2+} + H_2O \leftrightarrow \equiv FeOFeOH^0 \tag{2-14}$$
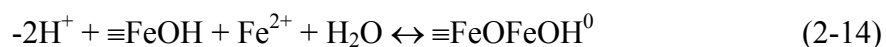
Reactivity of Fe(II) on iron oxides were observed to be dependent on the contact time of Fe(II) in solution, sorption density of Fe(II) (mole Fe(II)/surface area), and pH (23). Based on this observation, it was suggested that surface clusters or precipitates would be more reactive than simple species such as $\equiv$Fe(III)-O-Fe(II)-OH or $\equiv$Fe(III)-O-Fe$^+$ (23, 24).

The pathway for dechlorination of 1,1,1-TCA pathway might be different for clays reduced by biotic or abiotic mechanisms (45). Nearly complete removal of 1,1,1-TCA was observed with ferruginous smectite that was reduced microbially and approximately 60% of the 1,1,1-TCA was converted to 1,1-DCE by dehydrochlorination. In contrast, only 50% of the initial 1,1,1-TCA was removed by ferruginous smectite that

had been reduced chemically, and there was little conversion to 1,1-DCE (45). This indicates that 1,1,1-TCA can undergo different degradation pathways depending on the manner by which minerals were reduced. Molecular structure of chlorinated aliphatic compounds also can influence the pathways of reductive transformation by iron-bearing minerals (43). The effect of molecular structure on the fate of nine chlorinated aliphatic compounds degraded by iron-bearing smectites (SWa-R) was evaluated (43). This research demonstrated that trichloroacetonitrile (TCAN) and trichloronitromethane (CP) were reduced and PCA and 1,1,2,2-TetCA were dehydrochlorinated to PCE and TCE, respectively. In contrast, no transformation products for HCA, TCA, CT, TCE and PCE were observed, but they were sorbed to a moderate extent. Furthermore, it has been reported that the small susceptibility of HCA and PCM to sorption by SWa-R can be explained by the lack of polarity in their chemical structure or of substituents that facilitate charge delocalization. These factors affect how the compound relates to interlayer water molecules and the clay surface.

To characterize transformation of chlorinated compounds by iron–bearing phyllosilicates in the heterogeneous subsurface environment is very complicated. Reductive transformation of chlorinated aliphatic compounds by iron-bearing minerals should consider the following influencing factors: mineral type and quantity, contaminant molecular structure, reducing environment produced by biotic or abiotic processes, the density of reductant in the surface, and chemistry of clay surface.

CHAPTER III

MATERIALS AND METHODS

3.1   Experimental Plan

Two kinds of batch experiments were conducted to achieve two subordinate objectives of this research. First, batch kinetic experiments for three target organics were carried out in cement slurries. The effects of Fe(II) dose, pH, and target compound concentration were evaluated in cement slurries with Fe(II) added. Products of target organic compounds were identified in some batch experiments. Second, batch kinetic experiments with 1,1,1-trichloroethane were conducted in cement slurries with Fe(II) and iron-bearing phyllosilicates (soil minerals). In these experiments, type of soil mineral, Fe(II) dose, and mass ratio of cement to soil mineral were factors influencing the transformation of 1,1,1-TCA. A total of 36 batch kinetic experiments were conducted in this research and summarized in Table 3.1. In addition, experiments were conducted to evaluate the photochemical effect and the extent of sorption of target organic compound onto soil mineral surfaces.

3.1.1   Materials

The chemicals used as target organic compounds were 1,1,1-TCA (99.5%, anhydrous, Aldrich), 1,1,2,2-TetCA (98%, Aldrich) and 1,2-DCA (99.8%, Aldrich). To identify the products formed in degradation of target compounds, the following chemicals were used: TCE (99.5 +%, Fisher Scientific), c-DCE (97%, Aldrich), t-DCE

(98%, Aldrich), 1,1-DCE (97%, Aldrich), 1,1,2-TCA (97%, Aldrich), CA (100 mg/L in methanol, Chem Service), 1,1-DCA (99.5%, Chem Service), VC (200 mg/L, in methanol, Aldrich). Ethane (1000 ppm in He, C_1-C_6 paraffin mixture gas), ethylene (1000 ppm in He, C_2-C_6 olefin mixture gas), acetylene (1% in He), or gas mixtures of 1% CO, CO_2, methane, ethane, ethylene and acetylene in nitrogen were used for analysis of nonchlorinated products and they were purchased from Altech Associates, Inc. Portland cement (type I, Capitol Cement) and ferrous chloride (99+%, tetrahydrate, Sigma) were used as DS/S agents. The chemical composition of the Portland cement was determined by the manufacturer and is shown in Table 3.2. The specific surface area and Fe(III) content of cement, calcium hydroxide, and tricalcium silicate were measured by the manufacturers and are shown in Table 3.3. Stock solutions of chlorinated organics were prepared daily by diluting them in methanol (99.8%, HPLC grade, EM). Target organics (1,1,1-TCA and 1,1,2,2-TetCA) were extracted from the liquid phase with hexane (99.9%, HPLC grade, EM) containing 1,2-dibromopropane (1,2-DBP, 97%, Aldrich Chemical Company, Inc.) as an internal standard. Deaerated deionized water (ddw) was prepared by deoxygenating 18 MΩ-cm deionized water with 99.99% nitrogen for 2 hours and then was purged with mixed gases in an anaerobic chamber (95% nitrogen and 5% hydrogen) for 12 hours. 5N HCl (37%, Aldrich), 5N NaOH (97%, EM) diluted with ddw were used to control pH. Biotite (Bancroft, Ontario, Canada), vermiculite (Transvaal, Africa) and montmorillonite (Pather Creek, Colorado, USA) were purchased from Ward's Natural Science.

Biotite is included in the mica group as a 2:1 phyllosilicates. The general formula of biotite is $K(Mg, Fe)_3(AlSi_3O_{10})(OH)_2$. Biotite has high ferrous iron content of 5~25 % and contains potassium ion in the interlayer positions to satisfy the negative charge due to isomorphous substitution (66, 72). Potassium ions are strongly bonded between adjacent tetrahedral layers so that the basal spacing remains 10 Å (66).

The general formula for vermiculite is $(Mg,Ca)_{0.6-0.9}(Mg,Fe^{3+},Al)_{6.0}[(Al,Si)_8O_{20}]$-$(OH)_4$. Vermiculite is formed as a product of a weathering of micas, such as biotite (79). Therefore, the chemistry of vermiculite is very close to that of the parent mica or biotite (80). Total and ferrous iron content will be lower than that of biotite, because of oxidation of Fe(II) and loss during weathering (74). Another difference from biotite is that K^+ in the interlayer is replaced by exchangeable Mg^{2+}. When calcium and magnesium in interlayers are present, the basal spacing including two water layers is about 14 Å. Isomorphic substitution of Fe^{3+} or Al^{3+} for Mg^{2+} and Fe^{2+} in the octahedral sheet causes a positive charge and substitution of Al^{3+} for Si^{4+} in the tetrahedral sheet yields a negative charge, resulting in a net charge of -0.7 per unit formula. The layer charge in vermiculite causes its cation exchange capacity (CEC) to range from 1200 to 1500 mmol/kg, which is higher than that for montmorillonite (79). Vermiculite swells less than montmorillonite because of its higher layer charge. Total surface areas of vermiculite ranges from 600 to 800×10^3 m^2/kg when not saturated with K^+ or NH_4^+ (79).

The general formula of montmorillonite is $X_{0.7}(Mg_{0.7}Al_{3.3})Si_8O_{20}(OH)_4$. Montmorillonite is a 2:1 layer silicate with a large charge of 0.25 ~ 0.6 per formula unit. Because of the relatively low layer charge, the layers of montmorillonite are freely

expanded. Typical cation exchange capacities for montmorillonite range from 800 to 1200 mmol/kg (79). The surface area is in the range 600 to 800 m^2/g. The reduction of structural Fe^{3+} to Fe^{2+} in the octahedral sheet will increase layer charge and this will cause an increase in cation fixation or entrapment between layers (65).

Table 3.1 Conditions of batch kinetic experiments.

Type	Code	Influencing Factors	Target compound
DS/S-BKE-PC[a]	PC-TA-FE	6 different Fe(II) Dose	1,1,1-TCA (TA)
	PC-TA-pH	5 different pH	·
	PC-TA-C0	3 different target organic conc.	·
	PC-TE-FE	3 different Fe(II) Dose	1,1,2,2-TetCA (TE)
	PC-TE-pH	5 different pH	·
	PC-TE-C0	3 different target organic conc.	·
	PC-DA-FE	2 different Fe(II) Dose	1,2-DCA (DA)
DS/S-BKE-Soil[b]	PC/S-TA-SM	3 different soil mineral types	1,1,1-TCA (TA)
	PC/S-TA-FE	3 different Fe(II) Dose	·
	PC/S-TA-RA	3 different ratio of cement/soil	·

[a]DS/S-BKE-PC : Batch kinetic experiments in Portland cement slurries

[b]DS/S-BKE-Soil: Batch kinetic experiments in Portland cement with iron-bearing phyllosilicates.

Table 3.2 Chemical composition of the Portland cement (47, 81).

Oxide	CaO	SiO$_2$	Al$_2$O$_3$	Fe$_2$O$_3$	MgO	SO$_3$	Loss on ignition	Insoluble residue
wt%	64.85	20.26	5.46	2.52	1.26	3.20	1.65	0.1

Table 3.3 Specific surface area and Fe(III) content for solids (47, 81).

Surface	Specific surface are (m^2/g)	Fe(III) (wt %)
Portland cement[a]	0.35[b]	1.76
Calcium hydroxide (Ca(OH)$_2$)	n.a.	0.063
Tricalcium silicate (CaO)$_3$SiO$_2$)	0.355[b]	0.05

[a]94.8% passing 325 mesh(0.45 μm), [b]measured by the Blaine method

3.1.2 Experimental Procedures

3.1.2.1 Batch Kinetic Experiments in Cement Slurries

Clear borosilicate glass vials (24.2 ± 0.1 ml, nominally 20 ml) with triple-seal closures were used as batch slurry reactors. These closures consist of a Teflon lined silicon septum, lead foil tape (3M, adhesive backed), and Teflon tape (Norton Performance Plastics Co. nonadhesive, 2 mm thick). All samples were prepared in an anaerobic chamber. Anaerobic conditions were maintained in the chamber by a reactive palladium coated catalyst and were monitored by a colorless redox indicator (resazurin) which turns pink when redox potential increases above about 218 mV at pH 9 (82). Two

types of controls were prepared in duplicate and all other reactive samples were carried out in triplicate. One control consisted of water and a target organic and the other control included cement, water, and the target organic compound. The mass ratio of solid (cement) to solution was 0.1 in batch experiments with cement slurries. Fe(II) doses ranged from 1.96 mM to 196 mM. The Fe(II) dose was varied depending on the target organic compound. For 1,1,1-TCA, Fe(II) dose ranged from 1.96 mM to 78.4 mM. For 1,1,2,2-TetCA, it ranged from 39.2 mM to 196 mM. And the Fe(II) doses applied to experiments with 1,2-DCA were 39.2 mM and 196 mM. The pH of the 10 % cement slurries was approximately 12.5. For experiments to evaluate pH effects, 5 N HCl or 5 N NaOH were added to the samples to obtain the targeted pH.

The reaction was initiated by spiking 10 μL of the methanolic stock solution of 1,1,1-TCA, 1,1,2,2-TetCA, or 1,2-DCA into the slurries to yield a target organic concentration of 0.245 mM (respectively 32.7 mg/L, 41.1 mg/L and 24.2 mg/L). Three different initial target organic concentrations (0.01 mM, 0.1 mM and 1 mM) were prepared when it was an experimental factor. After spiking with the target organics stock solution, the vials were rapidly capped and were placed in a tumbler providing end-over-end rotation at 7 rpm at room temperature. At a specified reaction time, the reaction vials were removed from the tumbler and centrifuged at 2000 rpm (912 g) for 10 min (International equipment Co. model CS centrifuge). To extract target organics, 50 μL of supernatant was transferred into autosampler vials containing 1 mL hexane with 2.6 mg/L 1,2-DBP. After shaking at 250 rpm for 1 hour, the extractant was injected into the gas chromatograph using an automatic injection system.

3.1.2.2 Batch Kinetic Experiments in Cement and Soil Mineral Suspension

Batch kinetic experiments were conducted to characterize degradation kinetics of 1,1,1-TCA in cement slurries with Fe(II) and iron-bearing phyllosilicates. Biotite (Bancroft, Ontario, Canada), vermiculite (Transvaal, Africa), and montmorillonite (Pather Creek, Colorado, USA) are iron-bearing phyllosilicates that were used in this research. The soil minerals were also used by Lee et al. (72) and their properties are shown in Table 3.4. The soil minerals were ground with a grinder and sieved (sieve no. 60 with 0.25 mm openings). Soil minerals were used without pretreatment with a reductant, so they were probably in an oxidized state. After sieving, they were stored in an anaerobic chamber for 2 days.

Experiments were conducted using the same procedures previously described for the characterization experiments except as described here. Both the soil mineral and cement were considered in setting the mass ratio of solid to water at 0.1 (g/g). For vermiculite, pH was measured at eight different mass ratios of cement to soil mineral that ranged from 0.2 to 3. These pH values were maintained between 12.4 and 12.7 over 1 day. Mass ratios of cement to soil mineral of 0.2, 1, and 3 were determined and applied to all three soil minerals. All samples and controls for these experiments were prepared in duplicate. Three stock solutions of Fe(II) (0.1M, 0.05M, 0.025M) were used resulting in initial Fe(II) concentrations of 20 mM (11.2 mg/g solid), 10 mM (5.6 mg/g solid), and 5 mM (2.8 mg/g solid). For each soil mineral, three different Fe(II) doses were investigated at a constant mass ratio of cement to soil mineral of 1. A stock solution of 1,1,1-TCA (0.8 M) was prepared and 10 μL of it was spiked to the reactors, which

resulted in an initial concentration of 0.347 mM (46.3 mg/L). At each sampling time, the vials were centrifuged at 3000 rpm (1368 g) for 20 min to separate the solid and liquid phases. The concentration of target organic compound in the aqueous phase was measured after applying the same extraction procedure described for the characterization experiments.

Prior to the experiments in the presence of soil minerals, sorption tests of 1,1,1-TCA were performed for biotite and vermiculite. The mass ratio of solid to solution was 0.1 and 10 µL of 0.8 M stock solution of 1,1,1-TCA was spiked to the reactors. The kinetics of 1,1,1-TCA sorption onto soil minerals was observed over 5 days.

Table 3.4 Characteristics of iron-bearing phyllosilicates used in this research (72).

Soil minerals	Fe(II) (mg/g)	Fe(III) (mg/g)	Surface charge area (m^2/g)	Particle size (µm)
Biotite	114.1	3.1	1.9	63-250
Vermiculite	14.2	42.5	26.7	63-250

3.1.3   Analytical Procedures

Analytical procedures for gas chromatographic analysis of target organics (1,1,1-TCA, 1,1,2,2-TetCA, 1,2-DCA) were developed. Other procedures were developed to measure concentrations of chlorinated products (TCE, 1,1,2-TCA, 1,1-DCA, 1,1-DCE, c-DCE, t-DCE, CA, VC) and non-chlorinated products (ethane, ethylene, acetylene)

3.1.3.1   Chlorinated Aliphatic Hydrocarbons

Two target compounds (1,1,1-TCA, 1,1,2,2-TetCA) and TCE were analyzed with a Hewlett-Packard 6890 GC with a DB-VRX column (60 m x 0.25 mm i.d., with a film thickness of 1.4 μm, J&W scientific), and an electron capture detector (ECD). Aqueous samples of these compounds were extracted with hexane containing 1,2-DBP and injected using an autosampler with a split ratio of 20:1. The oven temperature program was as follows; 80 ºC for 2 min, ramp 5 ºC/min to 130 ºC and hold for 1 min. The temperature of the injector was 220 ºC and that of the detector was 240 ºC. The flow rate of make up gas was 60 mL/min and the sample injection amount was 1 μL. 1,2-DCA was analyzed by a Trace GC 2000 with a HP-5MS column and a flame ionization detector (FID). Chlorinated products formed in the degradation experiment (1,1,2,2-TetCA, TCE, 1,1,1-TCA, 1,1,2-TCA, 1,1-DCA, 1,1-DCE, c-DCE, t-DCE, CA, VC) were also analyzed with the Trace GC 2000 with a HP-5MS column and a FID. The temperatures of the injector and detector were 200 ºC. The oven temperature was programmed to be the isothermal at 50 ºC for 5 min. The column flow rate was 1.5 mL/min and makeup gas was helium at a flow rate of 40 mL/min. The ignition gases were hydrogen and oxygen and their flows were respectively 40 mL/min, and 450 mL/min. Headspace analysis procedures using GC/FID were developed to analyze these chlorinated products. A 10-mL sample of supernatant was rapidly transferred with 10-mL gas tight syringe to a 20-mL amber vial. The vial was tightly capped and shaken for 30 min at 250 rpm and then allowed to stand for 5 hours at room temperature to equilibrate between gas and liquid phases. Gas phase samples of 100 μL were

withdrawn from the headspace with a 100-μL gas-tight syringe (Hamilton) and manually introduced into the injection port. The concentrations of compounds by headspace analysis were quantified by comparing peak areas to standard calibration curves.

3.1.3.2 Non-Chlorinated Products

Non-chlorinated compounds including ethane, ethylene and acetylene were analyzed using a HP6890 GC with a GS-Alumina Column (30 m × 0.53 mm i.d., J&W Scientific) and a FID. The split/splitless injection port and detector were both at 150 °C and the oven temperature was isothermal at 100 °C for 5 min. Nitrogen was used both as carrier gas and makeup gas. Hydrogen and zero air were used as ignition gases. The flow rates of carrier gas and makeup gas were 6.3 and 60 mL/min, respectively. The same headspace sampling described for the analysis of chlorinated compounds was applied to non-chlorinated compounds. A sample of 100 μl was taken from the headspace and was manually introduced into the injection port at a split ratio of 5:1. The concentration of ethane, ethylene and acetylene were measured by comparing peak areas to a standard calibration curve.

CHAPTER IV

REDUCTIVE DECHLORINATION OF CHLORINATED ALIPHATIC

HYDROCARBONS BY FE(II) IN CEMENT SLURRIES

4.1   Treatment of Kinetic Data

Transformation kinetics of chlorinated aliphatic hydrocarbons by Fe(II) in cement slurries was investigated considering the influencing factors such as Fe(II) dose, pH, and initial target concentration. The degradation products in Fe(II)/cement system were also identified. Prior to conducting degradation kinetic experiments to examine three different influencing factors, the hydrolysis effect and the influence of oxygen and light on the degradation of 1,1,1-TCA in DS/S were investigated. For most experimental conditions, the kinetics was described by a pseudo-first-order rate model, which in a batch reactor can be described as follows.

$$\frac{dC_{CA,l}}{dt} = -k_{obs}C_{CA,l} \tag{4-1}$$

where k_{obs} is the observed pseudo-first-order rate constant (hour^{-1}), $C_{CA,l}$ is the concentration of chlorinated ethanes in the liquid phase (mM). Pseudo-first-order rate constants (k_{obs}) were obtained by conducting nonlinear regressions using MATLAB$^{®}$ for Windows (Version 6.5, The MathWorks, Inc.). Measured concentrations of a target organic in the aqueous phase of the reactors spiked with Fe(II) were regressed as a

function of reaction time. The MATLAB function 'nlinfit' calculates values of the model parameters (k_{obs}, $C_{CA,l}{}^0$) and the function 'nlparci' calculates their 95% confidence intervals. Two kinds of controls were used in these experiments. One type of control contained water and the target organic and the other contained water, cement and the target organic. In the control with cement, decay of chlorinated ethanes was observed, which would be the result of hydrolysis that occurs at the high pH caused by the cement. To obtain pseudo-first-order rate constants due to only the effect of reductive dechlorination by Fe(II), the rate constant in the control with cement ($k_{obs,control}$) was subtracted from the rate constant in the systems with Fe(II) (k_{obs}), as shown in equation 4-2,

$$-\frac{dC_{CA,l}}{dt} = (k_{obs} - k_{obs,control})C_{CA,l} = k'_{obs}\, C_{CA,l} \qquad (4\text{-}2)$$

where k'_{obs} is the pseudo-first-order rate constant (hr^{-1}) corrected by the control; $k_{obs,control}$ is the observed pseudo-first-order rate constant for the control that contained cement (hr^{-1}). If target organics were assumed to be partitioned into the liquid, gas and solid phases, then a material balance on target organics over all phases is:

$$
\begin{aligned}
M_{CA,t} &= V_l C_{CA,l} + V_g C_g + M_{solid} \\
&= V_l C_{CA,l} + V_g C_g + K_s C_{CA,l} V_l \\
&= V_l C_{CA,l}\left(1 + \frac{V_g C_g}{V_l C_{CA,l}} + K_s\right) \qquad (4\text{-}3) \\
&= V_l C_{CA,l}\left(1 + H\frac{V_g}{V_l} + K_s\right)
\end{aligned}
$$

$$C_{CA,t} = (1 + H\frac{V_g}{V_l} + K_s)C_{CA,l} = pC_{CA,l} \qquad (4\text{-}4)$$

$M_{CA,t}$ is the total mass of target organics; $C_{CA,t}$ is the total concentration of target organics; $C_{CA,l}$ is the concentration of target organics in the aqueous phase; C_g is the concentration of target organics in the gas phase; M_{solid} is the mass of target organics in solid phase; V_g (~0.3 ml) and V_l (~23 ml) are volumes of the gas and aqueous phases, respectively; H is the dimensionless Henry's constant for target organics (H=0.622 for 1,1,1-TCA) (35); K_s is the solid phase partition coefficient for the target organic (ratio of mass of target organic in the solid phase to mass of target organic in the aqueous phase). The solid phase partition coefficients (K_s) were determined as an average of K_s values calculated from controls without cement for eight experiments (K_s for 1,1,1-TCA=0.067). The value of the partitioning factor (*p*) calculated by equation 4-4 for 1,1,1-TCA was 1.07. The loss of target organic compound in controls with only water was shown to be caused by partitioning to the gas phase and to the solid phases, which included the triple-layered septum and the reactor wall (47).

In a heterogeneous system including cement and Fe(II), first-order rate kinetics was generally found to reasonably describe results of most experiments. However, under some conditions, a second-order rate model fitted the data better. In this chapter, three different kinetic models were used under different assumptions. The decay rate in reactions between target organics and Fe(II) generally can be described by equation 4-5.

$$r = k'(C_{RE})^m (C_{CA,l})^n \tag{4-5}$$

If it is assumed that the reductive capacity (C_{RE}) of a reductant is large enough and that the reaction order is first order with respect to target organics (n=1), then the reaction rate can be expressed as equation 4-6.

    I.   The first-order rate model (m=0, n=1)

$$-\frac{dC_{CA,t}}{dt} = kC_{CA,l} \tag{4-6}$$

$$-\frac{dC_{CA,l}}{dt} = \frac{k}{p}C_{CA,l} = k_{obs}C_{CA,l} \tag{4-7}$$

$$C_{CA,l} = C_{CA,l}{}^0 \exp(-k_{obs}t) \tag{4-8}$$

Equation 4-7 was obtained by substituting equation 4-4 into equation 4-6 and equation 4-8 is the solution of the differential equation of 4-7. Equation 4-8 was used to determine values of parameters ($C_{CA,l}{}^0$, k_{obs}) by a nonlinear-regression using MATLAB. The variable of k_{obs} is the observed pseudo-first-order rate constant and k is the pseudo-first-order rate constant calculated by the partitioning factor.

If it is assumed that the reductive capacity (C_{RE}) is large enough and that the reaction order is second order with respect to target organics (n=2), then the reaction rate can be expressed as equation 4-9.

    II.   The second-order rate model (m=0, n=2)

$$-\frac{dC_{CA,t}}{dt} = k(C_{CA,l})^2 \tag{4-9}$$

$$-\frac{dC_{CA,l}}{dt} = \frac{k}{p}(C_{CA,l})^2 = k_{obs}(C_{CA,l})^2 \qquad (4\text{-}10)$$

$$C_{CA,l} = \frac{C_{CA,l}{}^0}{1 + k_{obs}C_{CA,l}{}^0 t} \qquad (4\text{-}11)$$

Equation 4-11 is the result obtained by integrating equation 4-10. Equation 4-11 was used to estimate values of the parameters ($C_{CA,l}{}^0$, k_{obs}) by a nonlinear-regression using MATLAB.

Finally, if it is assumed that the reductive capacity (C_{RE}) is limited and the reaction order is first order with respect to the target organic (n=1) and with respect to the reductant (m=1), then the reaction rate can be expressed as equation 4-13. C_{RE} was determined as the difference between initial reductive capacity and the change of chlorinated ethanes in total concentration as described in equation 4-12.

III.   The dual concentration second-order rate model (m=1, n=1)

$$C_{RE} = C_{RE}{}^0 - \{C_{CA,t}{}^0 - C_{CA,t}\}$$

$$= C_{RE}{}^0 - p\{C_{CA,l}{}^0 - C_{CA,l}\} \qquad (4\text{-}12)$$

$$-\frac{dC_{CA,t}}{dt} = k'(C_{RE})(C_{CA,l})$$

$$= k'(C_{RE}{}^0 - p\{C_{CA,l}{}^0 - C_{CA,l}\})(C_{CA,l}) \qquad (4\text{-}13)$$

$$-\frac{dC_{CA,l}}{dt} = \frac{k'}{p}(C_{RE}{}^0 - p\{C_{CA,l}{}^0 - C_{CA,l}\})(C_{CA,l})$$

$$= k_{obs}(C_{RE}{}^0 - p\{C_{CA,l}{}^0 - C_{CA,l}\})(C_{CA,l}) \qquad (4\text{-}14)$$

Equation 4-14 was solved using the 'ode45' function in MATLAB with the values of parameters of C_{RE}^{0} and k_{obs} obtained by a nonlinear-regression.

4.2   1,1,1-Trichloroethane

The hydrolysis of 1,1,1-TCA and the effects of anaerobic condition and light on the degradation kinetics of 1,1,1-TCA were investigated prior to other kinetic experiments. The results are shown in Table 4.1. Base-catalyzed hydrolysis of 1,1,1-TCA at approximately pH 12.5 was examined using the control containing cement. Concentration of 1,1,1-TCA was monitored over time in 10% cement slurries without addition of Fe(II) and the results are shown in Figure 4.1 This shows hydrolysis of 1,1,1-TCA with a half-life of approximately 6.9 days. However, the pseudo-first-order rate constant for the control with cement was less than 1% of rate constant for reactors with cement and Fe(II). Therefore, the effect of hydrolysis was not significant and there was no need to modify the values of the pseudo-first-order rate constant for 1,1,1-TCA degradation measured in the Fe(II)/cement systems.

No products of 1,1,1-TCA degradation by hydrolysis was observed in gas chromatographic analysis for chlorinated or non-chlorinated products. The product of abiotic hydrolysis of 1,1,1-TCA has been reported to be acetic acid (HAc) (67), which would not be expected to be extracted into hexane and so would not be detected by subsequent gas chromatography.

$$\underset{1,1,1-TCA}{CH_3CCl_3} + 2H_2O \rightarrow \underset{HAc}{CH_3COOH} + 3H^+ + 3Cl^- \tag{4-15}$$
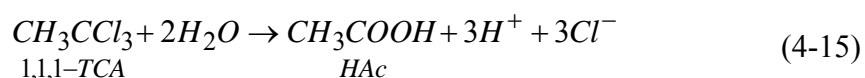
Table 4.1 Experiment conditions and pseudo-first-order rate constants for degradation of 1,1,1-TCA.

exp	solid[a]	C_0 (mM)	$Fe(II)$[b] (mM)	pH	k_{obs}(hour^{-1})	n[d]	condition
1	Cement	0.245	9.8	~12.5	0.588(±13.6%)[c]	19	Anaerobic
2	Cement	0.245	9.8	~12.5	0.077(±25.6%)	25	Aerobic
3	Cement	0.245	9.8	~12.5	0.441(±27.9%)	19	Not wrapped
4	Cement	0.245	9.8	~12.5	0.436(±16.0%)	19	wrapped
5	Cement	0.245	no	~12.5	0.004(±31.5%)	14	hydrolysis

[a]mass ratio of solid to solution was 0.1. [b]source of Fe(II) was $FeCl_2$ [c]uncertainties represent 95% confidence limits expressed in % relative to estimate for k_{obs}, [d]number of data points used in regression.
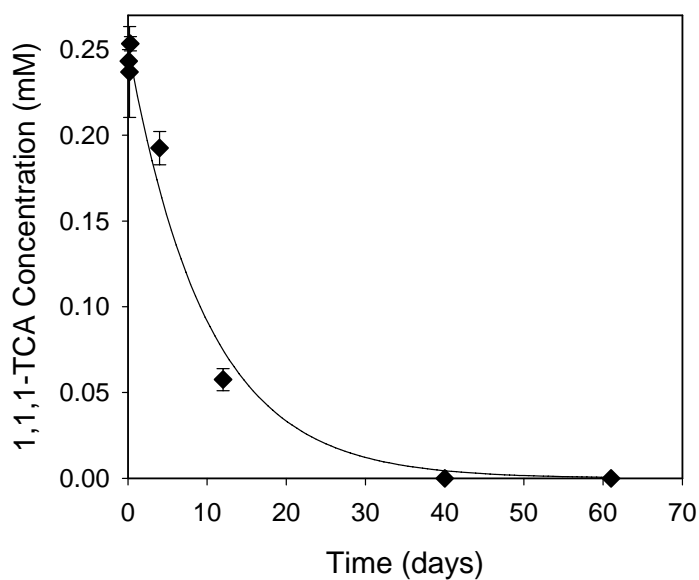
Figure 4.1 Hydrolysis of 1,1,1-TCA in control with cement (exp. 5). Error bars represent the standard deviation of measured 1,1,1-TCA concentrations. Some error bars are smaller than the symbols. The solid line represents the fit by a first-order model.

Figure 4.2 compares results of kinetic experiments conducted in an anaerobic chamber to those obtained outside the anaerobic chamber. The pseudo-first-order rate constant for the experiment conducted in the anaerobic environment was 7.6 times greater than that for the experiment conducted in an aerobic environment. It has been reported that only magnetite and GR(F$^-$) were detected in the XRD analysis of GR(F$^-$) after reducing PCE (83). Green rust (GR) is hypothesized to be the active reductant in DS/S-Fe(II). In an aerobic environment, oxidation of green rust to magnetite would be enhanced by the reaction with oxygen. Therefore, target organics and oxygen would compete as electron acceptors, resulting in slower rates of reduction of target organics.

The photochemical effect was investigated by conducting experiments in vials covered without aluminum foil and with foil. Results of these experiments are shown in Table 4.1 as exp. 3 and exp. 4 and Figure 4.3. The rate constants do not differ greatly, which indicates that the photochemical effect on the degradation kinetics of 1,1,1-TCA by Fe(II) in cement slurries was not significant. All subsequent degradation experiments were conducted without a cover of aluminum foil.
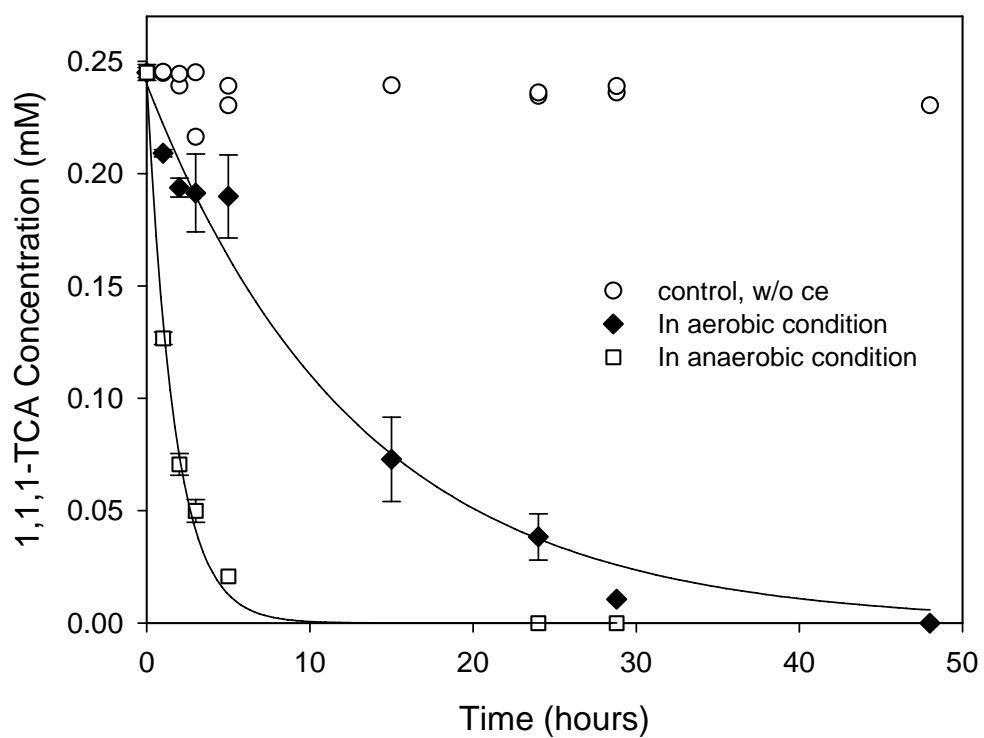
Figure 4.2 Degradation of 1,1,1-TCA by Fe(II) in 10% cement slurries in anaerobic and aerobic environments. Error bars represent the standard deviations of measured 1,1,1-TCA concentrations. Some error bars are smaller than the symbols. The solid lines represent the fit by a first-order model. $[1,1,1\text{-TCA}]_0$=0.245 mM and $[Fe(II)]_0$=9.8 mM (exp. 1& 2).
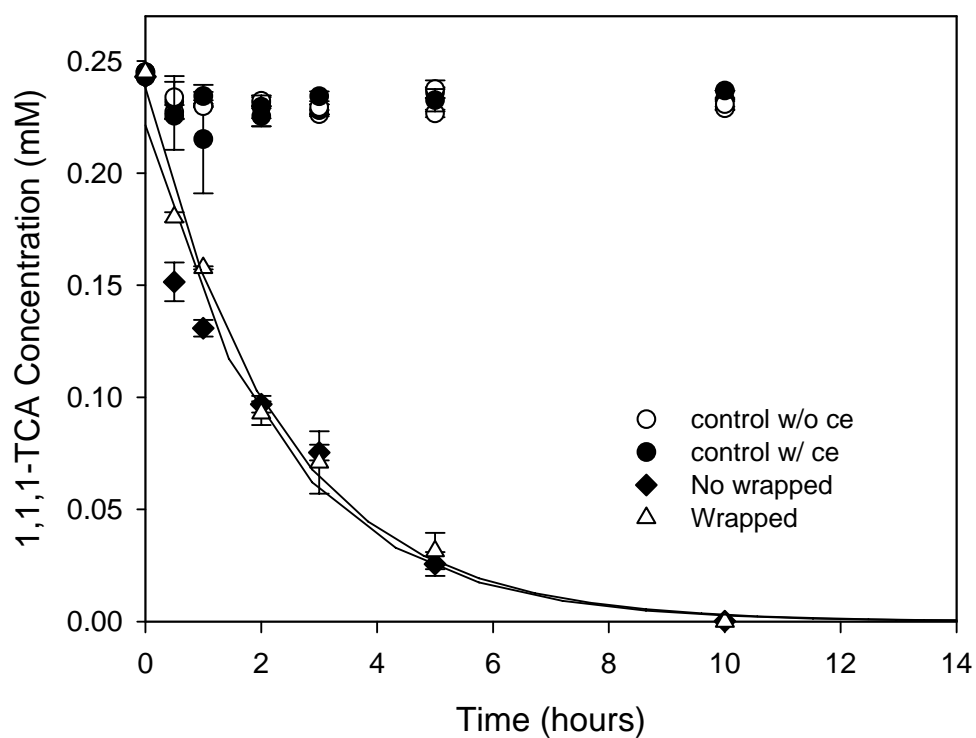
Figure 4.3 Photochemical effects on reduction of 1,1,1-TCA by Fe(II) in 10% cement slurries. Error bars represent the standard deviations of measured 1,1,1-TCA concentrations. Some error bars are smaller than the symbols. The solid lines represent the fit of a first-order model. $[1,1,1\text{-TCA}]_0$=0.245 mM and $[Fe(II)]_0$=9.8 mM (exp. 3& 4).

4.2.1 Effect of Fe(II) Dose

Figure 4.4 presents the results of 1,1,1-TCA degradation by Fe(II) in 10% cement slurries. Figure 4.4 shows that first-order kinetics can reasonably describe 1,1,1-TCA reduction kinetics for four selected Fe(II) concentrations that range from 4.9 mM to 39.2 mM. At a low concentration of Fe(II) (1.96 mM), the concentration of 1,1,1-TCA decreased slightly and then remained constant. This indicates that the reductant demand of the 1,1,1-TCA exceeded the reductive capacity of the reductants formed from Fe(II). First-order kinetics were not observed for the data obtained at a Fe(II) concentration of 1.96 mM, but the dual concentration second-order rate model (equation 4-14) fitted the data well.

Pseudo-first-order rate constants for these experiments are presented in Table 4.2 (exp. 6 to 10) and are plotted against Fe(II) dose in Figure 4.5, which shows a linear relationship. The increase of pseudo-first-order rate constants with Fe(II) dose indicates that added Fe(II) participates in formation of active reductants and higher formation of active reductants will result in the increase of rate constants. Here, the increase of k_{obs} corresponding to increase ratio of Fe(II) dose within the range investigated means that formation of active reductant can be stoichiometrically related to Fe(II) dose.

Table 4.2 Pseudo-first-order rate constants for degradation of 1,1,1-TCA at various experimental conditions.

exp	solid[a]	C_0 (mM)	$Fe(II)$[b] (mM)	pH	k_{obs}(hour^{-1})	n[f]
6	Cement	0.245	1.96	~12.5	0.005(±75.4%)[c]/0.485[d](±29.6%)	27
7	Cement	0.245	4.9	~12.5	0.154(±15.7%)	28
8	Cement	0.245	9.8	~12.5	0.415(±4.8%)	31
9	Cement	0.245	19.6	~12.5	0.864(±5.6%)	31
10	Cement	0.245	39.2	~12.5	1.928(±2.0%)	13
11	Cement	0.245	9.8	11.0	0.003(±34.5%)	28
12	Cement	0.245	9.8	11.9	0.024(±31.8%)	28
13	Cement	0.245	9.8	12.3	0.049(±19.5%)	28
14	Cement	0.245	9.8	12.5	0.428(±5.5%)	27
15	Cement	0.245	9.8	13.4	0.181(±22.1%)	25
16	Cement	0.01	4.9	~12.5	0.166(±12.7%)	22
17	Cement	0.1	4.9	~12.5	0.144(±15.8%)	25
18	Cement	1	4.9	~12.5	0.067(±39.2%)/0.138[e](±21.9%)	24

[a]mass ratio of solid to solution was 0.1.

[b]source of Fe(II) was $FeCl_2$.

[c]uncertainties represent 95% confidence limits expressed in % relative to estimate for k_{obs}.

[d]the rate constant was obtained from second-order rate model of equation 4-14.

[e]the rate constant was obtained from second-order rate model of equation 4-11.

[f]the number of data points used in nonlinear regression.
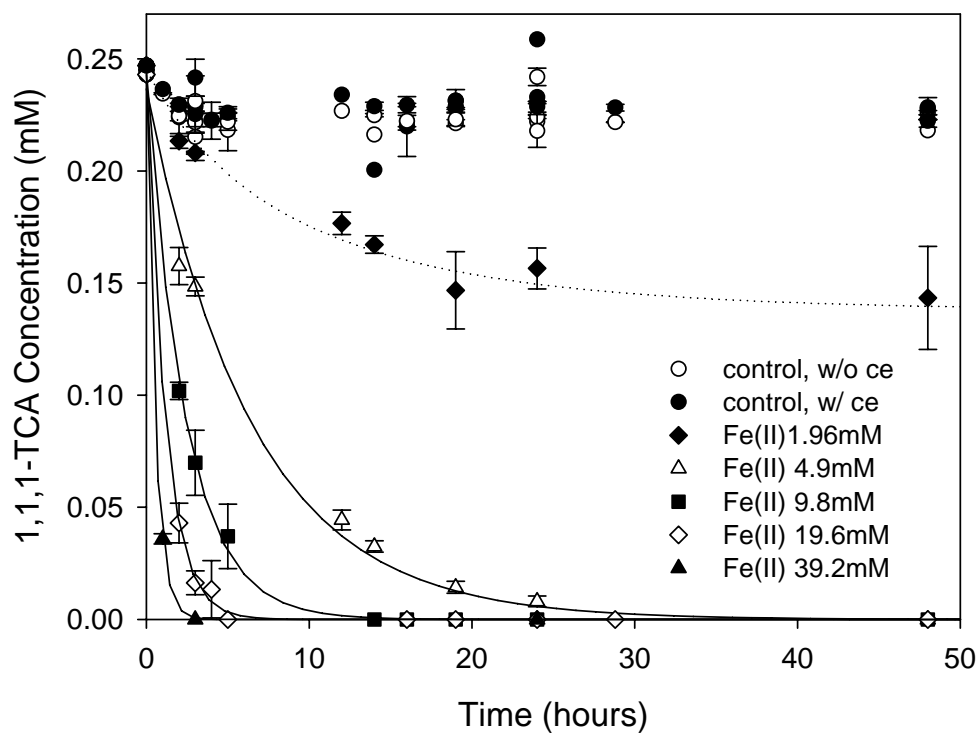
Figure 4.4 Kinetics of 1,1,1-TCA reduction by Fe(II) in 10% cement slurries at various Fe(II) dose. Error bars represent the standard deviations of measured 1,1,1-TCA concentrations. Some error bars are smaller than the symbols. Solid lines represent the fits of first-order models and dotted line represents the fit of a dual concentration second-order model (exp. 6 to 10). $[1,1,1\text{-TCA}]_0 = 0.245$ mM.
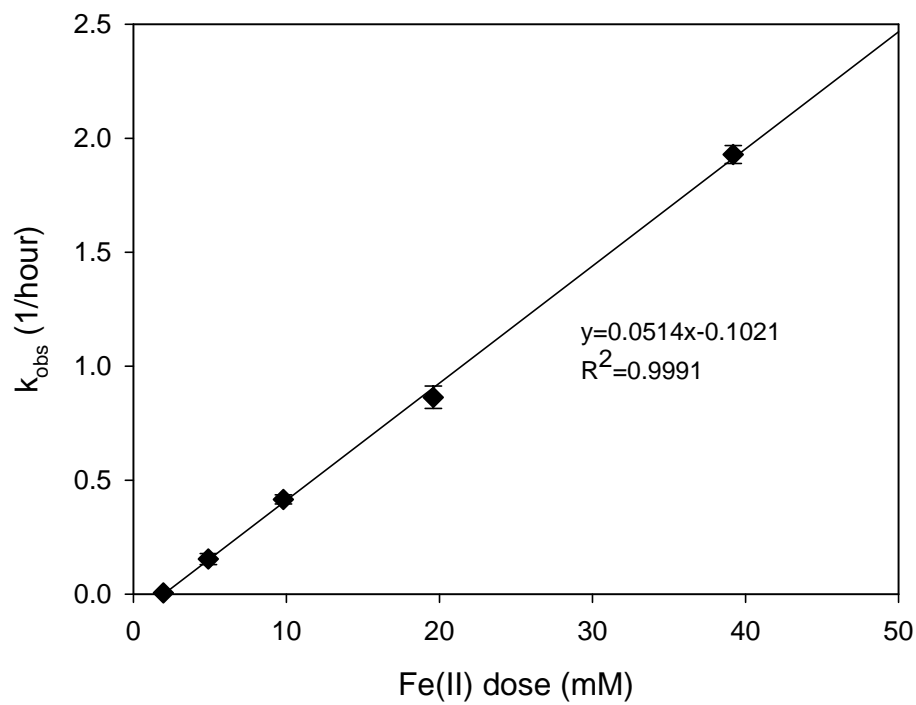
Figure 4.5 Dependence of pseudo-first-order rate constants on Fe(II) dose. Error bars are 95% confidence intervals for a estimated value. The solid line represents a linear model.

4.2.2   Effect of pH

The pH of the slurries was measured in each of the three replicate reactors at every sampling point and the average values are shown in Figure 4.6. The nominal pH was determined as the average value of all measured pH values for each experimental condition. The range of measured pH at nominal pH values of 11.0, 11.9, 12.3, 12.5, and 13.4 were ±0.2, ±0.3, ±0.2, ±0.1 and ±0.1, respectively. The pH in several experiments (nominal pH of 11.0, 11.9 and 12.3) showed a minimum near 24 hours.

The pH changes can be expected with the formation and oxidation of iron hydroxides such as green rust and with the reactions between target organics and reductants. The Fe^{2+} that is added in the presence of sufficient OH^- will form $Fe(OH)_2(s)$ and sufficient OH^- is expected in the presence of cement. $Fe(OH)_2(s)$ will be readily oxidized to green rust or on further oxidation, magnetite. Laboratory studies have reported that magnetite was found as the only oxidation product of green rust (31, 83). The formation of $GR(Cl^-)$ and its oxidation to magnetite by 1,1,1-TCA can be described by equations 4-16 and 4-17. These reactions assume that $Fe(OH)_2$ oxidation occurs in the presence of cement hydration products that contain Fe(III). The formula Fe_2O_3 is used to represent Fe(III) present in a cement hydration product such as tetracalcium aluminoferrite $((CaO)_2(Al_2O_3,Fe_2O_3)\cdot 6H_2O)$.

$$6Fe(OH)_2 + Fe_2O_3 + 2Cl^- + H_2O + 2H^+ = 2Fe^{II}_3Fe^{III}(OH)_8Cl \qquad (4\text{-}16)$$

$$CH_3CCl_3 + 2Fe^{II}_3Fe^{III}(OH)_8Cl + 11H^+ = C_2H_6 + Fe^{II}Fe^{III}_2O_4 + 5Cl^- + 5Fe^{2+} + 12H_2O \quad (4\text{-}17)$$
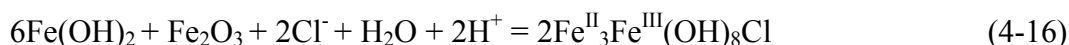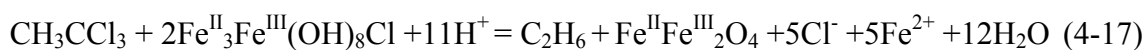
The effect of pH on degradation kinetics of 1,1,1-TCA was studied and the results are shown in Table 4.2 and Figures 4.7 and 4.8. Figure 4.8 shows that 1,1,1-TCA reduction reactions in cement systems are strongly dependent on pH. The pseudo-first-order rate constant increased with pH to a maximum near pH 12.5.
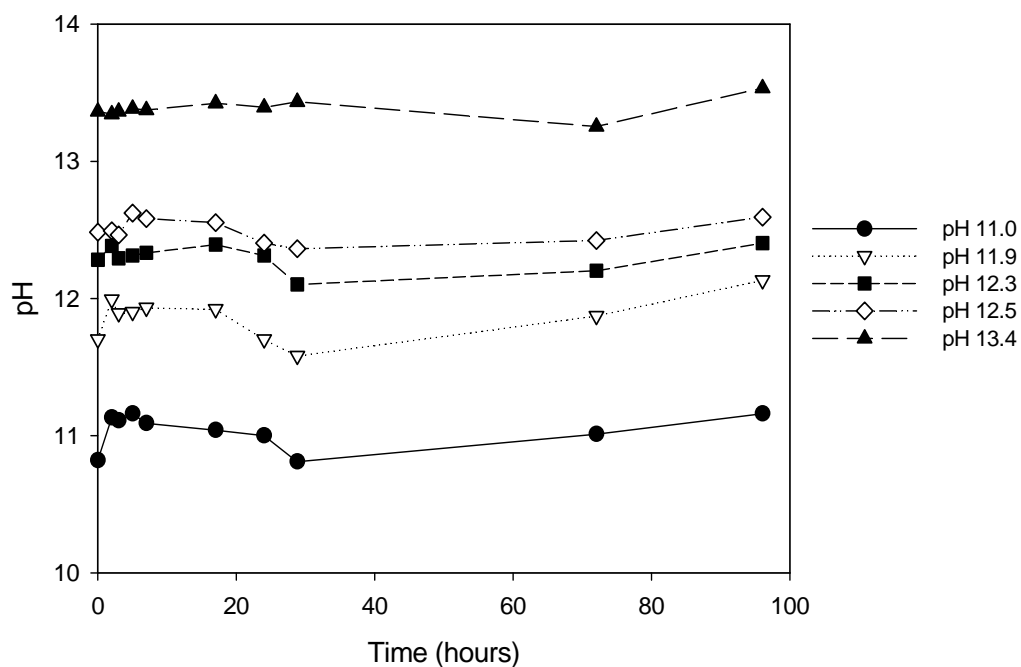
Figure 4.6 Changes in pH during the degradation of 1,1,1-TCA. Lines do not indicate a model fit but are to aid the eye (exp. 11 to 15).
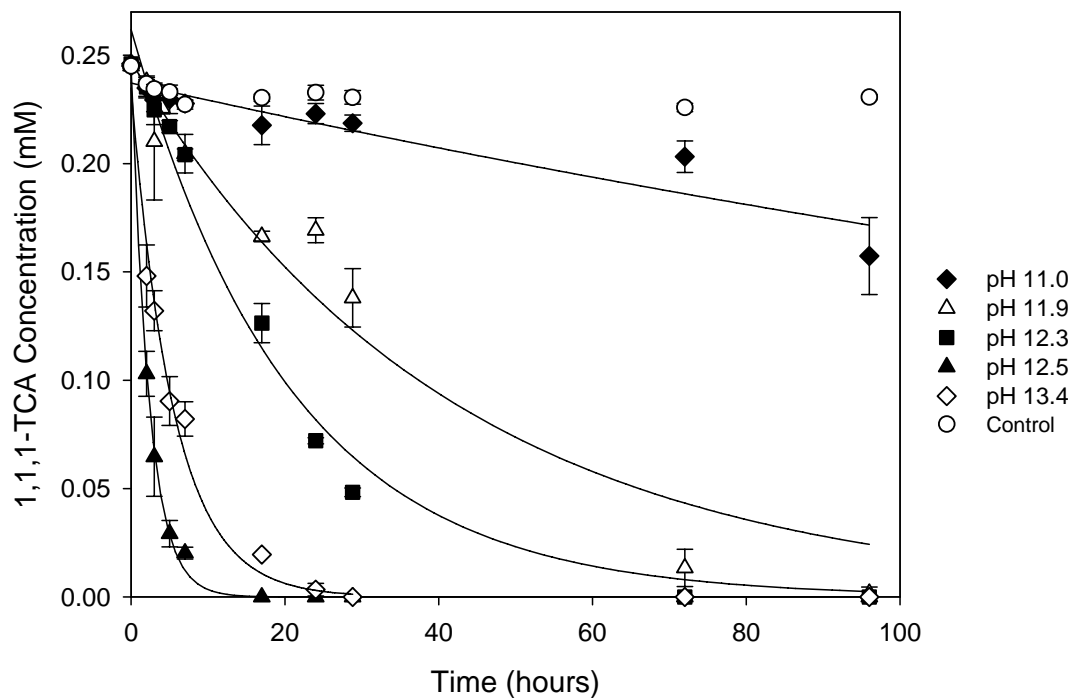
Figure 4.7 Kinetics of 1,1,1-TCA reduction by Fe(II) in 10% cement slurries at various pH. Error bars represent standard deviations of measured concentrations. Some error bars are smaller than the symbols. Solid lines represent fits of a first-order model. $[1,1,1\text{-TCA}]_0 = 0.245$ mM and $[Fe(II)]_0 = 9.8$ mM (exp. 11 to 15).
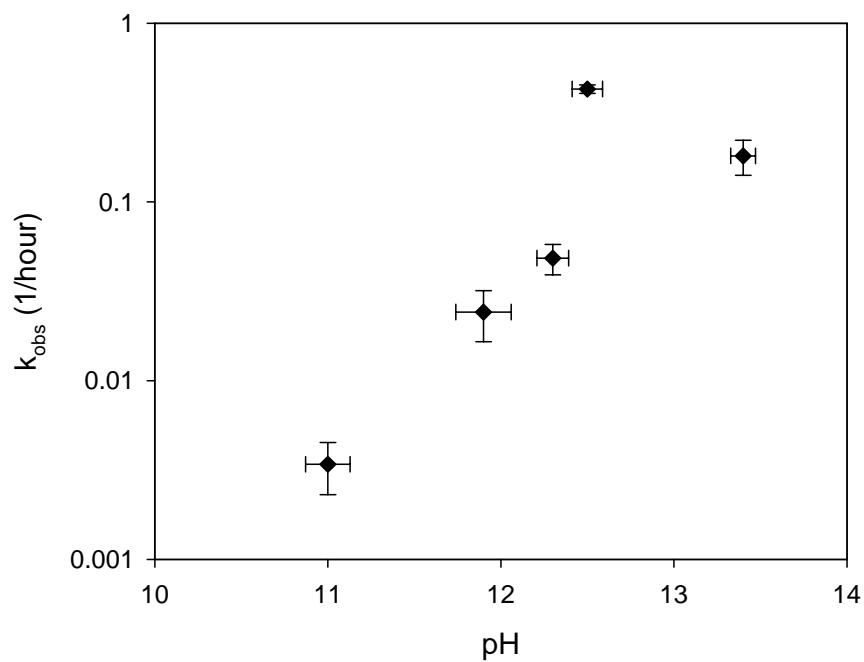
Figure 4.8 Dependence of pseudo-first-order rate constant on pH. Error bars for k_{obs} are 95% confidence intervals. Error bars for pH are ranges of measured pH values. $[1,1,1\text{-}TCA]_0$=0.245 mM and $[Fe(II)]_0$=9.8 mM (exp. 11 to 15).

4.2.3   Effect of Initial Target Organic Concentration

Figure 4.9 shows the kinetics of 1,1,1-TCA degradation when initial 1,1,1-TCA concentration varied between 0.01 mM and 1 mM and Fe(II) dose was 4.9 mM. The rate constants are shown in Table 4.2, exp. 16 to 18. Results of the degradation experiments at each initial concentration were well fitted by a first-order rate law. However, when the initial concentration of 1,1,1-TCA was 1 mM, a second-order rate model fit the data better than the first-order rate model. The parameters of the second-order rate model were estimated from equation 4.11 by nonlinear regression using MATALB.
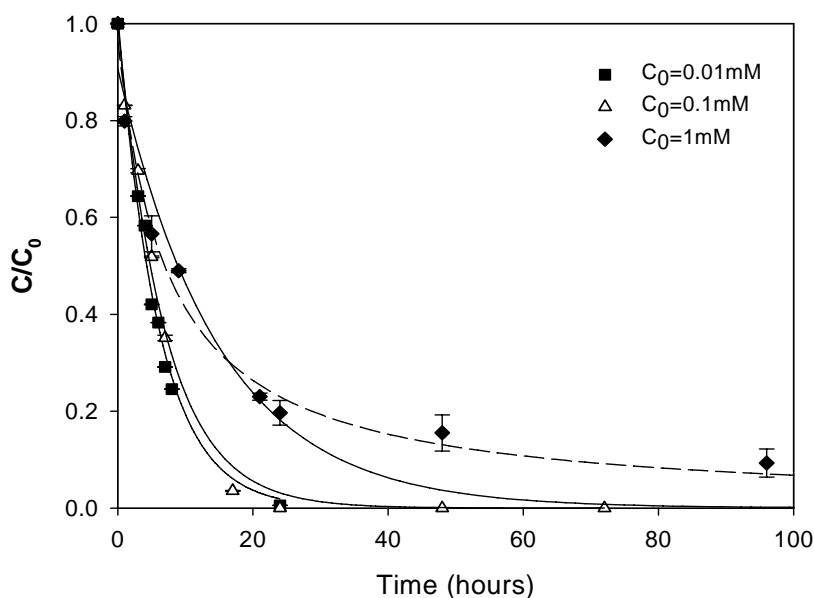
Figure 4.9 The effect of initial 1,1,1-TCA concentration on the dechlorination by Fe(II) in cement slurries. Error bars represent standard deviation of measured concentrations. Some error bars are smaller than the symbols. Solid lines represent fits of first-order rate models. The dotted line represents a fit by a second-order rate model. $[Fe(II)]_0$=4.9 mM (exp 16 to 18).

Figure 4.10 shows that the pseudo-first-order rate constant decreased with increasing initial concentration of 1,1,1-TCA over a range between 0.01 mM and 0.1 mM. This behavior is not consistent with the first-order rate model, which predicts that rate constants are independent of C_{TCA}^0. The behavior shown in Figure 4.10 is consistent with a saturation model. A saturation model is observed when a target organic adsorbs onto surface sites where it then reacts. Dechlorination reactions are expected to occur on surface sites and the process can be described as occurring by the following steps: mass transfer to and sorption of a target organic on the active sites, surface reaction, desorption of products, and mass transfer of products to solution. The saturation model is often called a modified Langmuir-Hinshelwood kinetic model, particularly when it is used to describe reactions on heterogeneous catalysts. Equation 4-18 presents a nonlinear relationship between initial degradation rate (r) and initial target organic concentration. Initial degradation rate (r) was calculated by multiplying the rate constant (k_{obs}) by the initial 1,1,1-TCA concentration (0.01, 0.1, 1.0 mM). As shown in Figure 4.11, initial degradation rate (r) will approach a maximum (r_{max}) at high concentrations. This means that the active sites are fully utilized at high concentration in the solution. At low concentration, degradation rates will be proportional to target organic concentration. The half-saturation constant (K_{TCA}) is a measure of the affinity of the target organic for the surface sites. The values of the constants in equation 4-18 (r_{max}, K_{TCA}) were determined by nonlinear regression to be 0.113 (mM/h) and 0.680 mM, respectively.

$$r = \frac{r_{\max} C_{TCA}{}^0}{K_{TCA} + C_{TCA}{}^0} \qquad (4\text{-}18)$$

where r is the initial degradation rate for 1,1,1-TCA (mM/h), $r_{\max}$ is the maximum degradation rate (mM/h), and K_{TCA} is the half-saturation constant for 1,1,1-TCA (mM).
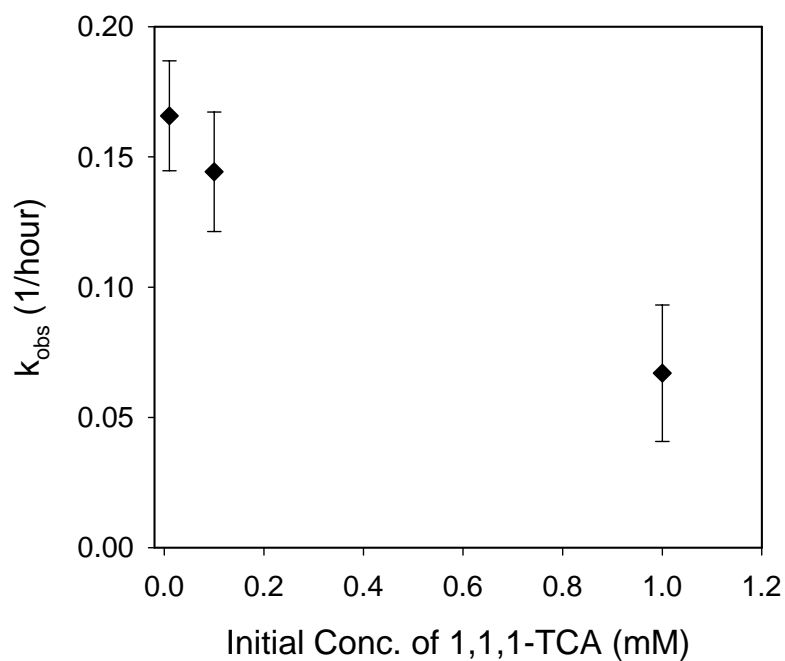
Figure 4.10 The effect of initial concentration on degradation first-order rate constants for degradation of 1,1,1-TCA. Error bars for k_{obs} are 95% confidence intervals. [1,1,1-TCA]$_0$=0.245 mM and [Fe(II)]$_0$=9.8 mM (exp. 16 to 18).
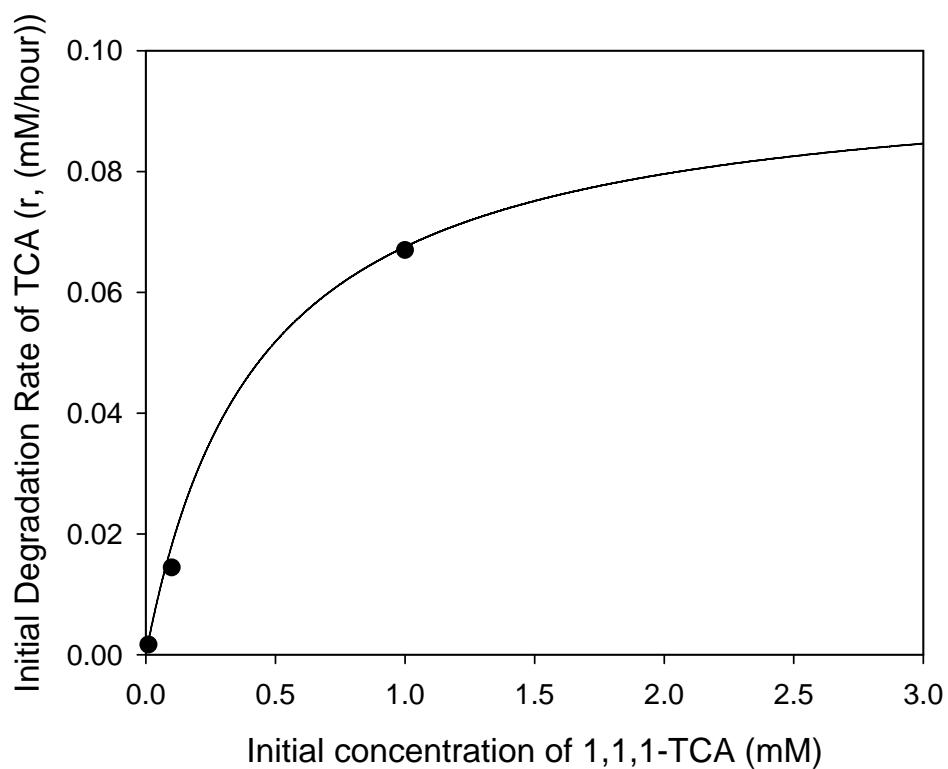
Figure 4.11 Dependence of initial degradation rates on initial concentration of 1,1,1-TCA. The solid line represents fit to a saturation model: $r = \dfrac{r_{max}[C_{TCA}]_0}{K_{TCA} + [C_{TCA}]_0}$, where r_{max} is the maximum degradation rate, $[C_{TCA}]_0$ is the initial concentration of 1,1,1-TCA, r_{max} is 0.113 (mM/hour) and K_{TCA} is 0.680 (mM) (exp. 16 to 18).

4.2.4 Degradation Products of 1,1,1-TCA

A potential transformation pathway of 1,1,1-TCA in DS/S-Fe(II) is shown in Figure 4.12.
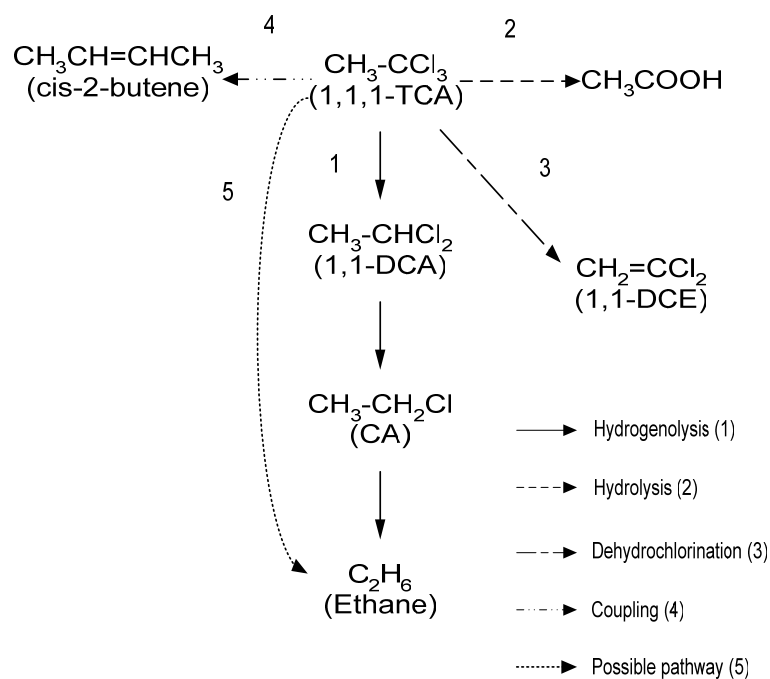
Figure 4.12 Potential transformation pathways of 1,1,1-TCA in Fe(II)/cement system.

Figure 4.12 shows several pathways for transformations of 1,1,1-TCA, including hydrolysis, dehydrochlorination and reductive dechlorination. It is known that the high pH environment of cement-based treatment promotes hydrolysis and dehydrochlorination of chlorinated aliphatic hydrocarbons (67). Acetic acid and 1,1-DCE would be produced by the hydrolysis (2) and the dehydrochlorination (3), respectively. Three

kinds of reductive dechlorination are possible: hydrogenolysis, in which chlorine atoms are replaced by hydrogen atoms; β-elimination, in which two chlorine atoms are removed and an additional carbon-carbon bond formed; and coupling, in which two alkyl groups connect together. Therefore, 1,1,1-TCA could be transformed into 1,1-DCA by hydrogenolysis (1) or into VC by β-elimination and cis-2-butene by coupling (4) (17).

Table 4.3 summarizes the pseudo-first-order rate constants for 1,1,1-TCA disappearance and transformation products of 1,1,1-TCA in cement slurries with Fe(II).

Table 4.3 Experimental conditions and results of transformation products of 1,1,1-TCA by Fe(II) in cement slurries.

exp^a	Fe(II) (mM)	$k_{obs}(min^{-1})^b / n^c$ (Eq. 4-8)	$k_1(min^{-1})^d /n$ (Eq. 4-21 & 4-22)	$t_{1/2}$ (min)^e	Products^f	recovery^g
19	4.9	$0.003(\pm8.8\%)^h/21$	$0.002(\pm7.4\%)^h/42$	~289	1,1-DCA	94.2%
20	9.8	$0.006(\pm9.0\%)/23$	$0.006(\pm6.4\%)/41$	~114	1,1-DCA	97.9%
21	19.6	$0.019(\pm29.7\%)/15$	$0.020(\pm12.8\%)/26$	~35	1,1-DCA/Ethane	95.4%
22	78.4	$0.038(\pm36.8\%)/21$	$0.054(\pm22.8\%)/39$	~13	1,1-DCA	105%

^{a}initial concentration of 1,1,1-TCA was 0.245 mM and the mass ratio of solid to solution was 0.1. $^b k_{obs}$ was calculated from equation 4-8, which considered only disappearance of 1,1,1-TCA. ^{c}the number of data points used in nonlinear regression. $^d k_1$ was calculated from equation 4-21 and 4-22, which considered both disappearance of 1,1,1-TCA and appearance of 1,1-DCA. ^{e}the half-life of 1,1,1-TCA was obtained from the rate constant (k_1). ^{f}major chlorinated product was presented. For only exp. 21, nonchlorinated products were analyzed. ^{g}the recovery was calculated from sum of 1,1,1-TCA and 1,1-DCA to initial 1,1,1-TCA concentration. ^{h}uncertainties represent 95% confidence limits expressed in % relative to estimates for k_{obs} and k_1.

1,1,1-TCA was observed to be rapidly transformed to 1,1-DCA in Fe(II)/cement system. Transformation of 1,1-DCA into other chlorinated products such as CA was not observed over the time period investigated, but a non-chlorinated compound, ethane, was measured. The fact that the concentration of 1,1,1-TCA remained constant in both controls (water, water/cement) and that 1,1-DCA was formed rapidly, indicates that 1,1,1-TCA readily undergoes hydrogenolysis (1). Electrons required for hydrogenolysis would be supplied from compounds formed by the reaction of Fe(II) and cement components. First, the disappearance rate of 1,1,1-TCA was evaluated without considering the formation of 1,1-DCA. The rate constant (k_{obs}) calculated from equation 4-8 was related to Fe(II) dose and compared with the data used in Figure 4.5. The linear relationship shown in Figure 4.5 describes the data well up to a dose of Fe(II) of 39.2 mM. However, a modified Langmuir-Hinshelwood model provided a better fit to the data at higher doses of Fe(II) as shown in Figure 4.13. This saturation behavior where the rate at higher Fe(II) doses approaches a maximum value corresponds to the basic idea of the Langmuir-Hinshelwood model. Second, pseudo first-order rate constant (k_1) for dechlorination of 1,1,1-TCA to 1,1-DCA was calculated from equation 4-21 and 4-22 by nonlinear regression. The results for k_{obs}, k_1 and degradation products of 1,1,1-TCA are shown in Table 4.3.

$$\frac{dC_{TCA,l}}{dt} = -k_1 C_{TCA,l} \tag{4-19}$$

$$\frac{dC_{DCA,l}}{dt} = k_1 C_{TCA,l} \tag{4-20}$$

$$C_{TCA,l} = C_{TCA,l}{}^0 \exp(-k_1 t) \qquad (4\text{-}21)$$

$$C_{DCA,l} = C_{TCA,l}{}^0 * (1 - \exp(-k_1 t)) \qquad (4\text{-}22)$$

Equations 4-21 and 4-22 were obtained by integrating equation 4-19 and 4-20. The data

for the disappearance of 1,1,1-TCA and the formation of 1,1-DCA at various Fe(II) dose

are shown in Figures 4-14 to 4.18.
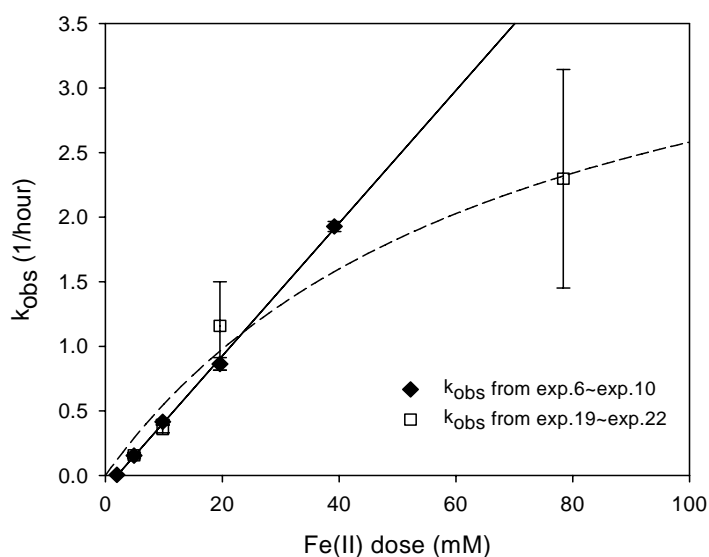
Figure 4.13 Dependence of pseudo-first-rate constants on Fe(II) dose. The solid line is a

linear model and values of rate constants ($\blacklozenge$) are based on data from exp. 6 to 10. The

dotted line is a saturation model and the rate constants ($\square$) are based on the data from

exp. 19 to 22. The saturation model is: $k_{obs} = \dfrac{k_{max}[Fe(II)]_0}{b + [Fe(II)]_0}$, k_{max} is the maximum

pseudo-first-order rate constant, $[Fe(II)]_0$ is the Fe(II) dose, and b is the constant. k_{max} is

4.37 (1/hour), and b is 69.14 (mM).
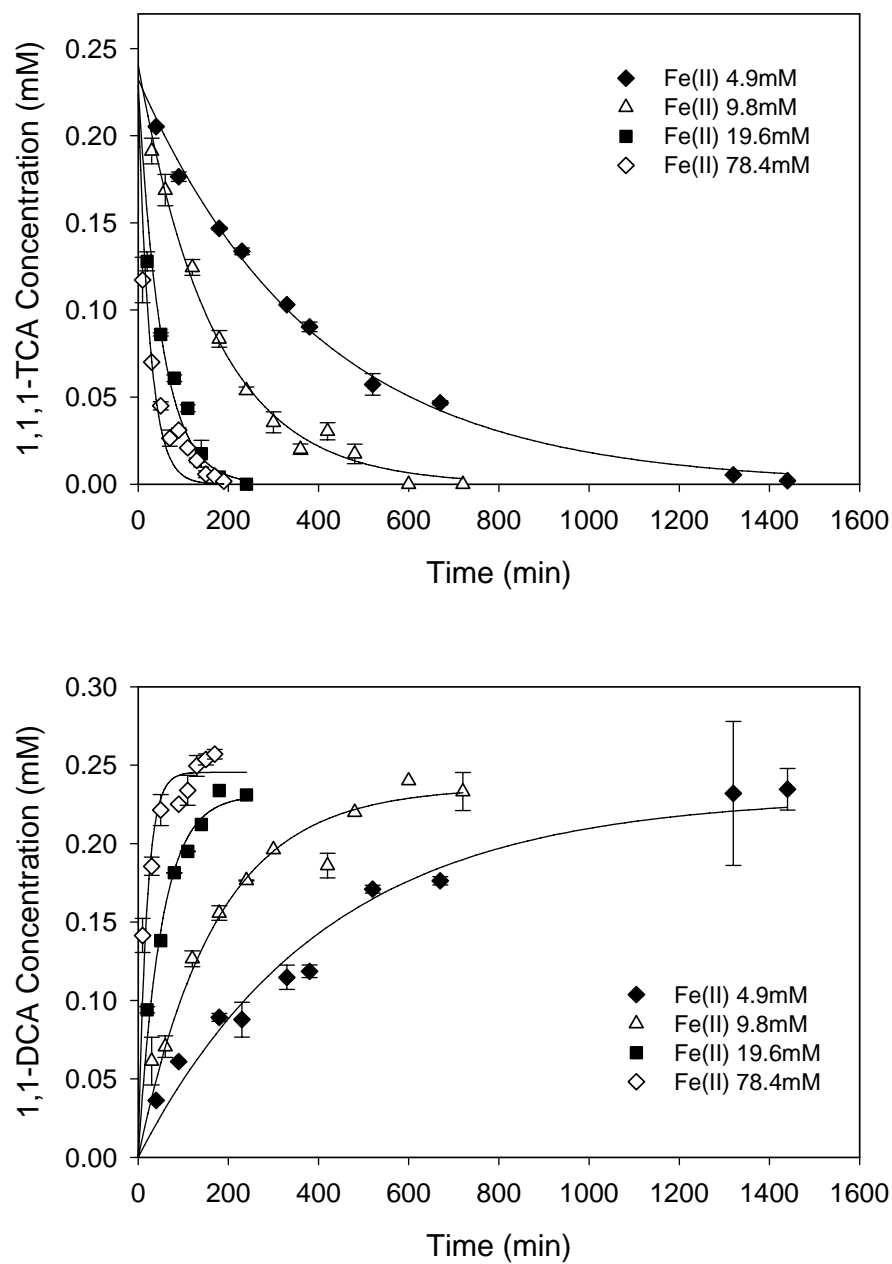
Figure 4.14 The effect of Fe(II) dose on disappearance of 1,1,1-TCA and appearance of 1,1-DCA. Error bars are represented by standard deviation of measured concentrations. Some error bars are smaller than the symbols. Solid lines represent the first-order kinetic model (Equations 4-21 and 4-22). $[1,1,1\text{-}TCA]_0 = 0.245$ mM.
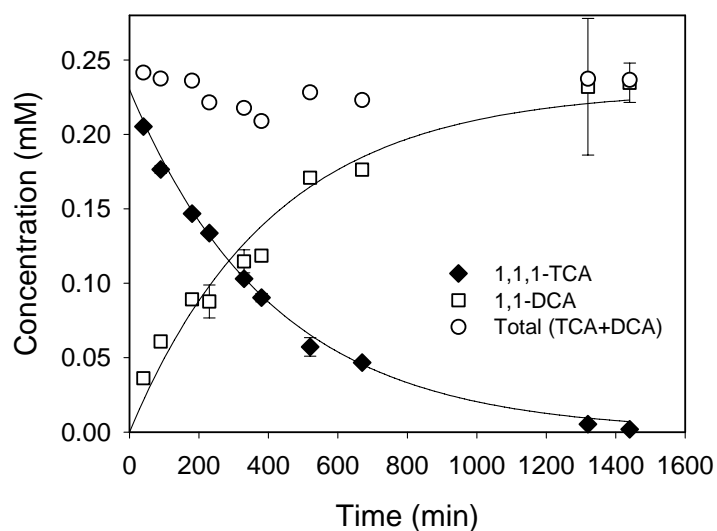
Figure 4.15 Conversion of 1,1,1-TCA to 1,1-DCA by Fe(II) at 4.9 mM in cement slurries with $[1,1,1\text{-TCA}]_0 = 0.245$ mM.
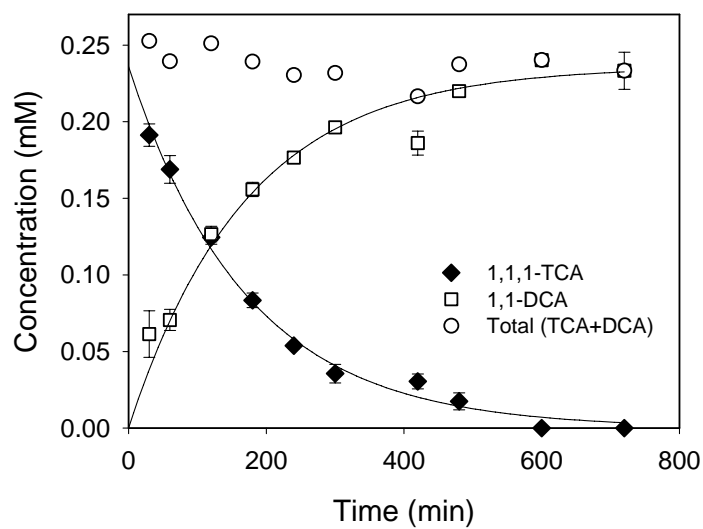
Figure 4.16 Conversion of 1,1,1-TCA to 1,1-DCA by Fe(II) at 9.8 mM in cement slurries with $[1,1,1\text{-TCA}]_0 = 0.245$ mM.
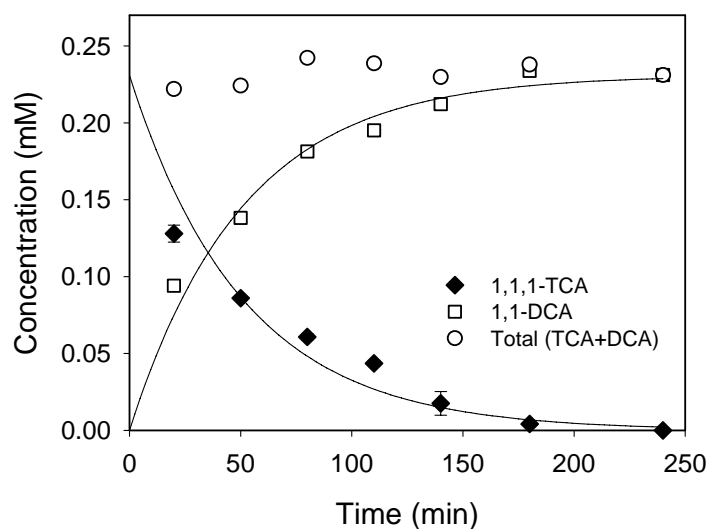
Figure 4.17 Conversion of 1,1,1-TCA to 1,1-DCA by Fe(II) at 19.6 mM in cement slurries with $[1,1,1\text{-TCA}]_0 = 0.245$ mM.
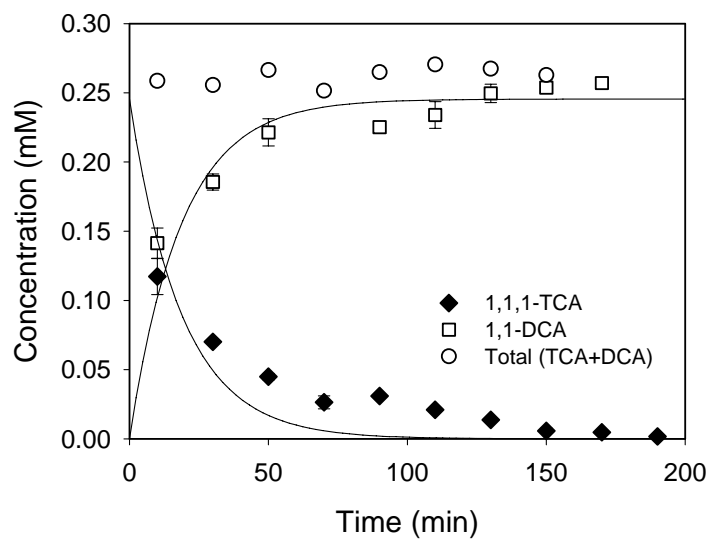
Figure 4.18 Conversion of 1,1,1-TCA to 1,1-DCA by Fe(II) at 78.4 mM in cement slurries with $[1,1,1\text{-TCA}]_0 = 0.245$ mM.

An analysis of non-chlorinated products was conducted for the degradation experiment where the concentration of target organic was 0.245 mM and the dose of Fe(II) was 19.6 mM (exp. 21). The disappearance of 1,1,1-TCA, the formation of primarily 1,1-DCA and a little ethane could be described by a parallel pseudo-first-order degradation model (1,1,1-TCA→1,1-DCA, 1,1,1-TCA→Ethane) or by the sequential pseudo-first-order degradation model (1,1,1-TCA→1,1-DCA→CA→Ethane). The data was analyzed by the parallel pseudo-first-order rate model now and the two models were compared in Chapter VI.

$$1,1,1-TCA \xrightarrow{k_{1,p}} 1,1-DCA \tag{4-23}$$

$$1,1,1-TCA \xrightarrow{k_{2,p}} Ethane \tag{4-24}$$

Both reactions were assumed to be irreversible and first-order with respect to reactants. This mechanism can be described by the following equations from 4-25 to 4-27:

$$\frac{dC_{TCA,l}}{dt} = -k_{1,p}C_{TCA,l} - k_{2,p}C_{DCA,l} \tag{4-25}$$

$$\frac{dC_{DCA,l}}{dt} = k_{1,p}C_{TCA,l} \tag{4-26}$$

$$\frac{dC_{Ethane}}{dt} = k_{2,p}C_{TCA,l} \tag{4-27}$$

$$C_{TCA,l} = C_{TCA,l}{}^0 \exp(-(k_{1,p} + k_{2,p})t) \qquad (4\text{-}28)$$

$$C_{DCA,l} = \frac{k_{1,p} C_{TCA,l}{}^0}{k_{1,p} + k_{2,p}}\{1 - \exp(-(k_{1,p} + k_{2,p})t)\} \qquad (4\text{-}29)$$

$$C_{Ethane} = \frac{k_{2,p} C_{TCA,l}{}^0}{k_{1,p} + k_{2,p}}\{1 - \exp(-(k_{1,p} + k_{2,p})t)\} \qquad (4\text{-}30)$$

where $k_{1,p}$ is the pseudo-first-order rate constant for dechlorination of 1,1,1-TCA to 1,1-DCA and $k_{2,p}$ is the pseudo-first-order rate constant for dechlorination of 1,1,1-TCA to ethane. The results of nonlinear regressions using equations 4-28 to 4-30 to obtain these parameters are presented in Table 4.4. The parallel reaction mechanism provides a good fit to the data of the disappearance of 1,1,1-TCA and formation of 1,1-DCA and ethane as shown in Figure 4.19. The pseudo first-order rate constant for disappearance of 1,1,1-TCA ($k_{1,p}+k_{2,p}$) was 0.021 min^{-1} and the rate constants for 1,1-DCA and ethane formation were 0.020 min^{-1}, and 0.001 min^{-1}, respectively.

Table 4.4 Kinetics of 1,1,1-TCA transformation by a parallel reaction pathway[a].

Parameters	Values calculated by nonlinear regression
$C_{TCA,l}{}^0$	0.238 (mM) ($\pm$4.4%)[b]
$k_{1,p}$	0.020 (min^{-1}) ($\pm$10.5%)
$k_{2,p}$	0.001 (min^{-1}) ($\pm$82.4%)

[a]data are from exp. 16.

[b]uncertainties represent 95% confidence limits expressed in % relative to estimates of $C_{TCA,l}{}^0$, $k_{1,p}$, $k_{2,p}$.
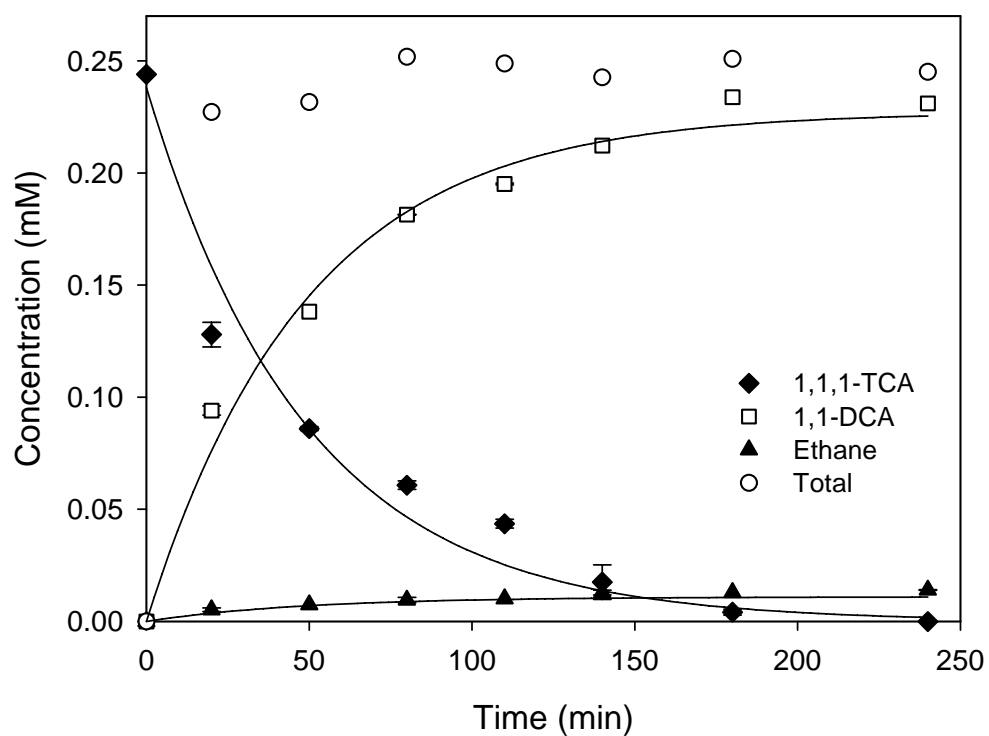
Figure 4.19 Degradation of 1,1,1-TCA by Fe(II) in cement slurries and formation of products. Error bars are represented by the standard deviations of measured concentrations. Some error bars are smaller than the symbols. The solid line is fitted with the model assuming a parallel reaction pathway: 1,1,1-TCA→1,1-DCA and 1,1,1-TCA→Ethane, $[1,1,1\text{-TCA}]_0$=0.245 mM.

4.3   1,1,2,2-Tetrachloroethane

Batch kinetic experiments with 1,1,2,2-TetCA were conducted to study the influence of Fe(II) dose, pH and initial target organic concentration on degradation kinetics. It is known that polychlorinated alkanes undergo dehydrochlorination under neutral or high pH conditions (67). 1,1,2,2-TetCA was observed to be completely and rapidly degraded into TCE[*] in the control that contained cement but not as rapidly as in reactors that contained Fe(II). Even in the control that contained only water, approximately 35% of 1,1,2,2-TetCA was degraded over a reaction time of 40 days (Figure 4.20). Therefore, the focus of research on the degradation of 1,1,2,2-TetCA was shifted to investigate the kinetics of TCE[*] dechlorination because 1,1,2,2-TetCA was completely transformed to TCE[*] within 1 hour in reactors that contained cement.
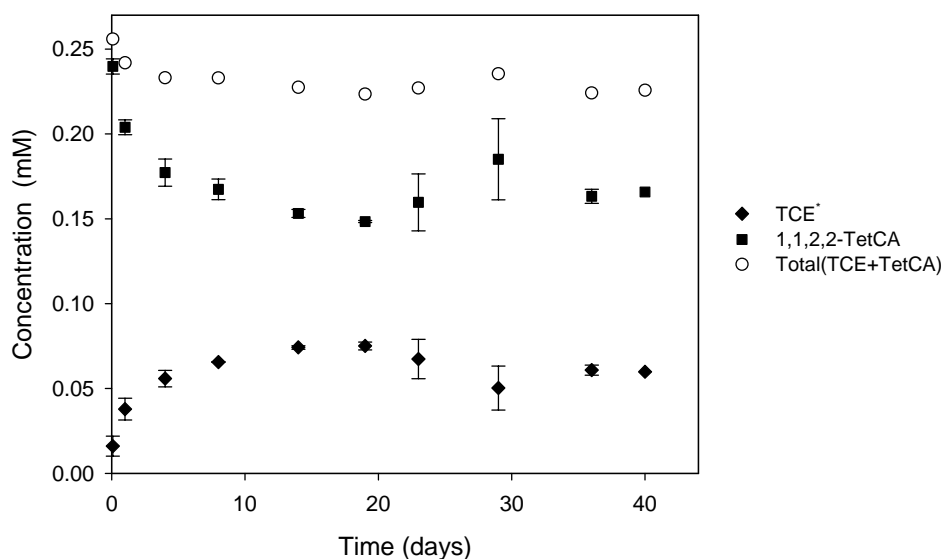
Figure 4.20 Dehydrochlorination of 1,1,2,2-TetCA to TCE[*] in water. TCE[*] represents the TCE produced in this reaction.

Table 4.5 shows the results of pseudo-first-order rate constants for dechlorination of TCE[*] produced by 1,1,2,2-TetCA transformation in Fe(II)/cement system.

Table 4.5 Pseudo first-rate constants of dechlorination of TCE[*] produced by 1,1,2,2-TetCA transformation at various conditions.

exp	solid[a]	C_0[b] (mM)	Fe(II)[c] (mM)	pH	k_{obs} (day^{-1})[d]	n[f]
23	Cement	0.245	39.2	~12.5	0.007(±41.5%)[e]	24
24	Cement	0.245	98	~12.4	0.046(±19.6%)	30
25	Cement	0.245	196	~12.0	0.088(±27.1%)	31
26	Cement	0.245	196	pH 10.6	0.010(±84.3%)	20
27	Cement	0.245	196	pH 11.5	0.008(±106%)	22
28	Cement	0.245	196	pH 12.1	0.044(±16.2%)	20
29	Cement	0.245	196	pH 12.3	0.019(±20.6%)	23
30	Cement	0.245	196	pH 13.3	0.016(±25.3%)	23
31	Cement	0.01	196	~pH 12.0	0.456(±33.9%)	21
32	Cement	0.1	196	~pH 12.0	0.185(±25.1%)	22
33	Cement	1	196	~pH 12.0	0.019(±16.6%)	25

[a]mass ratio of solid to solution was 0.1.

[b]the initial concentration of 1,1,2,2-TetCA that was added to the reactors.

[c]source of Fe(II) was FeCl$_2$. [d]k_{obs} is the pseudo first-order rate constant for dechlorination of TCE[*] that was produced from 1,1,2,2-TetCA transformation.

[e]uncertainties represent 95% confidence limits expressed in % relative to the estimate for k_{obs}.

[f]the number of data points used in the nonlinear regression.

4.3.1 Effect of Fe(II) Dose

Reductive kinetics of TCE[*] produced by 1,1,2,2-TetCA degradation was generally represented by a first-order kinetic model. A second-order kinetic model (Equation 4-14) was applied to the experiment where the concentrations of 1,1,2,2-TetCA and Fe(II) are 0.245 mM and 39.2 mM, respectively. Figure 4.21 shows the concentrations of TCE[*] produced by degradation of 1,1,2,2-TetCA in 10% cement slurries at three different Fe(II) doses. Pseudo-first-order rate constants for these experiments are presented in Table 4.5 (exp. 23~25) and are plotted against Fe(II) dose in Figure 4.22. This figure shows a linear relationship between a pseudo first-order rate constant and Fe(II) doses up to a dose of 196 mM. However, a saturation relationship between rate constants and Fe(II) dose is expected at much higher Fe(II) doses than was investigated, because similar behavior was observed for 1,1,1-TCA. A saturation relationship occurs because the amount of cement that is available is limited, so the amount of the active reductant that can be formed by Fe(II) and cement hydration product components will be limited, even as Fe(II) dose increases. Therefore, active surface sites available for TCE[*] transformation will reach a maximum as Fe(II) dose is increased.

Zero-order, first-order, and second-order rate models were applied to fit the data of exp. 23, 24 and 25 and the models with lower sum of squares errors were selected. The pseudo-first-order rate model for Fe(II) 98 mM and 196 mM and pseudo-second-order rate model for Fe(II) 39.2 mM were the models with the lowest sum of squares and the predictions of these models are shown as the lines in Figure 4.21.

Table 4.6 presents different rate constants for dechlorination kinetics of TCE[*] produced by 1,1,2,2-TetCA transformation at various Fe(II) doses. The rate constants of the controls were 9%, 2% and 0.6% of those for reactors with Fe(II) doses of 39.2 mM, 98 mM and 196 mM, respectively. The pseudo-first-order rate constant corrected only for the control (k_{obs}') was calculated by subtracting $k_{obs,control}$ from k_{obs}. The pseudo first-order rate constant corrected for both the control and for partitioning (k) was obtained by multiplying the partitioning factor (*p*) times the observed pseudo first-order rate constant (k_{obs}). The value of the dimensionless Henry's constant for TCE used was 0.419 (35). The values of V_g, V_l, and K_s used were 0.3 ml, 23 ml and 0.031. The solid phase partition coefficient (K_s) was determined as an average of K_s values calculated from controls for three experiments (exp. 23, 24 and 25). The value of the partitioning factor (*p*) for TCE[*] was calculated by equation 4-4 and was 1.04.

Table 4.6 Corrected pseudo-first-order rate constants for dechlorination of TCE[*] produced by 1,1,2,2-TetCA degradation in Fe(II)/cement system.

Exp	k_{obs} [a] (day^{-1})	k_{obs}' [b] (day^{-1})	$k_{obs,Fe(II)}$ [c] (day^{-1}·mM^{-1})	k [d] (day^{-1})
23	0.0067(±41.5%)	0.0061	2E-4	0.0070
24	0.0457(±19.6%)	0.0448	5E-4	0.0475
25	0.0881(±27.1%)	0.0876	4E-4	0.0916

[a]pseudo first-order rate constant from Equation 4-8 (k_{obs}). [b]pseudo-first-order rate constant corrected only for control ($k_{obs}'=k_{obs}-k_{obs,control}$). [c]pseudo-first-order rate constant normalized by Fe(II) dose ($k_{obs,Fe(II)}=k_{obs}/[Fe(II)]$). [d]pseudo-first-order rate constant corrected for control and for partitioning ($k=p*k_{obs}$, p=1.04).
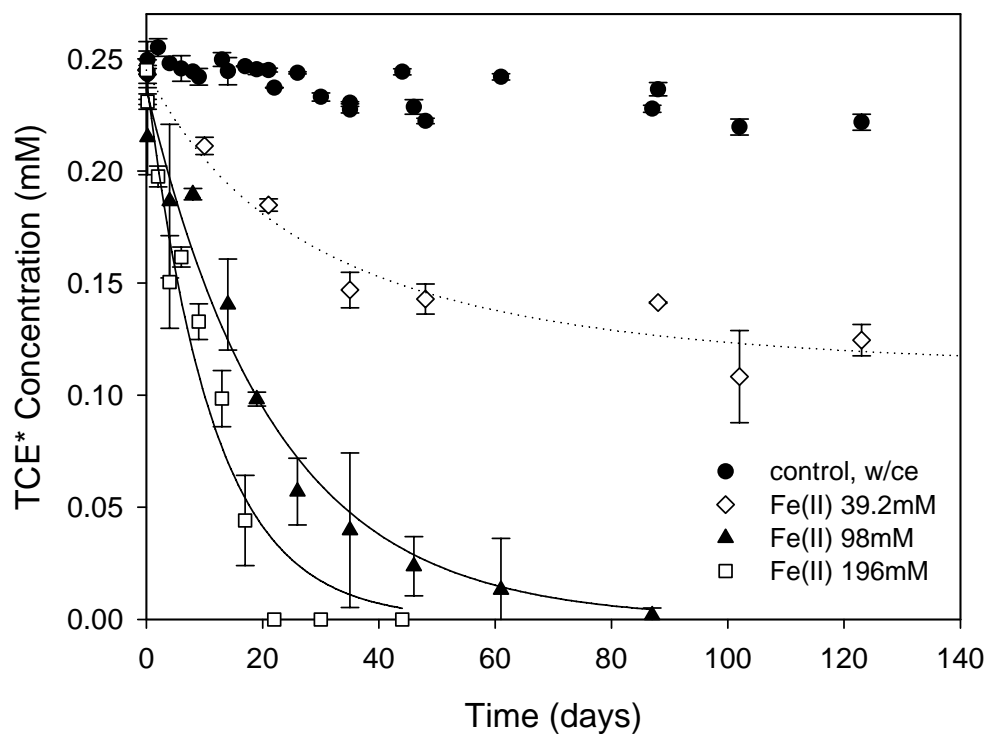
Figure 4.21 Effect of Fe(II) dose on kinetics of degradation of TCE* produced by transformation of 1,1,2,2-TetCA in 10% cement slurries. Error bars are the standard deviations of measured concentrations. Some error bars are smaller than the symbols. Solid lines are for the first-order model (Equation 4-8) and dotted line is for the second-order model (Equation 4-14).
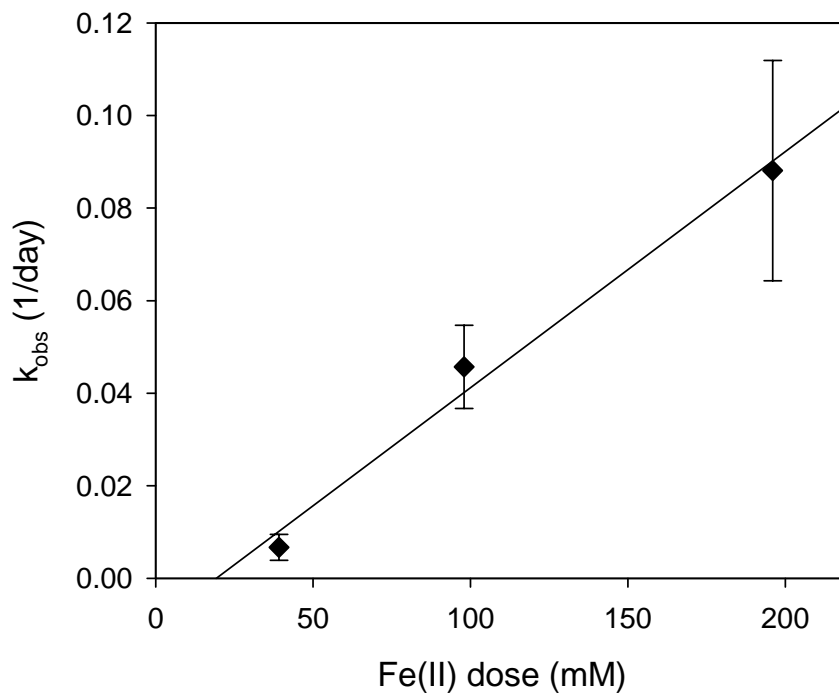
Figure 4.22 Dependence of pseudo-first-order rate constant of TCE[*] dechlorination on Fe(II) dose. Error bars represent 95% confidence intervals for predicted rate constants. Solid line is fitted by linear regression. The linear equation is k_{obs}=-0.0098+0.0005[Fe(II)] (R^2=0.9858).

4.3.2   Effect of pH

The effect of pH on kinetics of dechlorination TCE[*] was investigated at five nominal pH (pH 10.6, 11.5, 12.1, 12.3 and 13.3). The nominal pH was determined as the average value of measured pH, excluding the smallest value. The smallest pH value was excluded because it appears to be an outlier caused by incomplete mixing at the initial reaction time. Figure 4.23 represents the pH changes measured at every sampling point. During these experiments, pH changes were monitored over time. At nominal pH 10.6, pH was maintained within ±0.2 pH unit after reaction time of 3 days. At nominal pH 11.5, pH measured after 6 days was kept within ±0.3 pH unit. Experiments at nominal pH of 12.3 and 13.3 showed a constant pH until a reaction time of approximately 10 days. At that time, pH decreased by about 1.5 pH units and then increased. The experiment at a nominal pH 12.1 did not include additions of any acid and base solutions and it showed that pH was maintained at approximately about 12.1 and then pH was decreased to pH 11.1 after a reaction time of 17 days. Changes in pH could cause changes in the concentration or type of reactive solids that are able to reduce chlorinated organics, so changes in pH could influence dechlorination kinetics.

Figure 4.24 shows the effect of pH on degradation of TCE[*]. The relation between k_{obs} and pH is shown in Figure 4.25. The maximum value of the rate constant occurs around pH 12.1 at a Fe(II) dose of 196 mM in 10% cement slurries.
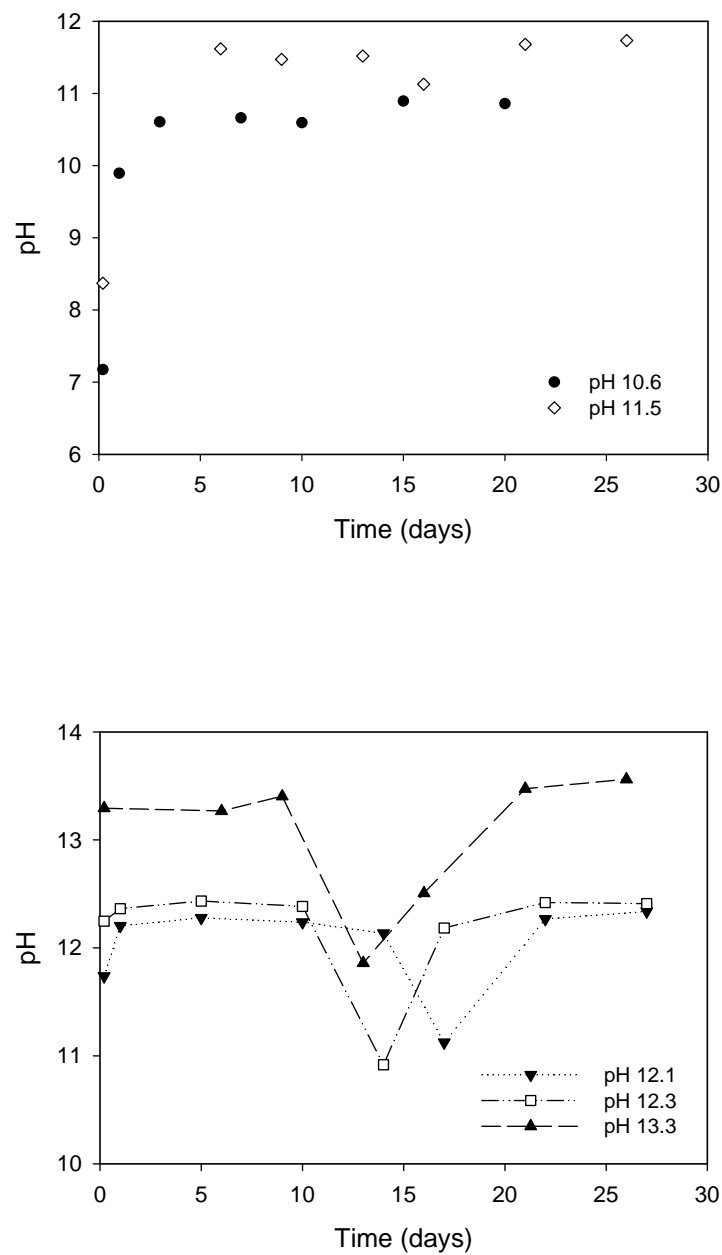
Figure 4.23 pH changes during experiments on degradation of 1,1,2,2-TetCA. Lines do not indicate a model fit but are used to help guide the eye.
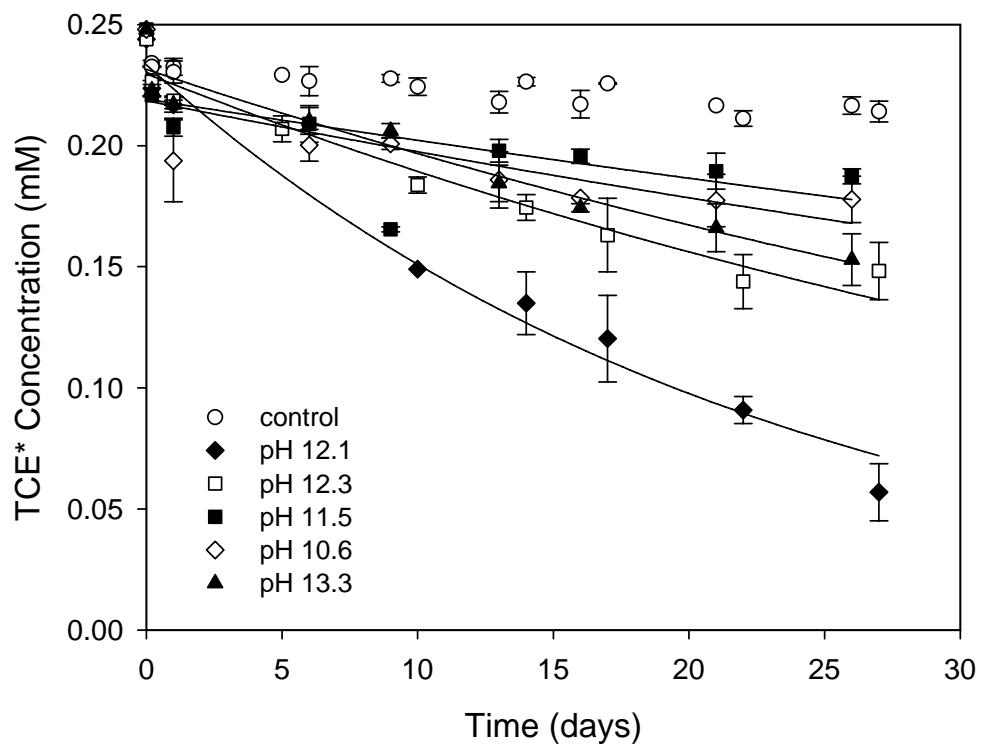
Figure 4.24 Concentrations of TCE* in 10% cement slurries with Fe(II) at various pH. Error bars are ranges of measured TCE* concentrations. Some error bars are smaller than the symbols. Solid lines represent first-order reaction fits. $[1,1,2,2\text{-TetCA}]_0 = 0.245$ mM, $[Fe(II)]_0 = 196$ mM
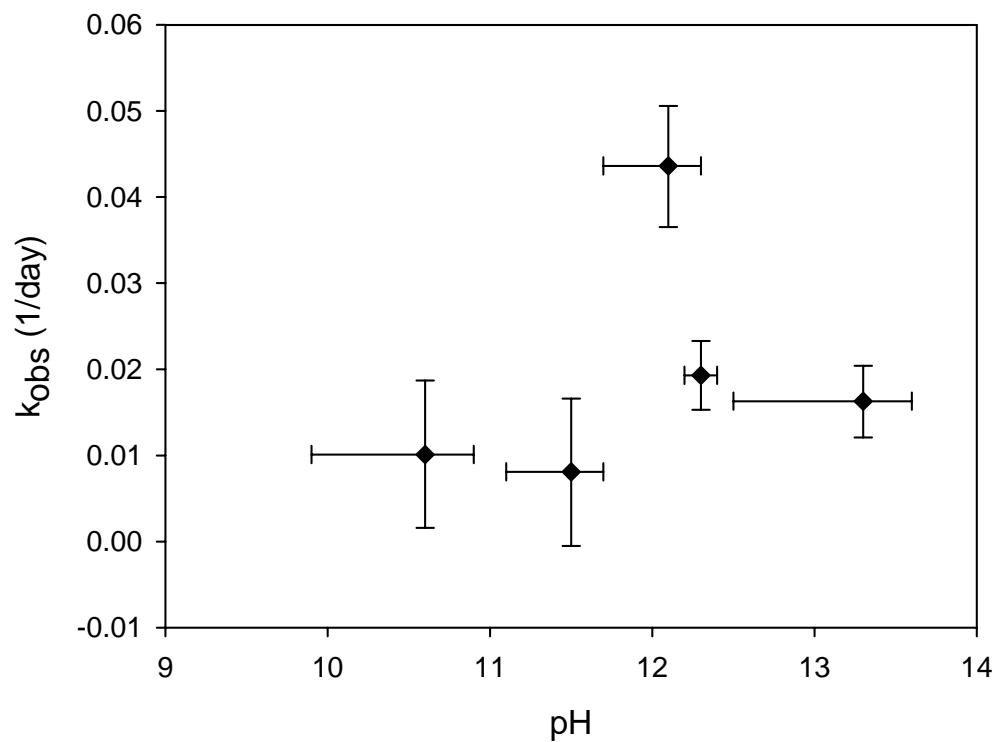
Figure 4.25 Dependence on pH of pseudo-first-order rate constants for reduction of TCE[*] produced in 1,1,2,2-TetCA transformation. Error bars for k_{obs} are 95% confidence intervals. Error bars for pH are ranges of measured pH values with the minimum pH value excluded.

Experiments to evaluate the effect of pH on the dechlorination of TCE[*] were conducted at two different doses of Fe(II) (98 mM and 196 mM). The rate constant measured for the control was large when the concentration of Fe(II) was 98 mM, so the pseudo-first-order rate constants corrected only for the control were compared for experiments with Fe(II) doses of 98 mM and 196 mM. The data used in this comparison are shown in Table 4.7. This comparison is made in Figure 4.26, which shows that the optimum pH for both Fe(II) doses is in the range of pH 12.0 to 12.4.

Table 4.7 Pseudo first-order rate constants and pseudo first-order rate constants corrected for the control obtained in experiments on effect of pH on degradation of 1,1,2,2-TetCA.

Fe(II) 98 mM		Fe(II) 196 mM	
pH	$k_{obs}{}^a/k_{obs}{}'^b$	pH	$k_{obs}{}^a/ k_{obs}{}'^b$
10.7	$0.006(\pm196\%)^c/0.003$	10.6	$0.010(\pm84.30\%)/0.007$
11.8	$0.035(\pm42.7\%)/0.032$	11.5	$0.008(\pm106\%)/0.005$
12.4	$0.062(\pm35.8\%)/0.057$	12.1	$0.044(\pm16.2\%)/0.041$
12.8	$0.016(\pm50.3\%)/0.011$	12.3	$0.019(\pm20.6\%)/0.016$
13.3	$0.018((\pm45.3\%)/0.012$	13.3	$0.016(\pm25.3\%)/0.013$

[a]pseudo-first-order rate constant from equation 4-8.

[b]pseudo-first-order rate constant corrected by control ($k_{obs}'=k_{obs}-k_{obs,control}$).

[c]uncertainties represent 95% confidence limits expressed in % relative to estimate for $k_{obs.}$
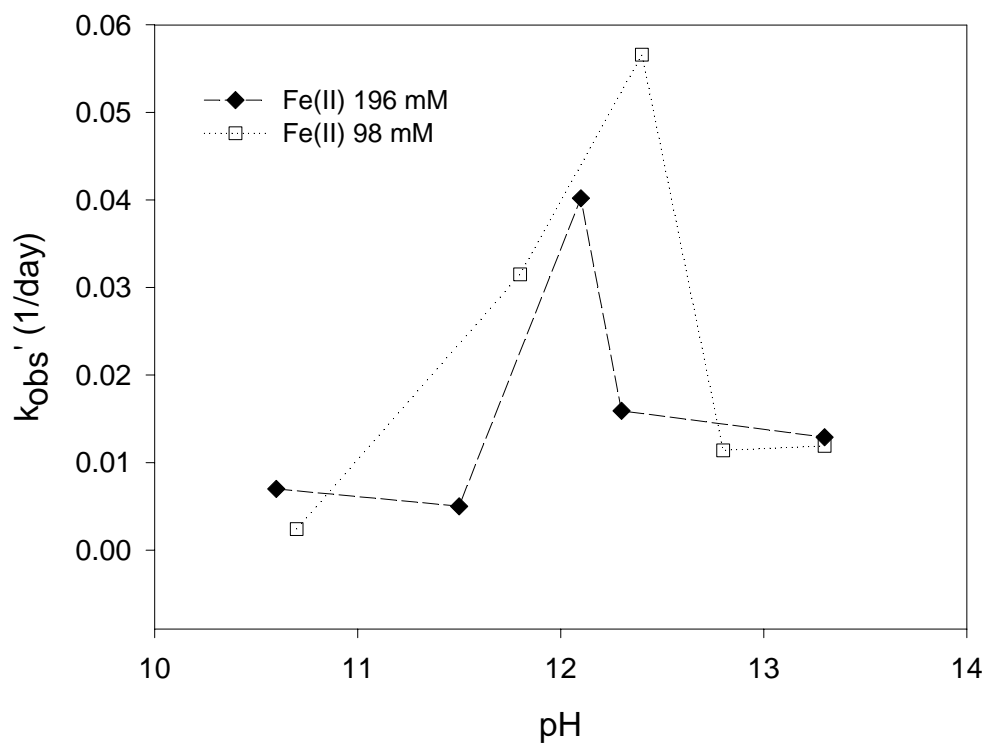
Figure 4.26 Dependence on pH of pseudo first-order rate constants corrected for the control at two different doses of Fe(II). Lines do not indicate a model fit but are used to help guide to eye.

4.3.3   Effect of Initial Target Organic Concentration

The effect of initial 1,1,2,2-TetCA concentration on the reductive dechlorination of TCE* in Fe(II)/cement system was investigated at concentrations of 0.01 mM, 0.1 mM and 1 mM. The concentration of Fe(II) was 196 mM and pH was approximately 12.1. Although 1,1,2,2-TetCA is the target organic, it was completely transformed to TCE* within less than 1 hour, so that the initial concentration of 1,1,2,2-TetCA and TCE* was treated as the same. The kinetic parameters for a first-order rate model are presented in Table 4.5. Figure 4.27 shows that a pseudo-first-order kinetic model fits well the normalized concentrations of TCE* (C/C_0) at four different initial concentrations. The result of exp.25 was included in this analysis.

A plot of pseudo-first-order rate constants for dechlorination of TCE* are shown as a function of initial TCE* concentration in Figure 4.28. The first-order rate model predicts that the rate constants should be independent of the initial target organic concentration, but this is not observed in Figure 4.28. This kind of behavior was also observed for 1,1,1-TCA degradation. The Langmuir-Hinshelwood kinetic model is generally used to describe many catalytic reactions and it assumes that all reactants adsorb onto the surface and they react on the surface. The hypothesis of this study that reactions of target organic compounds would occur on the active solid surface sites corresponds to the basic assumptions of the Langmuir-Hinshelwood kinetic model and appears to apply to both 1,1,1-TCA and TCE* produced by 1,1,2,2-TetCA transformation.

Figure 4.29 presents the relationship between initial degradation rates for TCE[*]

and initial target organic concentration between 0.01 mM and 1 mM. Nonlinear

regression on the data shown in Figure 4.29 gives $r_{max} = 0.022$ (mM/day) and $K_{TCE} =$

0.026 (mM). At very low initial target organic concentrations, the degradation rate

increases proportionally to concentrations, but the rate begins to decrease at higher

concentrations, approaching a maximum. This saturation behavior is also typical for

enzyme-catalyzed reactions (84). The half-saturation constant in enzyme reactions (K)

represents the affinity between the substrate and the enzyme. Similarly, the half-

saturation constant for dechlorination of TCE[*] or 1,1,1-TCA in slurries of cement with

Fe(II) is a parameter that indicates the affinity between surface sites and target organics.

Lower value of the half-saturation constant for TCE[*] ($K_{TCE} = 0.026$ mM) compared to

that for 1,1,1-TCA ($K_{TCA} = 0.68$ mM) indicates a stronger affinity of TCE for the surface,

which results in the maximum rate being reached at a relatively lower initial

concentration.
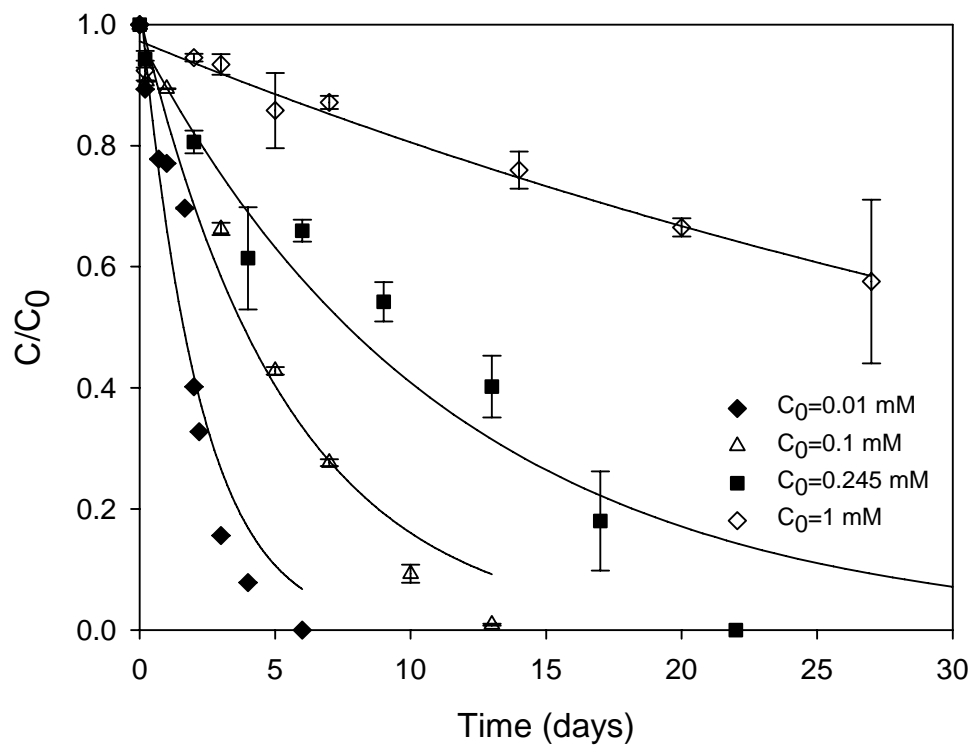
Figure 4.27 Effect of initial target concentration on degradation of TCE[*] produced by transformation of 1,1,2,2-TetCA. Error bars are standard deviations of measured concentrations. Some error bars are smaller than the symbols. Solid lines show predictions of a first-order kinetic model, (exp.25 and exp.31-33).
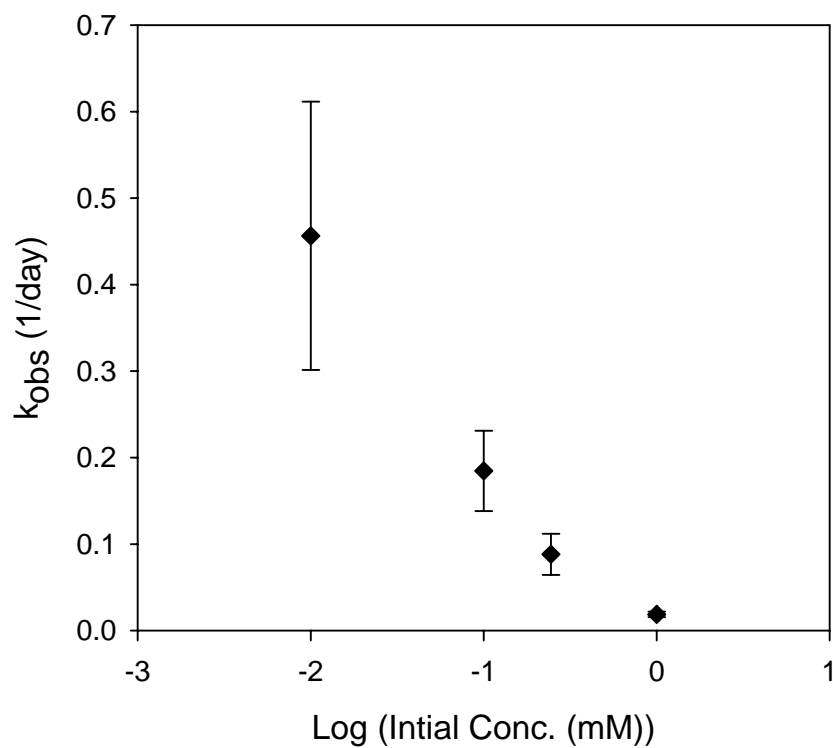
Figure 4.28 Influence of initial 1,1,2,2-TetCA concentration on degradation kinetics of TCE[*] produced by 1,1,2,2-TetCA transformation. (exp.25 and exp.31-33).
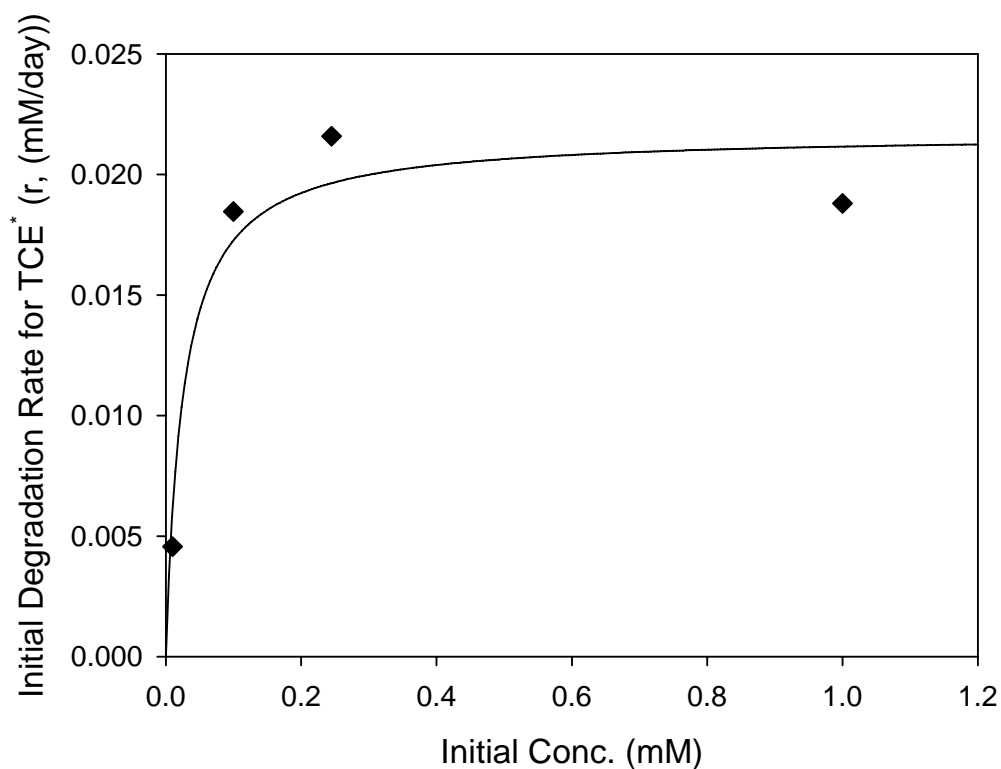
Figure 4.29 Dependence of initial degradation rate on initial concentration of TCE[*] produced by 1,1,2,2-TetCA transformation. Initial degradation rate (r) is a product of pseudo first-order rate constant and initial target organic concentration ($r = k_{obs} \times C_{TCE}^0$). r_{max} is the maximum initial degradation rate and K_{TCE} is the half-saturation constant for TCE[*]. The solid line shows the predictions of a saturation model: $r = r_{max}C_{TCE}^0/(K_{TCE}+C_{TCE}^0)$ where r_{max} is 0.022 mM/day and K_{TCE} is 0.026 mM. (exp.25 and exp.31-33).

4.3.4   Degradation Products of 1,1,2,2-TetCA

Potential transformation pathways for 1,1,2,2-TetCA in DS/S systems can be described as shown in Figure 4.30.
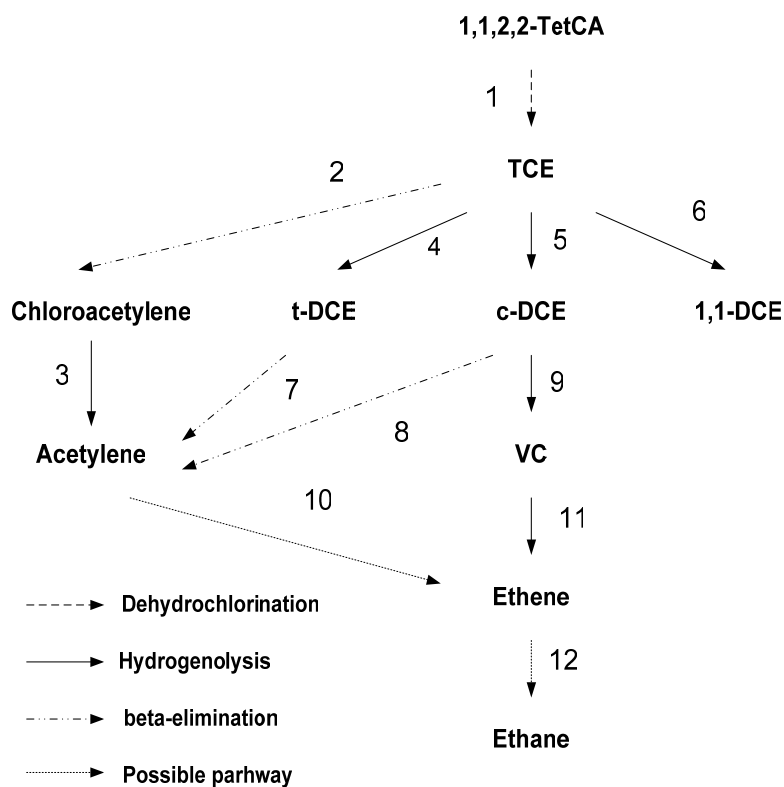
Figure 4.30 Possible pathways of 1,1,2,2-TetCA degradation in Fe(II)/cement system. Reaction 1 corresponds to the dehydrochlorination pathway. Reactions 3, 4, 5, 6, 9 and 11 are parts of the hydrogenolysis pathway. Reactions 2, 7 and 8 are parts of the reductive β-elimination pathway. Reactions 10 and 12 are hydrogenation reactions.

First, 1,1,2,2-TetCA rapidly transformed to TCE* by dehydrochlorination, which is a non-reductive reaction (pathway 1). The TCE* that is produced can undergo two major reductive dechlorination pathways, i.e., hydrogenolysis and beta-elimination. During degradation of 1,1,2,2-TetCA, only chlorinated compounds such as 1,1-DCE, c-DCE, t-DCE, VC were monitored over time by GC/FID (pathway 4, 5, 6 and 9). Peaks for these compounds were observed during analysis, but they represented negligible concentrations, although the peak area for c-DCE and t-DCE was larger than that of 1,1-DCE. It has been reported that the major product of PCE and TCE degradation by Fe(II) in cement slurries is acetylene (47, 69). This indicates that the major product of reductive dechlorination of TCE* produced from 1,1,2,2-TetCA would also be acetylene. Acetylene can be formed from chloroacetylene by hydrogenolysis or from t-DCE or c-DCE by β-elimination. It has been reported that the rates of formation of acetylene and VC during reduction of TCE by Zn(0) were constant over time compared to the rate of production of DCEs. It was also reported that degradation of chloroacetylene by Zn(0) was very rapid, so that there was no detectable accumulation of chloroacetylene (71). These results indicate that degradation of TCE* produced by transformation of 1,1,2,2-TetCA will follow a β-elimination pathway to produce acetylene, with chloroacetylene as an intermediate that does not accumulate (pathway 2 and 3). Hydrogenolysis might occur to a limited extent in parallel with β-elimination and result in formation of ethylene or ethane as minor products.

4.4   1,2-Dichloroethane

The DS/S-Fe(II) process effectively transformed chlorinated ethanes (1,1,1-TCA, 1,1,2,2-TetCA) in this study. Other research has shown that it effectively degrades chlorinated ethenes (PCE, TCE, DCEs, VC) and chlorinated methanes (CT, CF) (47, 49, 69). Batch kinetic experiments were conducted at two different Fe(II) concentrations (39.2 mM and 196 mM) to evaluate its ability to degrade 1,2-DCA at an initial concentration of 0.245 mM. However 1,2-DCA was not degraded by Fe(II) in cement slurries as is shown in Figure 4.31 and Figure 4.32. The nonreactive properties of 1,2-DCA were also observed in experiment using green rust alone, as well as with mixtures of green rust and Ag and Cu (33).
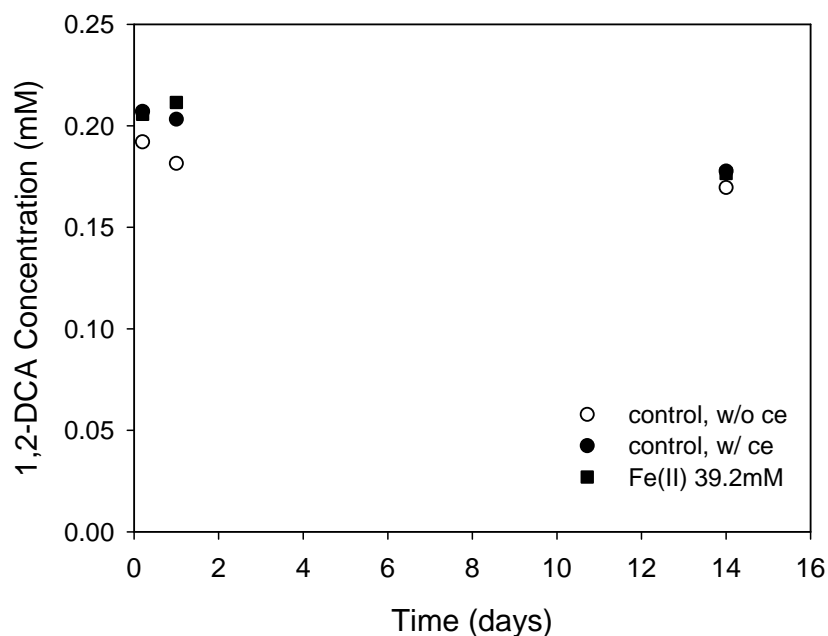
Figure 4.31 Concentration of 1,2-DCA in 10% cement slurries with 39.2 mM Fe(II). $[1,2\text{-DCA}]_0 = 0.245$ mM.
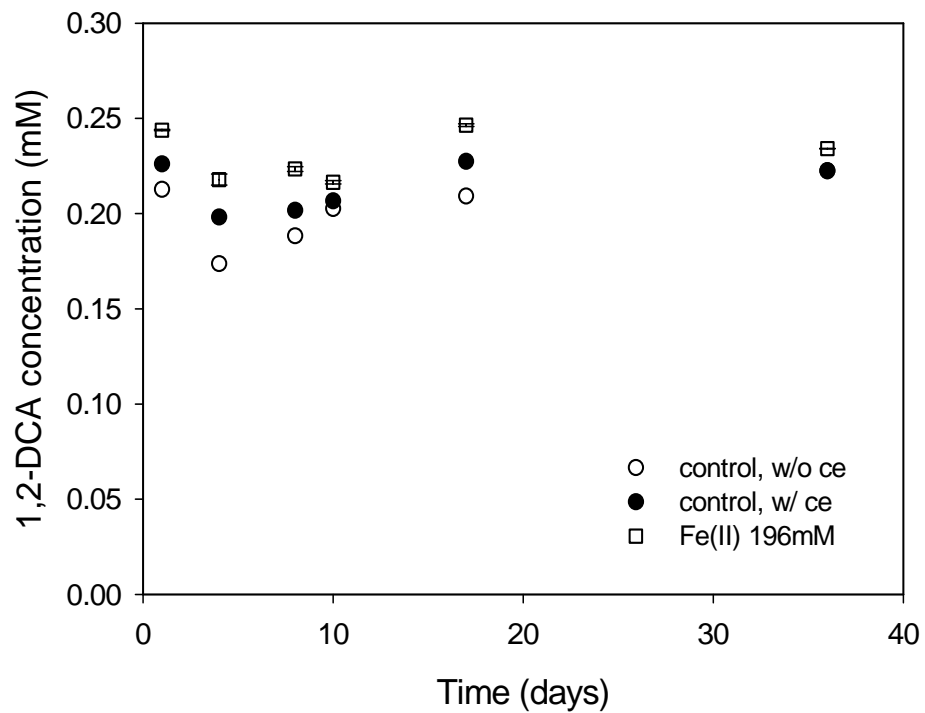
Figure 4.32 Concentration of 1,2-DCA in 10% cement slurries with 196 mM Fe(II).
[1,2-DCA]$_0$ = 0.245 mM.

CHAPTER V

**REDUCTIVE DECHLORINATION OF CHLORINATED ALIPHATIC HYDRO-
CARBONS BY FE(II) IN SLURRIES OF SOIL MINERALS AND CEMENT**

Structural and surface-bound Fe(II) of clay minerals is known to play an important role in reduction of chlorinated compounds. It has been reported that carbon tetrachloride was rapidly transformed in aqueous solutions containing dissolved hydrogen sulfide in the presence of biotite and vermiculite (38). In addition, nitroaromatic compounds (NACs) were reduced to anilines by structural Fe(II) and by Fe(II) complexed with surface hydroxyl groups of nontronite (42). The reactivity of iron-bearing phyllosilicates with chlorinated ethylenes as affected by pH, solid concentration and target organic concentration has been investigated (72). Knowledge of the redox chemistry at mineral surfaces will be a significant factor in understanding the reaction of chlorinated compounds on the mineral surfaces. However, it will be difficult to characterize the reactivity and the reaction mechanism of CAHs in a complex system containing Fe(II), cement and iron-bearing phyllosilicates.

It can be assumed that iron-bearing phyllosilicates will be present and that they can affect the dechlorination of CAHs when iron-based ds/s processes are applied to contaminated sites. It can also be assumed that structural Fe(II) or surface-bound Fe(II) of soil minerals can cause reductive dechlorination in addition to those active sites formed when Fe(II) reacts with components of cement. This chapter describes investigations on the reductive transformation of 1,1,1-TCA by Fe(II) in cement slurries

containing iron-bearing phyllosilicates. Reductive degradation of 1,1,1-TCA by Fe(II) in cement slurries with biotite, vermiculite, and montmorillonite was characterized using batch slurry reactors. Iron-bearing phyllosilicates were used without pretreatment by a reducing agent such as dithionite.

The effects on degradation of 1,1,1-TCA of mineral type (biotite, vermiculite and montmorillonite), Fe(II) dose (5 mM, 10 mM and 20mM) and the mass ratio of cement to phyllosilicates (0.2, 1 and 3) were studied. The extent of sorption of target organics onto clay mineral surfaces was also characterized. The controls and reactors were prepared in duplicates. A first-order kinetic model was used to describe dechlorination kinetics of 1,1,1-TCA in Fe(II)/cement system containing iron-bearing phyllosilicates. Table 5.1 represents the experimental conditions and pseudo-first-order rate constants obtained for these experiments.

Sorption of 1,1,1-TCA onto biotite and vermiculite was determined by the reduction of concentration in the control. 1,1,1-TCA concentration in aqueous phase was observed over 3 days and it showed less than a 4.5 % change, which was attributed to sorption to the Teflon liner or reactor walls. Such behavior was also observed in the experiments conducted with cement slurries and with suspensions of phyllosilicates. The sorption of 1,1,1-TCA was so small that apparent rate constants for 1,1,1-TCA degradation were not corrected for sorption onto the clay mineral surfaces.

Table 5.1 Experimental conditions and pseudo-first-order rate constants in Fe(II)/cement system containing iron-bearing phyllosilicates.

Exp.	Soil	Mass Ratio[a] (Cement/Soil)	Fe(II)[b] (mM)	k_{obs}	n[d]	pH[e]
34	Biotite	1	5	0.163($\pm$30.6%)[c]	21	12.8
35	Biotite	1	10	0.276($\pm$11.5%)	23	12.7
36	Biotite	1	20	0.353($\pm$35.5%)	20	12.6
37	Biotite	0.2	10	0.218($\pm$17.2%)	21	12.6
38	Biotite	3	10	0.323($\pm$19.0%)	20	12.7
39	Vermiculite	1	5	0.146($\pm$30.6%)	15	12.7
40	Vermiculite	1	10	0.290($\pm$14.6%)	23	12.7
41	Vermiculite	1	20	0.482($\pm$34.3%)	21	12.6
42	Vermiculite	0.2	10	0.054($\pm$37.5%)	20	12.5
43	Vermiculite	3	10	0.196($\pm$14.1%)	19	12.7
44	Montmorillonite	1	5	0.006($\pm$41.7%)	27	12.6
45	Montmorillonite	1	10	0.011($\pm$26.2%)	27	12.6
46	Montmorillonite	1	20	0.030($\pm$23.8%)	24	12.5
47	Montmorillonite	0.2	10	0.002($\pm$63.6%)	23	12.4
48	Montmorillonite	3	10	0.055($\pm$16.2%)	20	12.6

The initial of 1,1,1-TCA concentration was 0.347mM. The mass ratio of solid (sum of cement and soil minerals) to water was 0.1. [a]mass of cement/mass of soil. [b]the source of Fe(II) was $FeCl_2$. [c]uncertainties represent the 95% confidence intervals expressed relative to the estimate for k_{obs}. [d]the number of data points used regression. [e]The pH of solution was measured at the last sampling point of each experiment and the average value of duplicates is shown.

5.1   Biotite

Figure 5.1 shows results of experiments on 1,1,1-TCA degradation by Fe(II) in cement slurries containing biotite. These experiments were conducted at the mass ratio of cement to biotite of 1 and Fe(II) doses in the aqueous phase (5, 10, 20 mM) resulted in a range of Fe(II) loadings to the solids (2.8, 5.6, 11.2 mg/g). The pH was measured at the last sampling point and the average values were 12.8, 12.7 and 12.6 in the order of increasing Fe(II) dose. The results showed that first-order kinetics can reasonably describe 1,1,1-TCA reduction kinetics for the 3 Fe(II) doses. The concentrations of 1,1,1-TCA remaining stayed at approximately 94% of the initial values in controls without solids and at 95% of initial values in controls with solids (cement + biotite). When the concentration of Fe(II) was 5 mM, 1,1,1-TCA was completely removed within approximately 35 hours of reaction time. The first-order rate constant with the addition of 20 mM Fe(II) was 2.2 times greater than that with 5 mM Fe(II). The relationship between the first-order rate constants and Fe(II) dose was fitted by a saturation model (Figure 5.2).

Figure 5.3 shows the degradation of 1,1,1-TCA by Fe(II) in cement slurries at different mass ratios of cement to biotite (0.2 to 3.0) and Figure 5.4 shows the effect of the mass ratio on kinetic constants. As the mass ratio of cement to biotite was increased, the rate constant was increased as much 1.5 times.
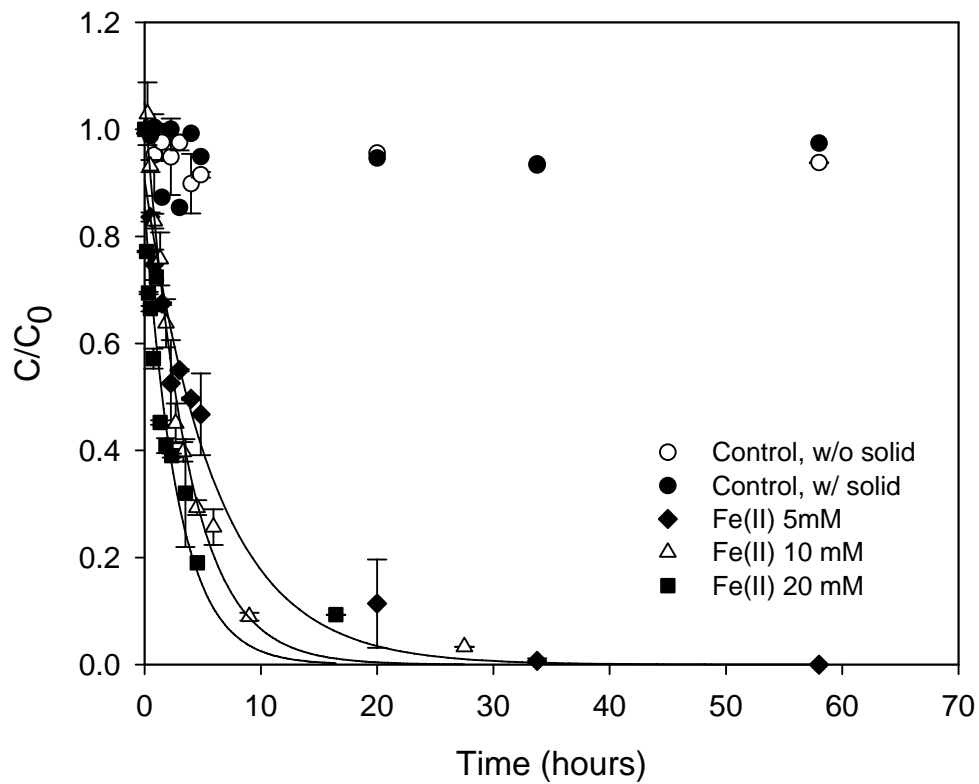
Figure 5.1 Reductive dechlorination of 1,1,1-TCA by Fe(II) in cement slurries containing biotite. Mass ratio of cement to biotite = 1, $[1,1,1\text{-TCA}]_0$=0.347 mM.
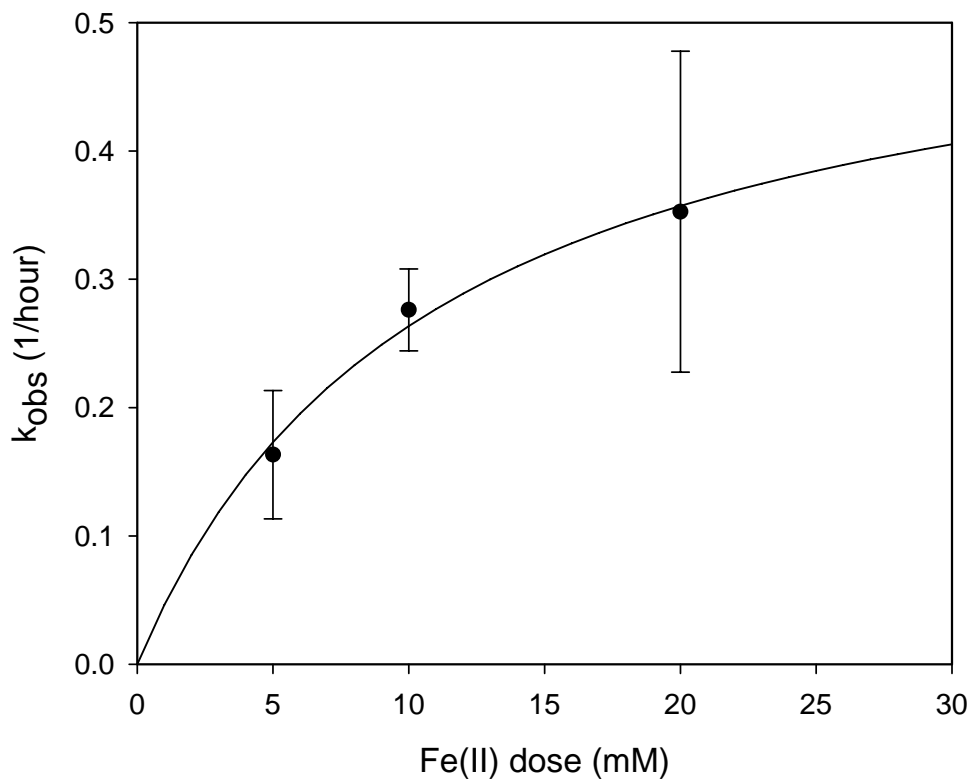
Figure 5.2 Dependence of pseudo first-order rate constants on Fe(II) dose in suspensions of biotite and cement. The solid line shows model predictions. Coefficients in a saturation model were determined by non-linear regression on data from exp. 34 to 36. The saturation model was: $k = \dfrac{k_{max}[Fe(II)]_0}{b + [Fe(II)]_0}$, where k_{max} is the maximum pseudo first-order rate constant, $[Fe(II)]_0$ is the Fe(II) dose, and b is the constant. k_{max} is 0.55 (1/hour), and b is 11.00 (mM)
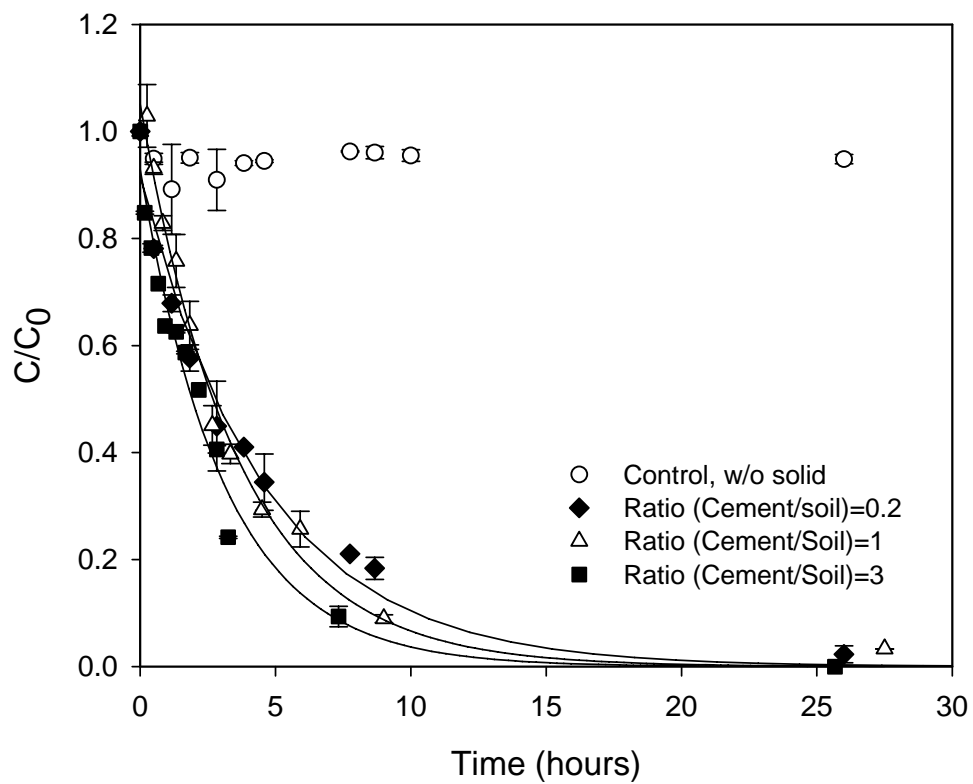
Figure 5.3 Degradation of 1,1,1-TCA in suspensions of biotite and cement at various mass ratios of cement to biotite. $[Fe(II)]_0 = 10$ mM, $[1,1,1\text{-}TCA]_0 = 0.347$ mM.
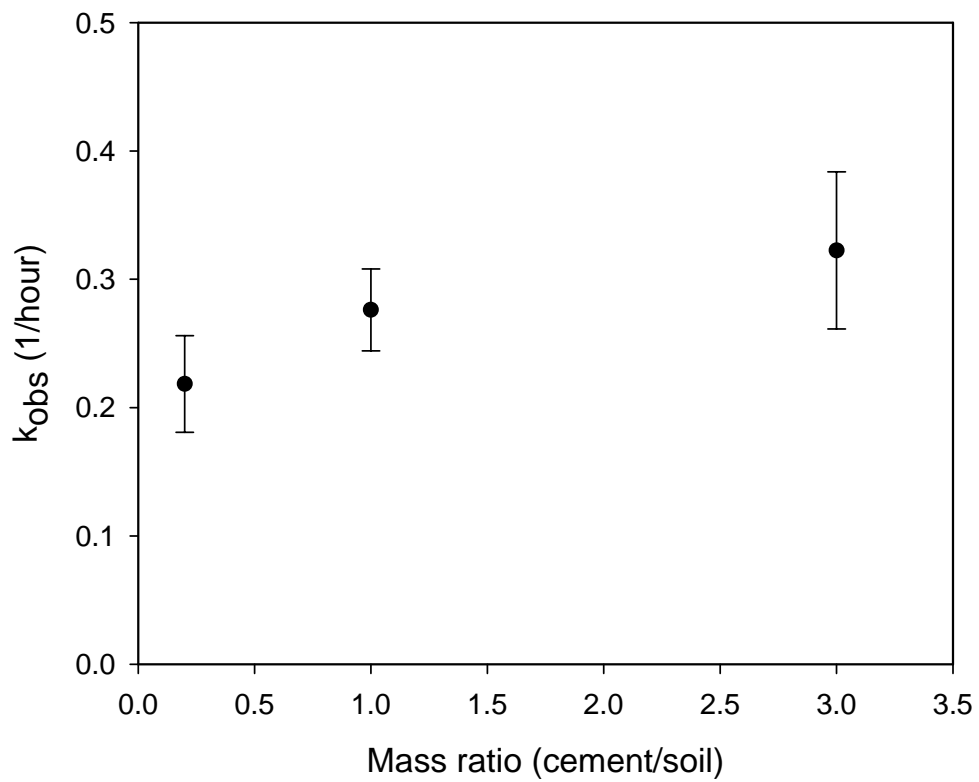
Figure 5.4 Dependence of pseudo-first order rate constant on the mass ratio of cement to biotite. $[Fe(II)]_0 = 10$ mM, $[1,1,1\text{-TCA}]_0 = 0.347$ mM

5.2   Vermiculite

Figure 5.5 shows the results of experiments on degradation of 1,1,1-TCA by Fe(II) in cement slurries containing vermiculite and that they are fit well by a first-order rate model. The mass ratio of cement to vermiculite was fixed at 1 and the mass ratio of all solids to water was 0.1. Final pH values of the three experiments (exp. 39, 40 and 41) were 12.7, 12.7, and 12.6 in the order of increasing Fe(II) dose. When the concentration of Fe(II) was 10mM, 1,1,1-TCA was completely removed at the reaction time of 24 hours. Figure 5.6 shows a linear relationship between pseudo-first-order rate constants and Fe(II) dose. This is contrary to observation that a saturation model provided a better fit to data from experiments with biotite and cement suspensions. The pseudo first-order rate constants were 0.146±0.045, 0.290±0.042, and 0.482±0.165 (1/hour) in the order of increasing Fe(II) dose (5 mM, 10 mM and 20 mM).

Figure 5.7 shows results of experiments on reductive dechlorination of 1,1,1-TCA by Fe(II) in cement slurries containing vermiculite at three different mass ratios of cement to vermiculite. The pH values at the last sampling point for experiments conducted at mass ratios of 0.2, 1 and 3 are 12.5, 12.7, and 12.7. The relationship between the pseudo-first-order rate constant and the mass ratio of cement to vermiculite is shown in Figure 5.8. Unlike the results observed in suspensions of biotite and cement, the first-order rate constant reached a maximum at the mass ratio of cement to vermiculite of 1.
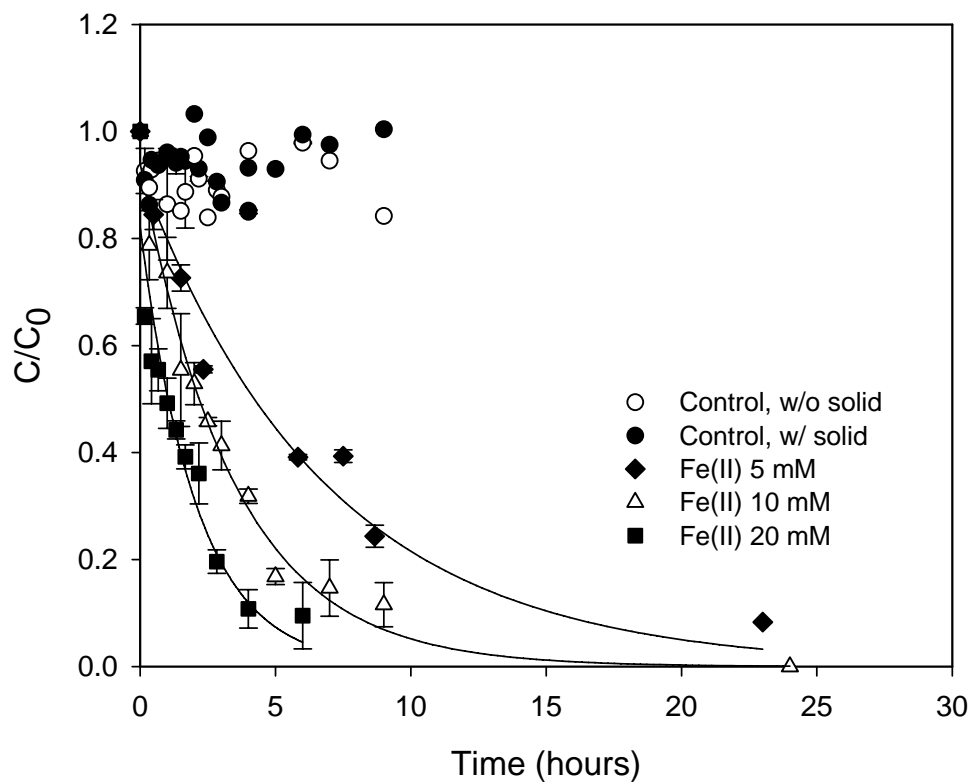
Figure 5.5 Degradation of 1,1,1-TCA by Fe(II) in cement slurries containing vermiculite. Mass ratio of cement to vermiculite = 1, $[1,1,1\text{-TCA}]_0$ = 0.347 mM.
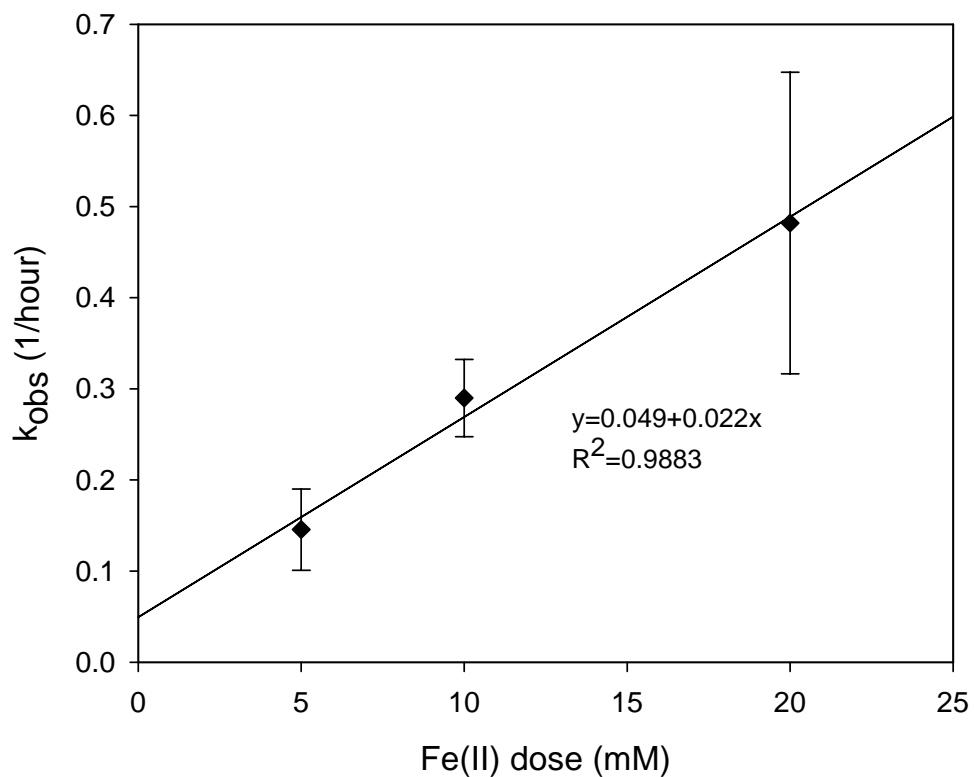
Figure 5.6 Dependence of pseudo-first-order rate constant on Fe(II) dose in suspensions of vermiculite and cement. The solid line was fitted by a linear regression. Mass ratio of cement to soil = 1, $[1,1,1\text{-}TCA]_0 = 0.347$ mM.
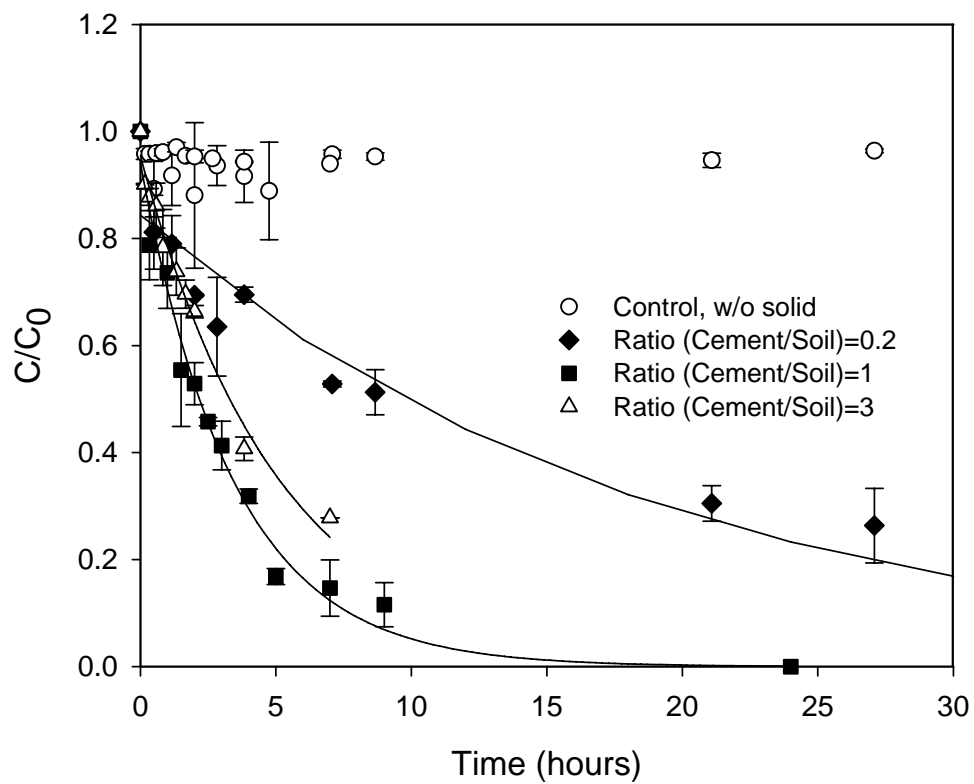
Figure 5.7 Degradation of 1,1,1-TCA by Fe(II) in suspensions of cement and vermiculite at various mass ratios of cement to vermiculite. $[Fe(II)]_0 = 10$ mM, $[1,1,1-TCA]_0 = 0.347$ mM.
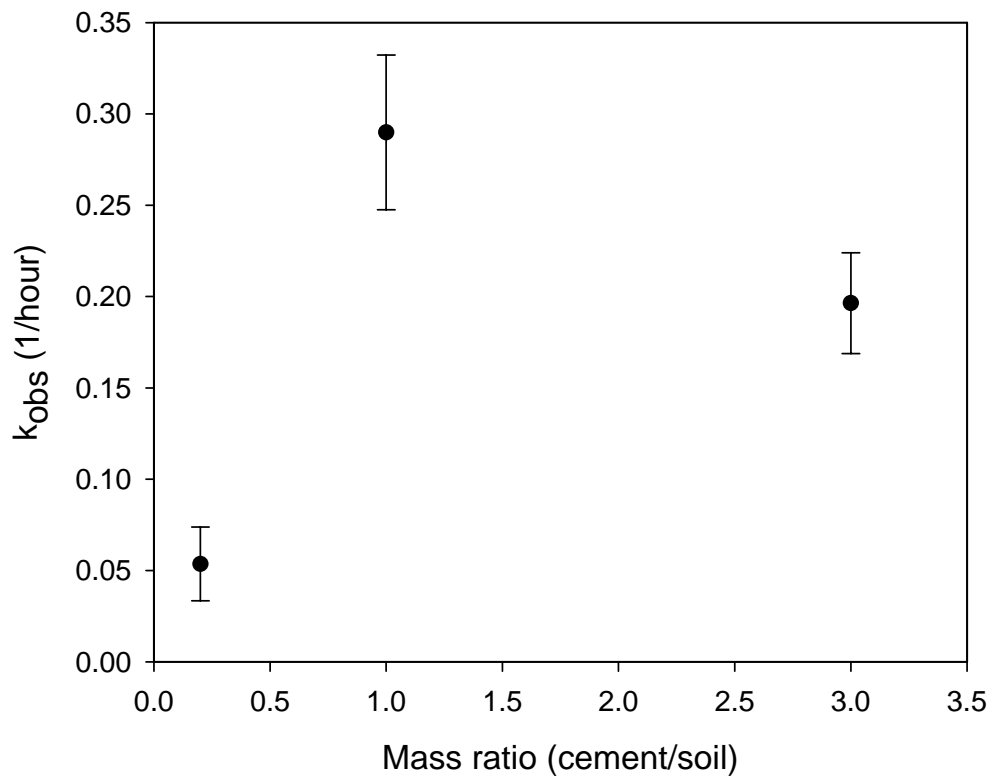
Figure 5.8 Dependence of pseudo-first-order rate constant on mass ratio of cement to vermiculite. $[Fe(II)]_0 = 10$ mM, $[1,1,1\text{-TCA}]_0 = 0.347$ mM.

5.3   Montmorillonite

Figure 5.9 shows results of experiments on degradation of 1,1,1-TCA by Fe(II) in cement slurries containing montmorillonite. A first-order kinetic model fits the data well. The effect of Fe(II) dose (5, 10, 20 mM) was investigated with a mass ratio of cement to montmorillonite of 1 and a mass ratio of solid to water of 0.1 and an initial concentration of 1,1,1-TCA of approximately 0.347 mM. The final pH in these experiments was 12.6, 12.6, and 12.5, in the order of increasing of Fe(II) doses. Kinetics of 1,1,1-TCA degradation in the presence of montmorillonite was slower than that observed with biotite or vermiculite. Percent removal of 1,1,1-TCA was about 28%, 62%, 82% at reaction time of 78 hours where Fe(II) concentration was respectively 5, 10 and 20 mM. The linear relationship between pseudo first-order rate constants and Fe(II) doses is shown in Figure 5.10.

Figure 5.11 shows the effect of mass ratio of cement to clay montmorillonite (0.2, 1, 3) on degradation of 1,1,1-TCA by Fe(II) in cement slurries containing montmorillonite. The pseudo-first-order rate constants were 0.002 ± 0.003, 0.011 ± 0.003, and 0.055 ± 0.007 (1/hour) for mass ratios of cement to montmorillonite of 0.2, 1 and 3. The relationship between the pseudo-first-order rate constant and the mass ratio of cement to montmorillonite is shown in Figure 5.12. As the mass ratio of cement to montmorillonite increases from 1 to 3 the first-order rate constant increases as much 5 times.
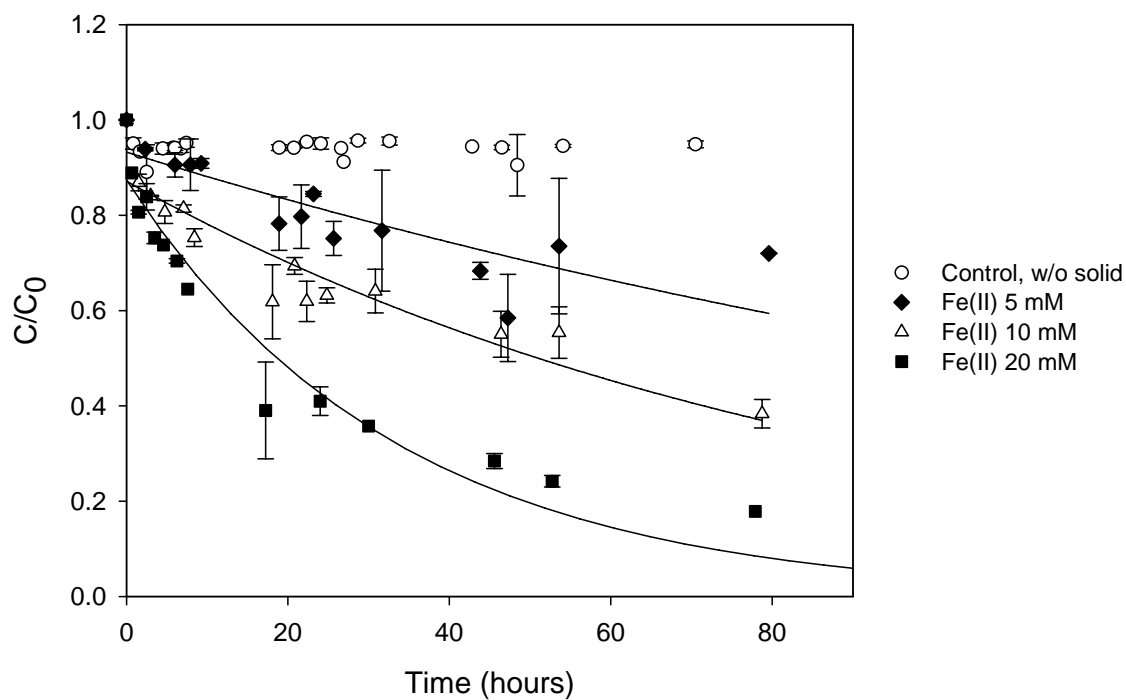
Figure 5.9 Reductive dechlorination of 1,1,1-TCA by Fe(II) in cement slurries containing montmorillonite. Mass ratio of cement to montmorillonite = 1, $[1,1,1\text{-TCA}]_0$ = 0.347 mM.
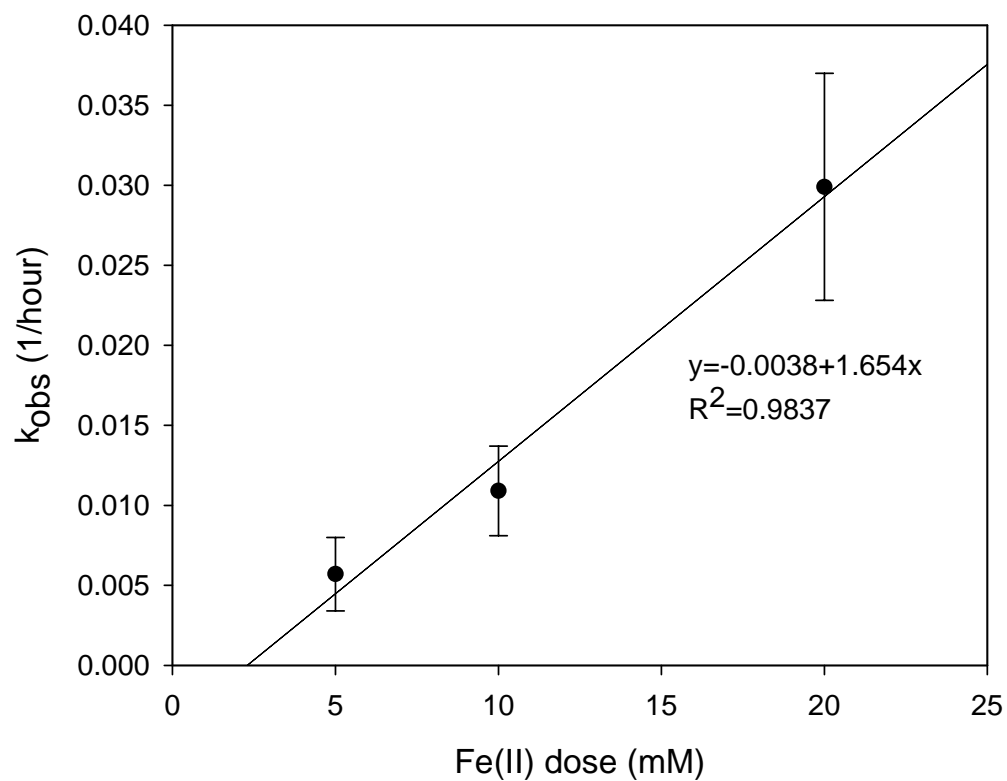
Figure 5.10 Dependence of pseudo-first-order rate constant on Fe(II) dose in suspensions of montmorillonite and cement. The solid line was fitted by linear regression. Mass ratio of cement to montmorillonite = 1, $[1,1,1\text{-TCA}]_0 = 0.347$ mM.
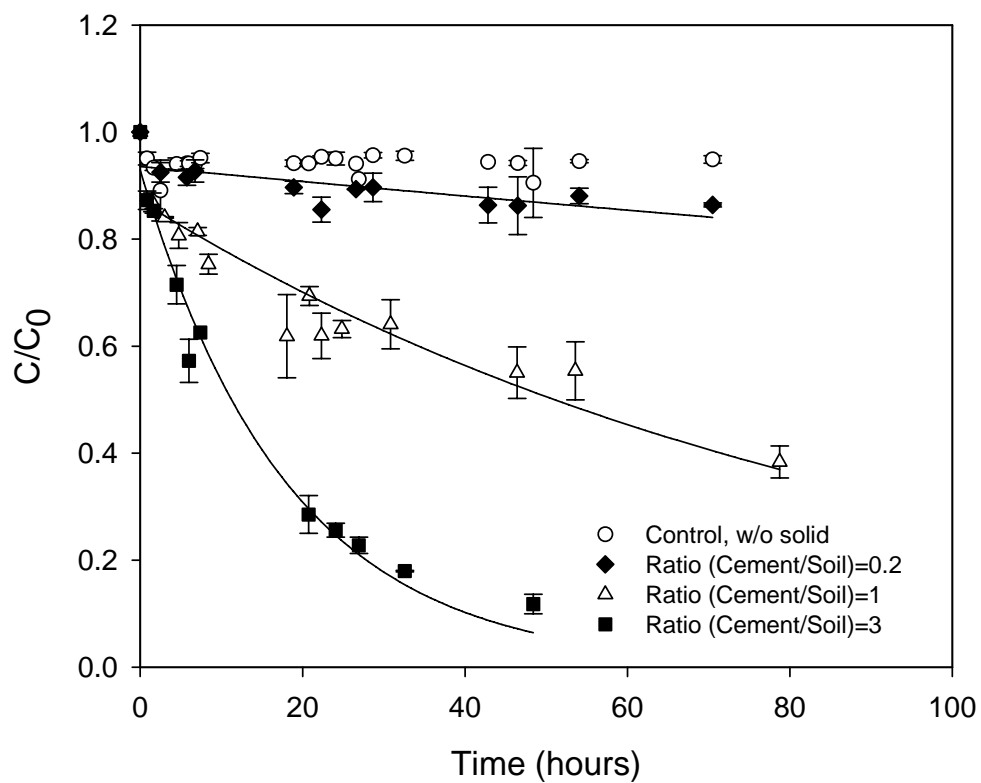
Figure 5.11 Degradation of 1,1,1-TCA by Fe(II) in suspensions of montmorillonite and cement at various mass ratios of cement to montmorillonite. $[Fe(II)]_0 = 10$ mM, $[1,1,1\text{-}TCA]_0 = 0.347$ mM.
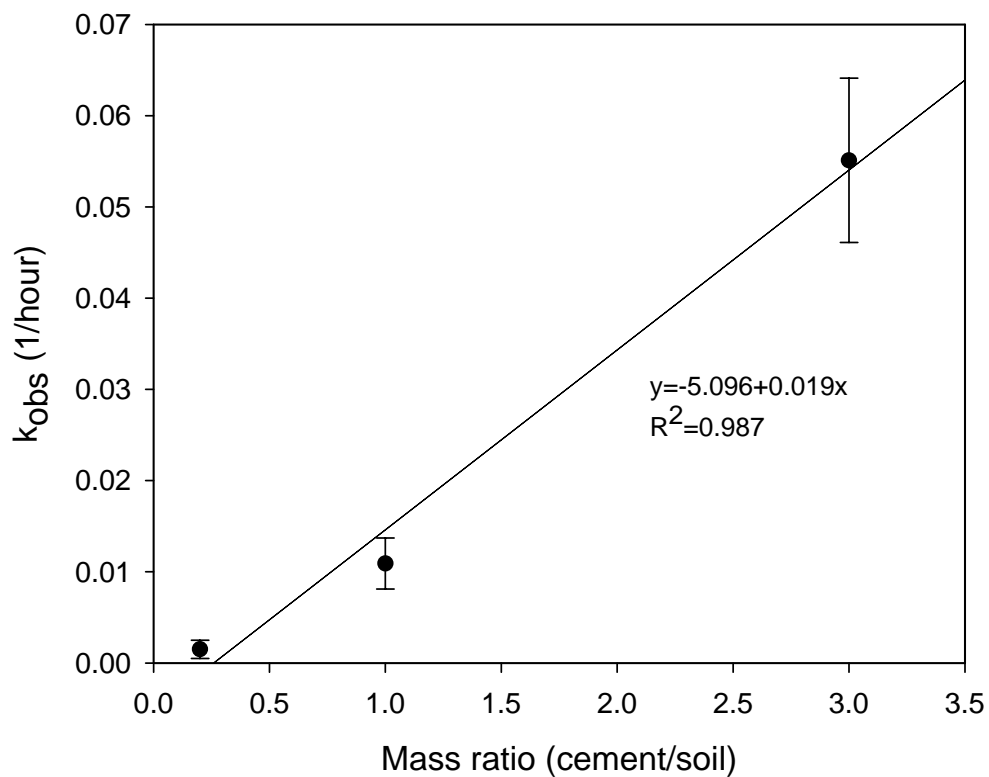
Figure 5.12 Dependence of pseudo-first-order rate constant on mass ratio of cement to montmorillonite. $[Fe(II)]_0 = 10$ mM, $[1,1,1\text{-}TCA]_0 = 0.347$ mM.

5.4   Effects of Soil Mineral Types on Dechlorination Kinetics

Degradation of 1,1,1-TCA over time was observed in the presence of Fe(II), cement and three different soil minerals (biotite, vermiculite, montmorillonite). All of the pseudo-first-order rate constants increased with Fe(II) dose as shown in Figure 5.13. However, the patterns of increases were different for different soil minerals.
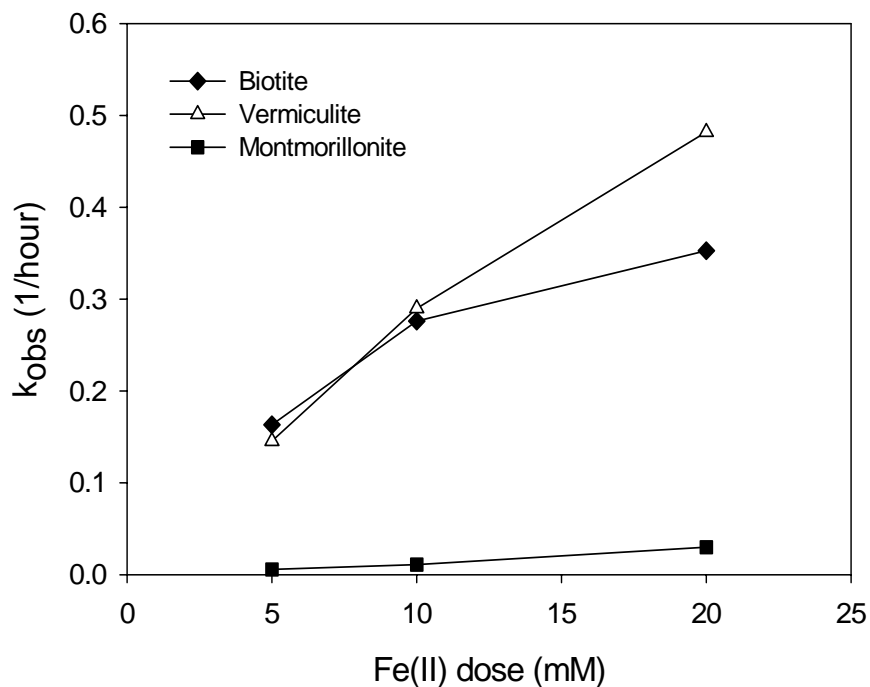
Figure 5.13 Dependence of pseudo first-order rate constants on Fe(II) doses for different soil minerals in suspensions of Fe(II) and cement. Solid lines do not represent a fitted model.

Similar values of the rate constants were observed for biotite and vermiculite when the doses of Fe(II) were 5 mM and 10 mM. This behavior is supported by the fact that these minerals have similar structures and that vermiculite is formed from weathering biotite. When the concentration of Fe(II) was increased to 20 mM, the rate constant in the presence of biotite was 1.4 times smaller than that in the presence of vermiculite. This contradicts reports that biotite is more reactive than vermiculite (38, 72). A possible explanation for this is that precipitation of Fe(II) could more easily cover the surface of biotite, because it has a smaller specific surface area (1.9 m^2/g) compared to vermiculite (26.7m^2/g). The relationship between the first-order rate constants and Fe(II) doses for biotite is best described by a saturation model while the relationship for vermiculite and montmorillonite is best described by a linear model.

Lee. (72) showed that increasing pH over the range of 5.5-8.5 increased the dechlorination rates of TCE in suspensions of biotite with and without addition of Fe(II). These higher rates could be caused by increased concentrations of reactive Fe(II) surface complexes on biotite resulting from higher pH. Also, it has been reported that 2:1 minerals have a point of zero charge (pH$_{pzc}$) of approximately 2.5 (85). Therefore, the surface charge of 2:1 clay minerals including biotite, vermiculite and montmorillonite will be negative at the high pH (pH 12.5) found in cement slurries. The negative surface sites of clay minerals could react with Fe(II) to form surface-bound Fe(II) sites that participate in reductive dechlorination of 1,1,1-TCA.

The pseudo-first-order rate constant in the presence of montmorillonite was much lower than that for biotite or vermiculite. This might be due to the higher cation

exchange capacity of montmorillonite which would allow greater amounts of reactive Fe(II) to be present in interlayers of montmorillonite. Furthermore, the large specific surface area of montmorillonite (500 m^2/g) indicates that montmorillonite might adsorb greater amounts of cement components, thereby reducing their ability to react with Fe(II) to form reactive species. In addition, the content of Fe(II) of montmorillonite is the lowest of the three clay minerals used in this study. Lee reported that the Fe(II) content of biotite was 8 and 97.5 times higher than that of vermiculite and montmorillonite, respectively (72).

Figure 5.14 shows the effect of cement/mineral ratio on the pseudo-first-order rate constant for three different soil minerals. The mass ratio of total solids (cement + mineral) to water was 0.1. The mass ratio of cement to mineral varied from 0.2 to 3.0. At the mass ratio of cement to mineral of 0.2, the first-order rate constant was the greatest with biotite, followed by vermiculite and montmorillonite. This result corresponds to reports that biotite was more reactive than two other phyllosilicates in the dechlorination of PCE with or without the addition of Fe(II) (72). This implies that biotite may provide more reactive sites than other clay minerals under the conditions investigated because of its higher natural content of Fe(II). The pseudo-first-order rate constants for experiments with biotite or montmorillonite increased regularly as the mass ratio of cement to clay mineral increased and the rate constants for montmorillonite were the lowest of the three soil minerals. In suspensions of Fe(II) and cement system without clay minerals, the active reductant was assumed to be a Fe(II)-Fe(III)hydroxide such as green rust. This compound is also assumed to be an important reductant in similar systems that also

contain phyllosilicates, although structural Fe(II) or surface-bound Fe(II) of the iron-bearing phyllosilicates may also act as reductants. This is supported by the observation that the rate constants for the dechlorination of chlorinated ethylene by iron-bearing phyllosilicates were approximately 1.9-21.5 times smaller than those for pyrite and $GR_{SO4.}$ Therefore, increased amounts of cement relative to phyllosilicates will cause increased rate constants. In contrast to the behaviors of biotite and montmorillonite, the first-order rate constant with vermiculate reached a maximum value at an intermediate value of the mass ratio of cement to mineral of 1. Kinetics of 1,1,1-TCA dechlorination by Fe(II) in cement slurries in the presence of iron-bearing phyllosilicates was dependent on soil mineral types as well as Fe(II) doses and the mass ratio of cement to clay minerals. But it is very complicated to separate effects of different factors on kinetic behaviors because of the complexity of the system. Several simplified models will be discussed in Chapter VI to help understand the reaction mechanism between chlorinated organic compounds and iron-bearing phyllosilicates in the Fe(II)/cement system.
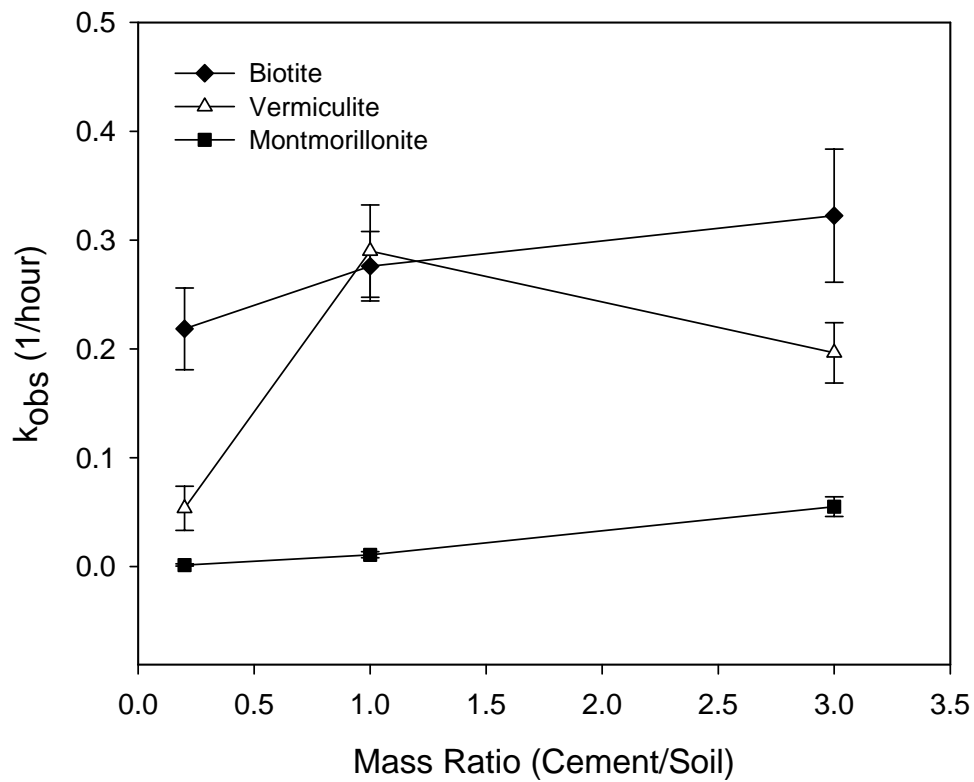
Figure 5.14 Dependence of pseudo first-order rate constant on the mass ratio of cement to soil mineral for three different soil mineral types in mixtures of Fe(II) and cement. The solid line does not represent a fitted model.

CHAPTER VI
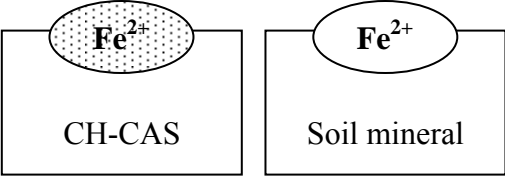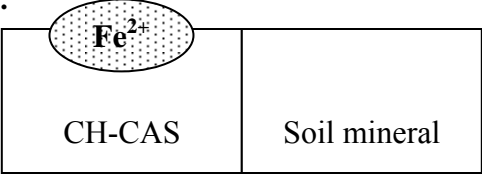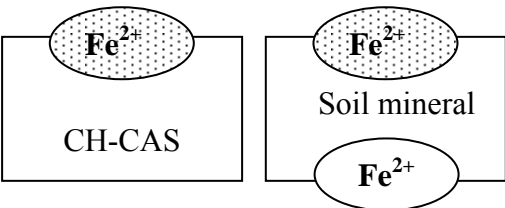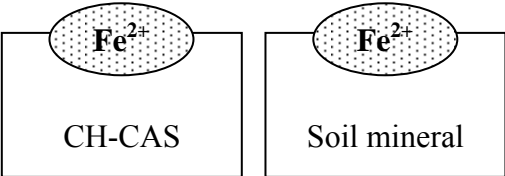
DISCUSSION

6.1   Reaction Mechanism in DS/S-Fe(II) process containing Iron-bearing phyllosilicates

It is known that solid phases such as iron oxides, iron sulfides and iron-bearing phyllosilicates are able to transfer electrons within in their structures (86). Therefore, these minerals will play an important role in reductive transformations in natural environments. Many researchers have demonstrated that reductive dechlorination in suspensions of soil minerals is strongly dependent on factors such as mineral type and quantity, contaminant molecular structure, density of reductant on the surface, chemistry of clay surface, and whether the reducing environment was caused by biotic or abiotic processes. Therefore, it will be more complicated to characterize transformation of chlorinated compounds in systems that contain several solid phases such as mixtures of Fe(II), cement and iron-bearing phyllosilicates. This chapter explains experimental results presented earlier for such a system by presenting several idealized reaction mechanisms. Table 6.1 presents the four different simplified models used to describe surface reactions of chlorinated aliphatic compounds (CAHs) with solids formed in mixtures of cement, soil minerals, and Fe(II). Results of XRD, SEM, and EDS analysis have been used to conclude that the compounds responsible for degradation in DS/S-Fe(II) system appear to be AFm phases, such as Friedel's salt, calcium aluminate hydrates and calcium aluminum silicate hydrates (87). These solids contain Ca, Al, and

SO_4 (52), so the sites that associate with Fe(II) will be represented as CH-CAS, which stands for cement hydration products (CH) consisting of Ca (C), Al (A) and sulfate (S).

Table 6.1 Simplified models that describe surface reactions of cement hydration products and soil minerals with Fe(II).

Idealized Model	Description
1. **Fe²⁺** (dotted oval) **Fe²⁺** (oval) CH-CAS Soil mineral	Assumption: Only cement components (CH-CAS)[a] will react with iron to form active reductants that degrade CAHs. Also, Fe(II) can be associated with soil minerals, but it will not participate in redox reactions with CAHs.
2. **Fe²⁺** (dotted oval) CH-CAS Soil mineral	Assumption: Only CH-CAS will react with iron to form active reductants that degrade CAHs. Clay minerals will physically cover the surfaces of the products of cement hydration.
3. **Fe²⁺** (dotted oval) **Fe²⁺** (dotted oval) CH-CAS Soil mineral **Fe²⁺** (oval)	Assumption: Active sites for degradation of CAHs can be formed by both reaction of CH-CAS with Fe(II) and reaction of soil minerals with Fe(II). Some iron will also be sorbed or exchanged with the soil minerals, but will not participate in redox reactions with CAHs.
4. **Fe²⁺** (dotted oval) **Fe²⁺** (dotted oval) CH-CAS Soil mineral	Assumption: Active sites for degradation of CAHs can be formed by both reaction of CH-CAS with Fe(II) and reaction of soil minerals with Fe(II). There is no inactive Fe(II) associated with the soil minerals.

The oval boxes with dots indicate iron that is active in degrading CAHs, while the oval boxes without dots indicate iron that is not reactive in degrading CAHs.

[a]represents cement hydration products including the components such as Ca, Al and SO_4.

In Model 1, the assumption is made that only CH-CAS will react with Fe(II) to form the active reductants that degrade CAHs and that the active reductant is a Fe(II)-Fe(III)-hydroxides. The model also assumes that Fe(II) can be sorbed onto the soil surface or can exchange with cations present in the interlayer of the phyllosilicates. However, this iron is assumed to be unable to react with CAH. Therefore, the iron associated with the soil minerals is not available to react with cement components to form active reductants. This model might be able to explain the lower rate constants observed for montmorillonite compared to other two soil minerals. The high cation exchange capacity (800-1200 mmol/kg) and large surface area of montmorillonite (500 m^2/g) will provide more sites for adsorption of Fe(II) or CH-CAS. If these compounds are adsorbed, they will not be available to react to form the active reductant.

In a Model 2, the assumption is that only CH-CAS will be responsible for the formation of active reductants and that soil minerals can physically cover the surface of the cement hydration products, but will not be able to degrade CAHs. The specific surface area of hydrated cement and montmorillonite was reported to be approximately 200 m^2/g and 500 m^2/g, respectively (72, 88). The specific surface area exclusive of interlayer zones of the smectites groups that include montmorillonite ranges from 50 to 120 m^2/g, while the specific surface area that is exposed by expanding the lattice ranges up to 840 m^2/g (66). The large surface area of montmorillonite (500 m^2/g, (72)) means that it could cover much of the surface of the cement hydration products and thereby reduce their ability to react with iron to form active reductants and reduce the ability of the active reductants to degrade CAHs.

The assumption applied in a Model 3 is that both CH-CAS and the structural Fe(II) or surface-bound Fe(II) of soil minerals provide active sites that can react with CAHs. This model also assumes that some of the iron that is sorbed or exchanged to soil surfaces is not able to take part in redox reactions with CAHs. The presence of iron-bearing phyllosilicates could enhance or degrade dechlorination rates of CAHs in mixtures of Fe(II) and cement. It has been reported that structural Fe(II) in clays and Fe(II) complexed to the clay surface can act as reductants for pollutant transformations, but Fe(II) bound by ion exchange has been reported to be non-reactive with nitroaromatic compounds (NACs) (42). The types of Fe(II) present in soil minerals will depend on the soil mineral types and will affect the dechlorination rates of CAHs.

In Model 4, the assumption is made that both CH-CAS and soil minerals react with iron to provide active sites for dechlorination of CAHs. Reactive sites can contain structural Fe(II) or surface-bound Fe(II), such as $\equiv$Fe(III)-O-Fe(II)-OH or $\equiv$FeOFe$^+$. It has been reported that Fe(II) in iron sulfides, lattice-bound Fe(II) in layered silicates (biotite or smectite), and Fe(II) sorbed onto Fe(III) oxides such as magnetite will be highly reactive with contaminants (77).

6.2 Reaction Pathway

There are two potential pathways (consecutive and parallel) that can describe the conversion of 1,1,1-TCA to ethane. The parallel reaction of 1,1,1-TCA (1,1,1-TCA→1.1-DCA and 1,1,1-TCA→Ethane) was discussed in Chapter IV. This section will discuss the consecutive reaction of 1,1,1-TCA to ethane that passes through 1,1-

DCA and CA (Equation 6-1). The degradation experiments on 1,1,1-TCA in cement slurries with Fe(II) were conducted with an initial concentration of 1,1,1-TCA of 0.245 mM and a dose of Fe(II) of 19.6 mM (exp.21). It was assumed that the reaction was irreversible and first-order with respect to reactants. Consecutive reactions were described using equation 6-2 to equation 6-5:

$$1,1,1-TCA \xrightarrow{k_{1,c}} 1,1-DCA \xrightarrow{k_{2,c}} CA \xrightarrow{k_{3,c}} Ethane \tag{6-1}$$
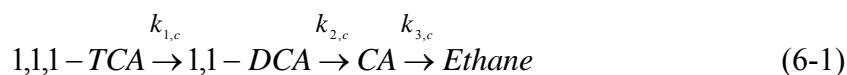
$$\frac{dC_{TCA,l}}{dt} = -k_{1,c}C_{TCA,l} \tag{6-2}$$

$$\frac{dC_{DCA,l}}{dt} = k_{1,c}C_{TCA,l} - k_{2,c}C_{DCA,l} \tag{6-3}$$

$$\frac{dC_{CA,l}}{dt} = k_{2,c}C_{DCA,l} - k_{3,c}C_{CA,l} \tag{6-4}$$

$$\frac{dC_{Ethane,l}}{dt} = k_{3,c}C_{CA,l} \tag{6-5}$$

where $k_{1,c}$ is the pseudo first-order rate constant for dechlorination of 1,1,1-TCA to 1,1-DCA and $k_{2,c}$ is the pseudo first-order rate constant for dechlorination of 1,1-DCA to CA in consecutive reaction, and $k_{3,c}$ is the pseudo first-order rate constant for transformation of CA to Ethane in consecutive reaction. The values of these parameters calculated by nonlinear regression are presented in Table 6.2. The regression fitted experimental data to the kinetic model described by Equation 6.2 to Equation 6.5. This set of ordinary differential equations was solved by MATLAB function ode45.

Table 6.2 Kinetic parameters for 1,1,1-TCA transformation by a consecutive reaction pathway.

Parameter	Value calculated[a]
$C_{TCA,l}{}^0$	$0.236(\pm 5.5\%)^b$ (mM)
$k_{1,c}$	$0.020(\pm 11.3\%)$ (1/min)
$k_{2,c}$	$0.0003(\pm 175.9\%)$ (1/min)
$k_{3,c}$	$2(\pm 5.6E4\%)$ (1/min)

[a]the values were calculated by a nonlinear regression using the kinetic model described by Eq. 6-3 to Eq.6-5. [b]uncertainties represent 95% confidence limits expressed in % relative to estimates for $C_{TCA,l}{}^0$, $k_{1,c}$, $k_{2,c}$, and $k_{3,c}$.

The relative magnitudes of the rate constants in Table 6.2 mean that the reaction rate from 1,1-DCA to CA will be very slow and the reaction rate from CA to ethane will be very rapid. The model with these rate coefficients would predict that the concentration of 1,1-DCA would decrease over time. However, disappearance of 1,1-DCA was not observed over the reaction time investigated. The high level of uncertainty for $k_{2,c}$ and $k_{3,c}$ is due to the fact that the reaction of 1,1-DCA to produce CA did not occur. In addition, the concentration of ethane should gradually increase but a constant concentration was measured. The pseudo-first-order rate constant for the conversion of 1,1,1-TCA to 1,1-DCA ($k_{1,p}$) and the rate constant for conversion of 1,1,1-TCA to ethane ($k_{2,p}$) in the parallel model were calculated as 0.020 ($\pm 10.5\%$) (min^{-1}) and 0.001 ($\pm 82.4\%$) (min^{-1}), respectively. The uncertainties for parameters in the parallel model were lower than those in the consecutive model shown in Table 6.2. The model predictions obtained from the consecutive and parallel pathways are compared in Figure 6.1. This figure shows that it is likely that the parallel reaction mechanism is the better way to explain

reductive transformation of 1,1,1-TCA by Fe(II) in cement slurries over the range of reaction time investigated.
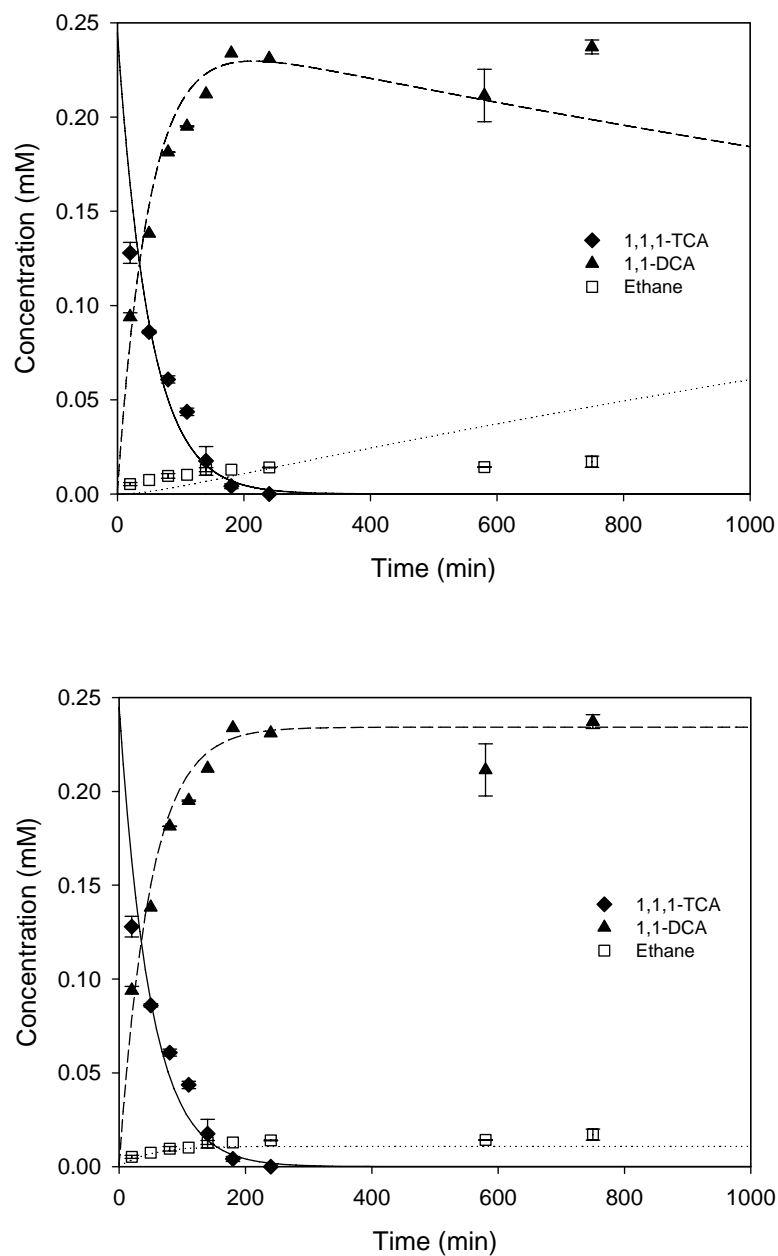
Figure 6.1 Transformation of 1,1,1-TCA by Fe(II) in cement slurries by (a) the consecutive reaction mechanism and (b) the parallel reaction mechanism.

6.3   Reductive Dechlorination Kinetics Dependent on Chemical Molecular Structure

Chapter IV discussed the effects of Fe(II) dose, pH, and initial target organic concentration on dechlorination kinetics of 1,1,1-TCA and TCE[*] produced from 1,1,2,2-TetCA transformation. The general behavior of rate constants was similar for both 1,1,1-TCA and TCE[*]. Rate constants increased with Fe(II) dose and the maximum rate constant was observed at the pH obtained without additions of supplemental acid or base. The optimum pH for 1,1,1-TCA was about 12.5, while the optimal pH for TCE[*] was near pH 12.1. The rate constants decreased with increasing initial target organic concentration. Furthermore, a saturation model described the relationship between initial concentration and reaction rates for disappearance of 1,1,1-TCA and TCE[*]. This indicates that reductive dechlorination of both compounds occurs at the same sites on surfaces formed in mixtures of Fe(II) and cement.

However, the rate constants for removal of 1,1,1-TCA were about 2~3 orders of magnitude greater than those for removal of TCE[*] as shown in Figure 6.2. Half-lives ($t_{1/2}$) for 1,1,1-TCA were estimated to be in the range of 22 min to 9 day, while half-lives for TCE[*] were in the range from 1.6 day to 104 day. Analysis of degradation products showed that 1,1,1-TCA underwent hydrogenolysis to produce 1,1-DCA, while TCE[*] was degraded through a β-elimination pathway. Differences in reaction rate constants and degradation pathways will be dependent on the molecular properties of the chlorinated hydrocarbons.
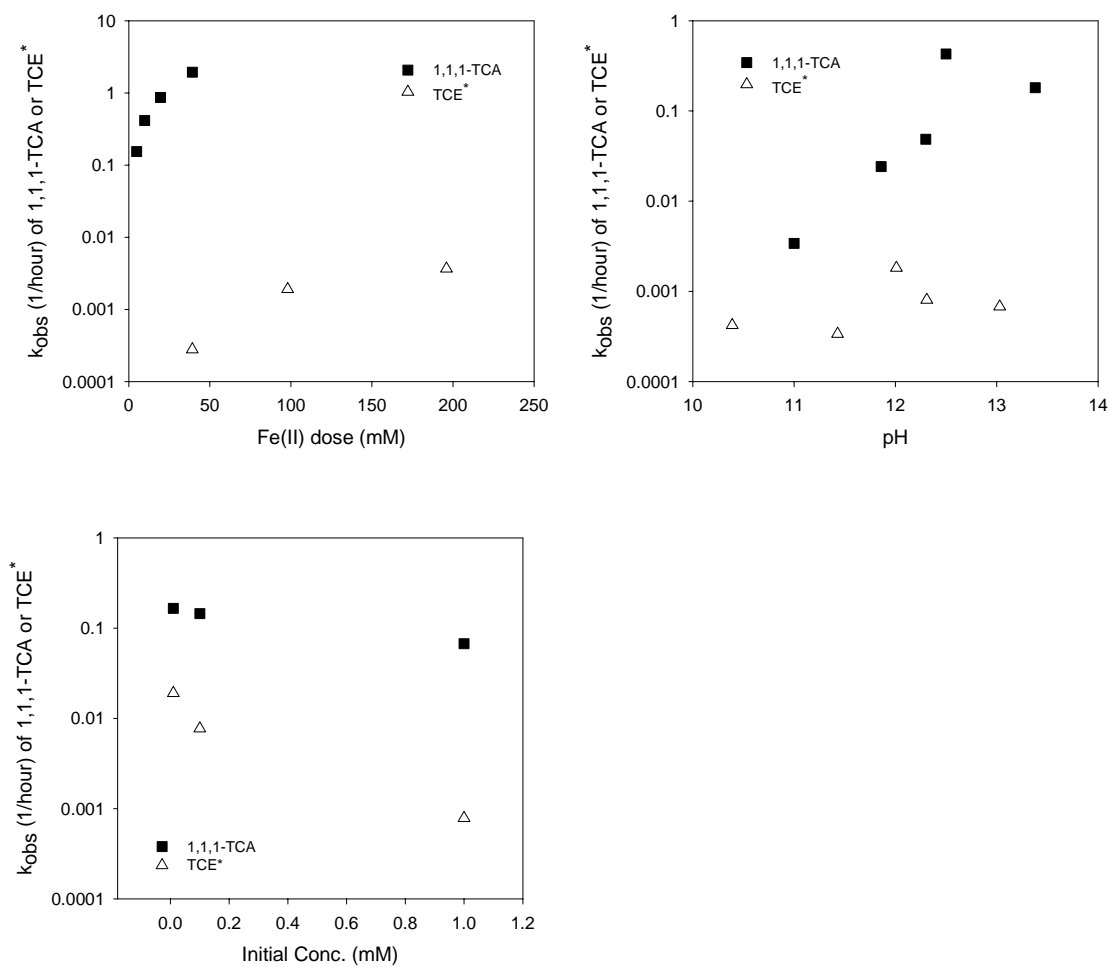
Figure 6.2 Effects of different factors on pseudo first-order rate constants for degradation of 1,1,1-TCA and TCE[*]. (a) effect of Fe(II) dose, (b) effect of pH, (c) effect of initial concentration of target compound. TCE[*] was produced by dehydrochlorination of 1,1,2,2-TetCA by Fe(II) in cement slurries. Detailed experimental conditions were presented in Table 4.2 and Table 4.5.

6.4   Correlation Analysis of Rate Constants

The applicability of Fe(II)-based ds/s process to degrade chlorinated ethylenes, chlorinated ethanes, and chlorinated methanes including PCE, PCB, TCE, 1,1-DCE, VC, 1,1,1-TCA, 1,1,2,2-TetCA, 1,2-DCA, CT, CF has been investigated (48, 49, 69, 70). It has been demonstrated that different molecular properties of target chlorinated organics as well as factors such as Fe(II) dose, pH and initial target organic concentration affect reduction kinetics (89). Therefore, data is available to conduct a correlation analysis of rate constants for a range of chlorinated hydrocarbons degraded by Fe(II)-based ds/s. The approach to correlation analysis is to relate first-order rate constants corrected by a partitioning factor (p) with one-electron reduction potential (E_1^o), two-electron reduction potential (E_2^o) and bond dissociation energy (D_{R-X}). Kinetic data for PCE, CT, TCE, 1,1-DCE and VC in Fe(II)-based ds/s process were obtained from published reports (49, 69, 70). Values of E_1^o (90, 91) , E_2^o (67) and D_{R-X} (35) were obtained from the literature and used in calculation procedures that are described in more detail in Appendix C.

Reductive dechlorination consists of a two-step process. The first-step is that a single electron from an electron donor is transferred and the alkyl radical is formed. This compound can undergo several reactions, including hydrogenolysis, β-elimination, and coupling (74). It has been reported that the initial reaction forming the radical is the rate-limiting step (92). This supports the assumption that the one-electron reduction potential should be used as the independent variable for correlation analysis, rather than the two-electron reduction potential.

Table 6.3 presents rate constants for degradation of chlorinated hydrocarbons in mixtures of Fe(II) and cement and Table 6.4 presents thermodynamic reduction potentials.

Table 6.3 Kinetic data for degradation of chlorinated hydrocarbons in mixtures of Fe(II) and cement.

Parent compound	Products[b]	C_0 (mM)	Fe(II)(mM)/k[c](1/hr)	Fe(II)(mM)/k[d](1/hr)	Ref.
CT	CF	0.26	41.6/12 (±20%)		(49)
CF[*a]	MC	0.26	41.6/0.011(±18%)		(49)
1,1,1-TCA	1,1-DCA	0.245	39.2/2.063(±0.1%)		
PCE	Acetylene	0.245	39.2/0.004(±5.4%)	98/0.007 (±6.5%)	(70)
TCE[*a]	Acetylene	0.245	39.2/0.0003(±2.4%)	98/0.002(±1.6%)	
TCE	Acetylene	0.25	40/0.012(±5.4%)	100/0.019(±4.4%)	(69)
1,1-DCE	Ethene	0.25		100/0.008(±11.1%)	
VC	Ethene	0.15		100/0.003(±23.8%)	

The kinetic data of CAHs except 1,1,1-TCA and TCE* were used from ref. (49, 69, 70) [a] * indicates that CF and TCE were not original target compounds but were produced by transformation of CT and 1,1,2,2-TetCA. [b] The final reduction product observed. [c,d] The first-order rate constant was obtained at each Fe(II) dose. And the values of [c] and [d] represent the first-order rate constants corrected for partitioning among the aqueous, gas and solid phases; k=p×k$_{obs}$, where p is the partitioning factor of each target organic compound (p = mass in all phases/mass in aqueous phase).

Table 6.4 Thermodynamic reduction potentials.

Parent compound (RX)	Radical[a] (R•)	Hydrogenolysis Product[b]	$E_1^o(V)^c$	$E_2^o(V)^e$	D_{R-X}^e (kJ/mole)
CT	$Cl_3C•$	CF	0.13	0.67	304.1
CF	$HCl_2C•$	MC	-0.23	0.56	
1,1,1-TCA	$H_3CCl_2C•$	1,1-DCA	-0.23	0.57	316.8
PCE	$Cl_2CClC•$	TCE	-0.36	0.58	334.6
TCE	$Cl_2CHC•$	1,1-DCE	-0.91^d	0.50	357.4
1,1-DCE	$H_2CClC•$	VC	-0.72	0.4	
VC	$H_2CHC•$	Ethene	-0.95	0.49	

[a]radicals are products of one-electron reduction reaction (92). [b]products are those produced by hydrogenolysis pathway (67). [c]one-electron reduction potential from ref. (90), [d]one-electron reduction potential from ref. (91), [e]two-electron reduction potential from ref.(67). [e]gas-phase bond dissociation enthalpy from ref.(35).

Figure 6.3 presents the first-order rate constants corrected for partitioning. The rate constants for chlorinated methanes and chlorinated ethanes are higher than those for chlorinated ethenes under the similar experimental conditions. The rate constant for TCE* (TCE produced by 1,1,2,2-TetCA dehydrochlorination) was lower than that reported for TCE that was added as target compound. This might be explained by considering the steps in surface reaction. 1,1,2,2-TetCA will sorb onto the solids and will transform to TCE* by a non-reductive reaction. Then, TCE* can be dechlorinated by electron transfer if it is sorbed to an active site. However, if it is sorbed to a non-active site, electron transfer does not occur and TCE* will diffuse into the bulk solution. TCE*

from solution can react by the following steps; sorption, surface reaction, desorption and diffusion into the solution. These steps might be slow enough to affect the overall rate of degradation of TCE*.
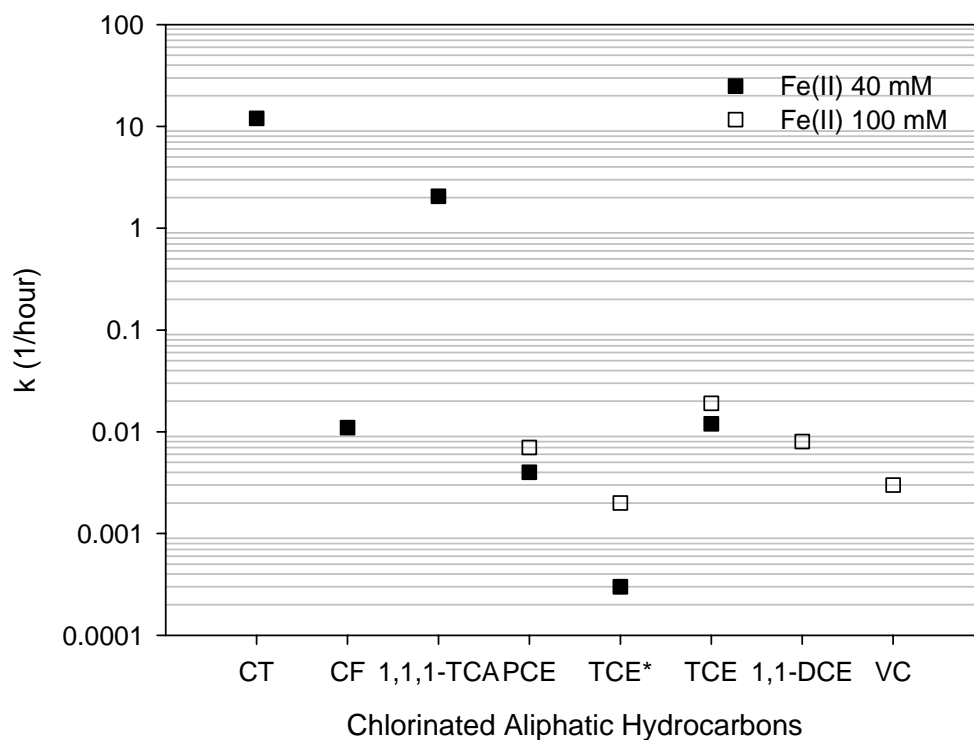
Figure 6.3 Pseudo-first-order rate constants for degradation of various chlorinated hydrocarbons by Fe(II) in cement slurries. Detail experimental conditions are shown in Table 6.3. The solid and open symbols represent rate constants obtained in experiments conducted with Fe(II) doses of 40 mM and 100 mM, respectively.

The redox potential of a reaction (E_h) can also be expressed as the electron activity (pE) (93):

$$pE = \frac{E_h}{\dfrac{2.303RT}{F}} = \frac{E_h}{0.059(V)}$$ (6-6)

when T is absolute temperature (K), R is the gas constant = 8.314 J/mol·K and F is Faraday constant = 96.486 kJ/equiv-V.

Linear relationships between log k and E_1^o, E_2^o and $D_{R\text{-}X}$ were assumed as shown in equations 6-7 and 6-8. The potentials were divided by 0.059 to convert them to electron activities.

$$\log k = a(\frac{E^o}{0.059}) + b$$ (6-7)

$$\log k = a(D_{R-X}) + b$$ (6-8)

The results of the regressions are described in Table 6.5. Figure 6.4 shows the correlation between the rate constants for six different target organics and one-electron reduction potential and Figure 6.5 shows the relation between the rate constants and two-electron reduction potential. Figure 6.6 shows the correlation between the rate constants of eight different target organics and one-electron reduction potential. The additional rate constants are for experiments with 1,1-DCE and VC that was conducted with different experimental conditions as described in Table 6.3. Figure 6.7 shows the correlation between rate constants and gas-phase bond dissociation enthalpy.

The regression results show that one-electron reduction potential does not correlate better with rate constants than the two-electron reduction potential. This could be due to the fact that the rate constants represent degradation by both hydrogenolysis and β-elimination, so they would not be as dependent on one-electron reduction potentials. Other mechanisms could also be at work and other steps could be rate limiting (90). Table 6.5 shows that the correlation between log k and D_{R-X} is the statistically best relationship, because of a higher value of R-squared.

Table 6.5 Results of correlation analysis.

	Log k= $a \times E^o/0.059$ (V) + b			Descriptor variables
	a	b	R^{2a}	
Figure 6.4	0.194	-0.028	0.610	One-electron reduction potential
Figure 6.5	1.281	-13.635	0.613	Two-electron reduction potential
Figure 6.6	0.177	-0.061	0.625	One-electron reduction potential
	Log k= $a \times D_{R-X}$(kJ/mole)+ b			Descriptor variables
Figure 6.7	-0.073	22.992	0.816	Gas-phase bond dissociation enthalpy

[a] R-squared value is the fraction of the variance in the data relative to the model that can be explained by changes in the independent variable.
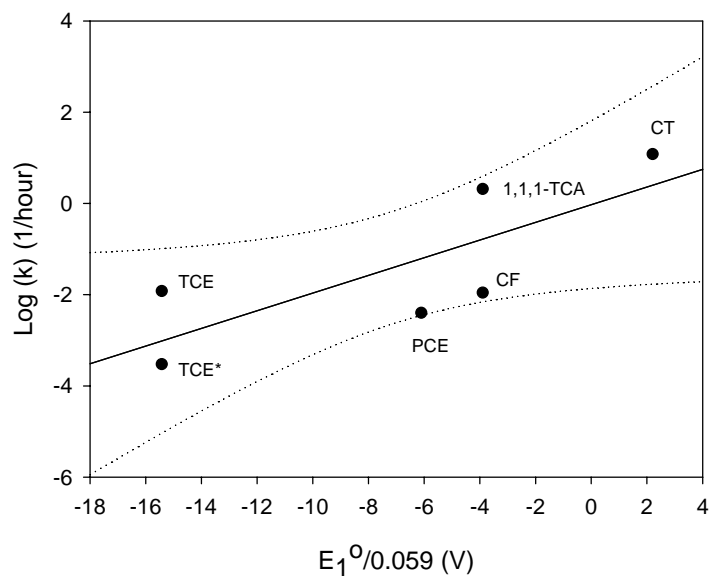
Figure 6.4 Correlation between rate constants and one-electron reduction potential. The dotted line represents the 95% confidence interval
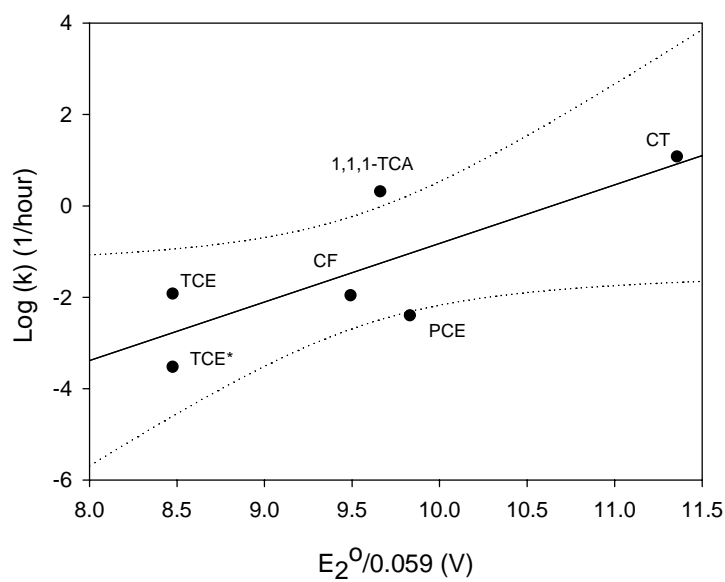
Figure 6.5 Correlation between rate constants and two-electron reduction potential. The dotted line represents the 95% confidence interval
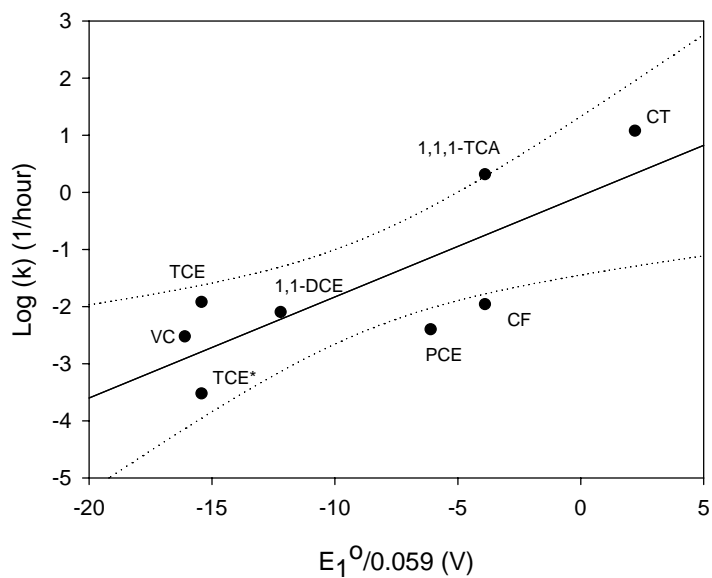
Figure 6.6 Correlation between rate constants and one-electron potential. The dotted line represents the 95% confidence interval.
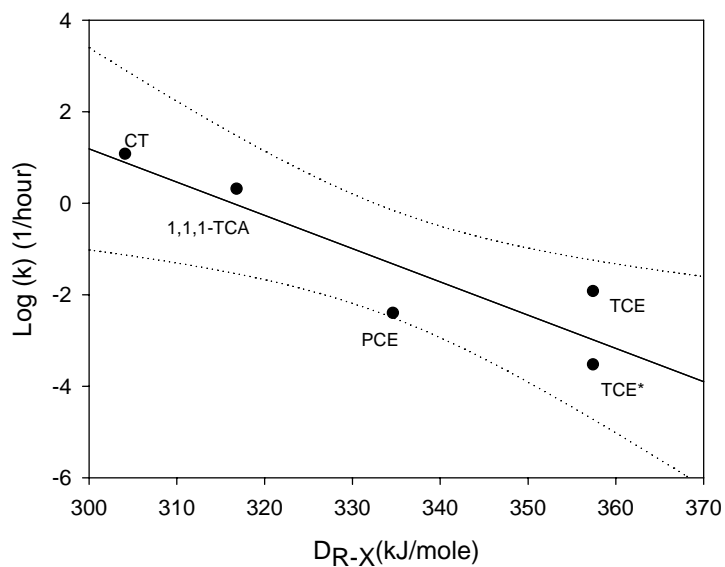
Figure 6.7 Correlation between rate constants and gas-phase bond dissociation enthalpy. The dotted line represents the 95% confidence interval.

CHAPTER VII

SUMMARY AND CONCLUSION

7.1 Summary

Degradative solidification/stabilization (s/s) technology is an attractive treatment method that combines a chemical degradation process with conventional s/s. The effectiveness of DS/S-Fe(II) has already been proven for chlorinated hydrocarbons including PCE, TCE, DCEs, VC, CT, PCBs. The goal of this research is to determine the applicability of DS/S-Fe(II) process to various chlorinated aliphatic hydrocarbons. The electron donors that participate in redox reactions that dechlorinate organics was hypothesized to be a Fe(II)-Fe(III)-hydroxides such as green rust that is formed by reaction of ferrous iron and the components of Portland cement. Another hypothesis of this research was that transformations of CAHs will occur on the surfaces of reactive solids.

First, degradation kinetics of 1,1,1-TCA, 1,1,2,2-TetCA, 1,2-DCA by Fe(II) in cement slurries was characterized using batch slurry reactors. Factors such as Fe(II) dose, pH, initial target organic concentration were investigated and degradation products were identified. Experimental evidence suggested that the rate constants were very strongly dependent on the influencing factors and that degradation kinetics of 1,1,1-TCA and TCE* (TCE produced by dehydrochlorination of 1,1,2,2-TetCA) was well described by a first-order kinetic model. In contrast, 1,2-DCA was not degraded by the Fe(II)-DS/S process within the time period of the experiments conducted.

Second, transformation of 1,1,1,-trichloroethane by Fe(II) in cement slurries containing iron-bearing phyllosilicates was studied. The effects of mineral type (biotite, vermiculite, montmorillonite), Fe(II) dose, and the mass ratio of cement to soil on degradation of 1,1,1-TCA were measured. Laboratory results showed that how first-order rate constants were affected by Fe(II) dose or solid mass ratio depended on mineral type. This dependence is affected by the type of Fe(II) in the soil minerals.

The accomplishments of this research are that: 1) The effectiveness of DS/S-Fe(II) for degrading chlorinated ethanes (1,1,1-TCA, 1,1,2,2-TetCA) and a chlorinated ethene (TCE[*]) was proven; 2) The effects of factors that affect reduction kinetics were characterized; 3) Understanding of the reaction mechanism of chlorinated aliphatic hydrocarbons in DS/S-Fe(II) system was improved through identification the degradation products and the variety of reaction mechanisms that depend on chemical molecular structure; and 4) Knowledge of the effects on rate constants of factors such as mineral type, Fe(II) dose, and the mass ratio of cement to soil mineral in Fe(II)/cement system containing soil minerals provided information for optimizing the DS/S-Fe(II) process in contaminated soils/sediments.

7.2   Conclusion

1. DS/S-Fe(II) process was successful in degrading 1,1,1-TCA and TCE[*] (TCE produced by dehydrochlorination of 1,1,2,2-TetCA), however, it was not able to degrade, 1,2-DCA within the time period of experiments conducted.

2. The half-life for the hydrolysis reaction of 1,1,1-TCA was approximately 6.9 days. The pseudo-first-order rate constant for the experiment conducted in an anaerobic environment was 7.6 times greater than that for the experiment conducted in an aerobic environment. The photochemical effect on the degradation kinetics of 1,1,1-TCA by Fe(II) in cement slurries was not significant.

3. Degradation of 1,1,1-TCA in cement slurries including Fe(II) was very rapid and generally described by a pseudo-first-order rate law. Half-lives for 1,1,1-TCA were measured between 0.4 and 5 hours when Fe(II) dose ranged from 4.9 mM to 39.2 mM. Transformation kinetics of 1,1,1-TCA was strongly dependent on Fe(II) dose, pH and initial target organic concentration. Saturation behavior was observed over the range of Fe(II) dose between 4.9 mM and 78.4 mM. The pseudo-first-order rate constant increased with pH to a maximum near pH 12.5. The relationship between initial degradation rates and initial target organic concentration (0.01 mM to 1 mM) was also described by a saturation model when Fe(II) dose was 4.9 mM.

4. The fact that a saturation model (modified Langmuir-Hinshelwood kinetic model) described measurements at higher Fe(II) doses and target organic concentrations indicates that dechlorination reactions occur on active surfaces that contain a limited number of sites.

5. The major transformation product of 1,1,1-TCA in mixtures of Fe(II) and cement system was 1,1-DCA, which indicates that degradation occurred by a hydrogenolysis pathway. A small amount of ethane was observed. The conversion of 1,1,1-TCA to ethane was better described by a parallel reaction model than by a consecutive reaction model.

6. 1,1,2,2-TetCA rapidly transformed to TCE* in the control that contained cement and as well as in the reactor with Fe(II). Therefore, the focus of research on the degradation of 1,1,2,2-TetCA was shifted to investigate the kinetics of TCE* dechlorination.

7. A linear relationship was shown to describe the relationship between the pseudo-first-order rate constant for TCE* disappearance and Fe(II) dose up to a dose of 196 mM. However, it is expected that saturation behavior will be observed at higher Fe(II) dose. The optimum pH was observed in the range of pH 12.0 to 12.4 for Fe(II) doses of 98 mM and 196 mM. Degradation rates for TCE* showed saturation relationship with initial target organic concentration for concentrations between 0.01 mM and 1 mM.

8. The final product of dechlorination of TCE* would be acetylene if the pathway were β-elimination. The fact that no intermediate chlorinated products were

detected supports this reaction pathway as occurring in mixtures of Fe(II) and cement.

9. Degradation of 1,1,1-TCA in the presence of Fe(II), cement and soil minerals (biotite, vermiculite and montmorillonite) was monitored. The relationship between the first-order rate constants and Fe(II) dose for biotite was well described by a saturation model. In contrast, the relationship for vermiculite and montmorillonite was best described by a linear model. The pseudo-first-order rate constant for montmorillonite was lower than that for biotite and vermiculite by factors of 11 to 27. The effect of cement/mineral ratio on rate constants with three different soil minerals indicates that biotite was more reactive than the other two phyllosilicates. This may be due to the high natural Fe(II) content in biotite. Also, the observation that increased amounts of cement relative to phyllosilicates caused rate constants to increase supports the hypothesis that Fe(II)-Fe(III)-hydroxides are important reductants in mixtures of Fe(II) and cement that contain phyllosilicates as well as those without phyllosilicates.

10. Factors such as Fe(II) dose, pH and initial target organic concentration showed similar effects on dechlorination kinetics of 1,1,1-TCA and TCE [*]. However rate constants for removal of 1,1,1-TCA were about 2 to 3 orders of magnitude greater than those for removal of TCE[*]. Half-lives ($t_{1/2}$) for 1,1,1-TCA were calculated to be in the range of 22 min to 9 day, while half-lives for TCE[*] were in the range from 1.6 day to 104 day. Analysis of degradation products showed that 1,1,1-TCA and TCE[*] tended to be degraded by the hydrogenolysis and β-

elimination pathways, respectively. Differences in reaction rate constants and degradation pathways demonstrate that rate constants are dependent on the molecular properties of the chlorinated organics.

11. Kinetic data for degradation of 1,1,1-TCA and TCE[*] determined by this study was combined with kinetic data for degradation of PCE, TCE, 1,1-DCE, and VC by the DS/S-Fe(II) process and were used to investigate importance of various chemical molecular properties on degradation kinetics. The results showed that the rate constants for chlorinated methanes and chlorinated ethanes were higher than those for chlorinated ethenes under the similar experimental conditions. Correlation analysis related the logarithm of first-order rate constants with one-electron reduction potential ($E_1°$), two-electron reduction potential ($E_2°$) and bond dissociation energy (D_{R-X}). The relationship of log k with D_{R-X} was statistically better than those with $E_1°$ and $E_2°$.

LITERATURE CITED

(1)   Ferguson, J. F.; Pietari, J. M. H. *Environmental Pollution* **2000**, *107*, 209-215.

(2)   Ramamoorthy, S. *Chlorinated Organic Compounds in the Environment.* Lewis Publishers: New York, 1997.

(3)   Kovalick, W. W. Remediation Technologies in the U.S.:Current Practice and New Development. 1st International Workshop on Geo-Environmental Restoration, Washington, D.C. 1998.

(4)   Riley, R. G. *Chemical Contaminants on DOE lands and Selection of Contaminant Mixtures for Subsurface Science Research*: DOE/ER-0547T, U.S. Department of Energy, Office of Energy Research, Subsurface Science Program. Springfield,Virginia, 1992.

(5)   *ToxFAQs for 1,1,1-trichloroethane*; Agency for Toxic Substances and Disease Registry:Division of Toxicology, 1996; http://www.atsdr.cdc.gov/toxfaq.html (November, 2003).

(6)   *ToxFAQs for 1,1,2,2-tetrachloroethane*; Agency for Toxic Substances and Disease Registry, 1997; http://www.atsdr.cdc.gov/toxfaq.html (November, 2003).

(7)   *Public Health Statement for 1,2-Dichloroethane*; Agency for Toxic Substances and Disease Registry, 1997; http://www.atsdr.cdc.gov/toxfaq.html (November, 2003).

(8)   Arnold, W. A.; Winget, P.; Cramer, C. J. *Environ. Sci. Technol.* **2002**, *36*, 3536-3541.

(9)   http://ptcl.chem.ox.ac.uk/MSDS/carcinogens.html (January, 2005).

(10)   LaGrega, M. D.; Buckingham, P. L.; Evans, J. C. *Hazardous Waste Management.* 2nd ed.; Thomas Casson: New York. NY, 2001.

(11)   *Soil Washing* http://www.frtr.gov/matrix2/section4/4_21.html (February, 2005).

(12)   *Soil Vapor Extraction* http://chemelab.ucsd.edu/sve/ (February, 2005).

(13)   *Incineration* http://www.frtr.gov/matrix2/section4/4-23.html (February, 2005).

(14)   Conner, J. R. *Chemical Fixation and Solidification of Hazardous Wastes.* Van Nostrand Reinhold: New York, 1990.

(15)   Anderson, W. C. *Innovative Site Remediation Technology: Stabilization/Solidification.* Water Environment Federation: Alexandria, Virginia, 1994; Vol. 4.

(16)   Wiedemeier, T. H.; Rifai, H. S.; Newell, C. J.; Wilson, J. T. *Natural Attenuation of Fuels and Chlorinated Solvents in the Subsurface.* John Wiley & Sons, Inc., New York, NY, 1999.

(17)   Fennelly, J. P.; Roberts, A. L. *Environ. Sci. Technol.* **1998**, *32*, 1980-1988.

(18)   Doong, R.; Chen, K.; Tsai, H. *Environ. Sci. Technol.* **2003**, *37*, 2575-2581.

(19)   Lookman, R.; Bastiaens, L.; Borremans, B.; Maesen, M.; Gemoets, J.; Diels, L. *Journal of Contaminant Hydrology* **2004**, *74*, 133-144.

(20)   Doong, R.; Wu, S. *Chemosphere* **1992**, *24*, 1063-1075.

(21)   Klecka, G. J.; Gonsior, S. J. *Chemosphere* **1984**, *13*, 391-402.

(22)   Charlet, L.; Liger, E.; Gerasimo, P. *Journal of Environmental Engineering* January **1998**, *124*, 25-30.

(23)   Pecher, K.; Haderlein, S. B.; Schwarzenbach, R. P. *Environ. Sci. Technol.* **2002**, *36*, 1734-1741.

(24)   Lee, W.; Batchelor, B. *Environ. Sci.Technol.* **2002**, *36*, 5147-5154.

(25)   Refait, P.; Memet, J. B.; Bon, C.; Sabot, R.; Genin, J. M. R. *Corrosion Science* **2003**, *45*, 833-845.

(26)   Danielsen, K. M.; Hayes, K. F. *Environ. Sci. Technol.* **2004**, *38*, 4745-4752.

(27)   Mccormick, M. L.; Adriaens, P. *Environ. Sci. Technol.* **2004**, *38*, 1045-1053.

(28)   Maithreepala, R. A.; Doong, R. *Environ. Sci. Technol.* **2004**, *38*, 6676-6684.

(29)   Maithreepala, R. A.; Doong, R. A. *Environ. Sci. Technol.* **2004**, *38*, 260-268.

(30)   Erbs, M.; Hans, H. C. B.; Olsen, C. E. *Environ. Sci. Technol.* **1999**, *33*, 307-311.

(31)   Lee, W.; Batchelor, B. *Environ. Sci. Technol.* **2002**, *36*, 5348-5354.

(32)   O'Loughlin, E. J.; Kemner, K. M.; Burris, D. R. *Environ. Sci. Technol.* **2003**, *37*, 2905-2912.

(33)   O'Loughlin, E. J.; Burris, D. R. *Environmental Toxicology and Chemistry* **2004**, *23*, 41-48.

(34)   Gander, J. W.; Parkin, G. F.; Scherer, M. M. *Environ. Sci. Technol.* **2002**, *36*, 4540-4546.

(35)   Butler, E. C.; Hayes, K. F. *Environ. Sci. Technol.* **2000**, *34*, 422-429.

(36)   Butler, E. C.; Hayes, K. F. *Environ. Sci. Technol.* **1999**, *33*, 2021-2027.

(37)   Kriegman-King, M. R.; Reinhard, M. *Environ. Sci. Technol.* **1994**, *28*, 692-700.

(38)   Kriegman-King, M. R.; Reinhard, M. *Environ. Sci. Technol.* **1992**, *26*, 2198-2206.

(39)   Roberts, A. L.; Sanborn, P. N.; Gschwend, P. M. *Environ. Sci. Technol.* **1992**, *26*, 2263-2274.

(40)   Amonette, J. E.; Rosso, K. M.; Gorby, Y. A.; Divanfard, H. R. *Redox Chemistry at Mineral Surfaces*, William R. Wiley Environmental Molecular Sciences Laboratory. Richland, Washington, 1999.

(41)   Amonette, J. E.; Workman, D. J.; Kennedy, D. W.; Fruchter, J. S.; Gorby, Y. A. *Environ. Sci. Technol.* **2000**, *34*, 4606-4613.

(42)   Hofstetter, T. B.; Schwarzenbach, R. P.; Haderlein, S. B. *Environ. Sci. Technol.* **2003**, *37*, 519-528.

(43)   Cervini-Silva, J.; Larson, R. A.; Wu, J.; Stucki, J. W. *Environ. Sci. Technol.* **2001**, *35*, 805-809.

(44)   Cervini-Silva, J.; Larson, R. A.; Wu, J.; Stucki, J. W. *Chemosphere* **2002**, *47*, 971-976.

(45)   Cervini-Silva, J.; Kostka, J. E.; Larson, R. A.; Stucki, J. W.; Wu, J. *Environmental Toxicology and Chemistry* **2003**, *22*, 1046-1050.

(46)   Lee, W.; Batchelor, B. *Chemosphere* **2004**, *56*, 999-1009.

(47)   Hwang, I. Ph.D. Dissertation, Texas A&M University: College Station, Texas, 2000.

(48)   Son, S. Ph.D. Dissertation, Texas A&M University: College Station, Texas, 2002.

(49)   Hwang, I.; Batchelor, B. *Chemosphere* **2002**, *48*, 1019-1027.

(50)   Means, J. L.; Smith, L. A.; Nehring, K. W.; Brauning, S. E.; Gavaskar, A. R.; Sass, B. M. *The Applications of Solidification/Stabilization to Waste Materials.* Lewis Publishers: Boca Raton, Florida, 1995.

(51)   *"Treatment Technologies for Site Cleanup"*: EPA-542-R-03-009, U.S.EPA/National Service Center for Environmental Publications. Cincinnati, Ohio, 2004.

(52)   Ko, S. MS. thesis, Texas A&M University: College Station, Texas, 2001.

(53)   Adaska, W. S.; Tresouthick, S. W.; West, P. B. Solidification and Stabilization of Wastes Using Portland Cement 2nd ed. Portland Cement Association: Skokie, Illinois, 1998.

(54)   Taylor, H. F. W. *Cement Chemistry.* 2nd ed.; Academic Press: London, 1997.

(55)   Kosmatka, S. H.; Panarese, W. C. *Design and Control of Concrete Mixtures.* Portland Cement Association, 1990; Vol. EB001.

(56)   Bensted, J.; Barnes, P. *Structure and Performance of Cements.* 2nd ed.; Spon Press: New York, NY, 2002.

(57)   Soroka, I. *Portland Cement Paste and Concrete.* The Macmillan Press Ltd.: New York, NY, 1979.

(58)   Hewlett, P. C. *Lea's Chemistry of Cement and Concrete.* 4th ed.; ARNOLD, New York, NY, 1998.

(59)   Kalinichev, A. G.; Kirkpatrick, R. J. *Chem. Mater.* **2002**, *14*, 3539-3549.

(60)   Newman, S. P.; Jones, W. *New J. Chem.* **1998**, 105-115.

(61)   Khan, A. I.; O'Hare, D. *J. Mater. Chem.* **2002**, *12*, 3191-3198.

(62)   You, Y.; Zhao, H.; Vance, G. F. *Colloids and Surfaces A.* **2002**, *205*, 161-172.

(63)   Yong, R. N.; Mohamed, A. M. O.; Warkentin, B. P. *Principles of Contaminant Transport in Soils.* Elsevier: Amsterdam, The Netherlands, 1992.

(64) Sparks, D. L. *Environmental Soil Chemistry.* Academic Press, San Diego, California, 1995.

(65) Amonette, J. E. Soil Mineralogy with Environmental Applications, *SSSA Book Series 7*; Soil Science Society of America, Inc., Madison, Wisconsin, 2002.

(66) Mitchell, J. K. *Fundamentals of Soil Behavior.* 2nd ed.; John Wiley & Sons, Inc., New York, NY, 1992.

(67) Vogel, T. M.; Criddle, C. S.; McCarty, P. L. *Environ. Sci. Technol.* **1987**, *21*, 722-736.

(68) Jeffers, P. M.; Ward, L. M.; Woytowitch, L. M.; Wolfe, N. L. *Environ. Sci. Technol.* **1989**, *23*, 965-969.

(69) Hwang, I.; Park, H.; Kang, W.; Park, J. *Journal of Hazardous Materials* **2005**, *B118*, 103-111.

(70) Hwang, I.; Batchelor, B. *Environ. Sci. Technol.* **2000**, *34*, 5017-5022.

(71) Arnold, W. A.; Roberts, A. L. *Environ. Sci. Technol.* **1998**, *32*, 3017-3025.

(72) Lee, W. Ph.D. Dissertation, Texas A&M University: College Station, Texas, 2001.

(73) Lien, H.; Zhang, W. *Journal of Environmental Engineering* January **2005**, 4-10.

(74) Kriegman-King, M. R. Ph.D. Dissertation, Stanford University: Stanford, California, 1993.

(75) Nzengung, V. A.; Castillo, R. M.; Gates, W. P.; Mills, G. L. *Environ. Sci. Technol.* **2001**, *35*, 2244-2251.

(76) Stucki, J. W.; Lee, K.; Zhang, L.; Larson, R. A. *Pure and Applied Chemistry* **2002**, *74*, 2145-2158.

(77) Elsner, M.; Schwarzenbach, R. P.; Haderlein, S. B. *Environ. Sci. Technol.* **2004**, *38*, 799-807.

(78) Charlet, L.; Silvester, E.; Liger, E. *Chemical Geology* **1998**, *151*, 85-93.

(79) Bohn, H. L.; McNeal, B. L.; O'connor, G. A. *Soil Chemistry.* 2nd ed.; John Wiley & Sons, Inc.: New York, 1985.

(80)   Newman, A. C. D. *Chemistry of Clays and Clay Minerals.* Longman Scientific & Technical, New York, NY, 1987.

(81)   Capitol Cement Company, Mill Test [Certificate]. San Antonio, Texas, 1997.

(82)   Clark, W. M. *Oxidation-Reduction Potentials of Organic Systems.* The Williams & Wilkins Company: Baltimore, Maryland, 1960.

(83)   Choi, J. Ph.D. Dissertation, Texas A&M University: College Station, Texas, 2005.

(84)   Rittmann, B. E.; McCarty, P. L. *Environmental Biotechnology: Principles and Applications.* McGraw-Hill, New York, NY, 2001.

(85)   Kaplan, D. I.; Serkiz, S. M. *Influence of surface charge of an Fe-oxide and an organic matter dominated soil on Iodide and pertechnetate sorption*: http://sti.srs.gov/fulltext/ms2002090/ms2002090.html (January, 2005).

(86)   Sparks, D. L.; Grundl, T. J. *Mineral-Water Interfacial Reactions: Kinetics and Mechanisms.* ACS Symposium Series, 1998.

(87)   Ko, S. Ph.D. Dissertation, Texas A&M University: College Station, Texas, 2005.

(88)   Lea, F. M. *The Chemistry of Cement and Concrete.* 3rd ed.; Chemical Publishing Co. Inc.: New York, 1971.

(89)   Johnson, T. L.; Scherer, M. M.; Tratnyek, P. G. *Environ. Sci. Technol.* **1996**, *30*, 2634-2640.

(90)   Scherer, M. M.; Balko, B. A.; Gallagher, D. A.; Tratnyek, P. G. *Environ. Sci. Technol.* **1998**, *32*, 3026-3033.

(91)   Roberts, A. L.; Totten, L. A.; Arnold, W. A.; Burris, D. R.; Campbell, T. J. *Environ. Sci. Technol.* **1996**, *30*, 2654-2659.

(92)   Curtis, G. P. Ph.D. Dissertation, Stanford University: Stanford, California, 1991.

(93)   Stumm, W.; Morgan, J. J. *Aquatic Chemistry.* 3rd ed.; John Wiley & Son. Inc., 1996.

(94)   Curtis, G. P.; Reinhard, M. *Environ. Sci. Technol.* **1994**, *28*, 2393-2401.

APPENDIX A

NOTATION

The following symbols are used in this dissertation.

Chemicals

1,1,1-TCA	1,1,1-Trichloroethane
1,1,2,2-TetCA	1,1,2,2-Tetrachloroethane
1,1,2-TCA	1,1,2-Trichloroethane
1,1-DCA	1,1-Dichlroethane
1,1-DCE	1,1-Dichloroethylene
1,2-DBP	1,2-Dibromopropane
1,2-DCA	1,2-Dichloroethane
CA	Chloroethane
c-DCE	Cis-Dichloroethylene
CF	Chloroform
CP	Trichloronitromethane
CT	Carbon tetrachloride
HAc	Acetic acid
HCA	Hexachloroethane
HS-	Hydrogen sulfide
MC	Methylene chloride
NAC	Nitroaromatic compounds
PCA	Pentachloroethane
PCE	Tetrachloroethylene
TCAN	Trichloroacetronitrile
TCE	Trichloroethylene
t-DCE	Trans-Dichloroethylene
VC	Vinyl chloride
VOCs	Volatile organic compounds

Solid Phase

AFm	Aluminate-ferrite-monosubstituted
AFt	Aluminate-ferrite-trisubstituted
C_2S	Dicalcium silicate
C_3A	Tricalcium aluminate
C_3S	Tricalcium silicate
C_4AF	Tetracalcium aluminoferrite
$Ca(OH)_2$	Calcium hydroxide
$Fe_{10}O_{15} \cdot 9H_2O$	Ferrihydrite
$\alpha\text{-}Fe_2O_3$	Hematite
$\gamma\text{-}Fe_2O_3$	Maghemite
Fe_3O_4	Magnetite
$\alpha\text{-}FeOOH$	Goethite
$\gamma\text{-}FeOOH$	Lepidocrocite
$\delta\text{-}FeOOH$	Feroxyhyte
$\beta\text{-}FeOOH$	Akaganeite
FeS	Iron sulfide
FeS_2	Pyrite
GR	Green rust
$GR(Cl^-)$	Green rust containing chloride
$GR(F^-)$	Green rust containing Fluoride
$K(Mg\ Fe)_3(AlSi_3O_{10})(OH)_2$	Biotite
LDH	Layered double hydroxides
$Mg_{0.33}(Mg,Al,Fe^{3+})3(Si_3Al)O_{10}(OH)_2$	Vermiculite
$M_x(Si_8)Al_{3.2}Fe_{0.2}Mg_{0.6}O_{20}(OH)_4$	Montmorillonite

Symbols

b	Saturation model constant
$C_{CA,l}$	Concentration of chlorinated ethanes in liquid phase
$C_{CA,l}{}^0$	Initial concentration of chlorinated ethanes in liquid phase calculated by a model

$C_{CA,t}$	Total concentration of target organics
C_g	Concentration of target organics in the gas phase
C_{RE}	Reductive capacity of a reductant
H	Dimensionless Henry's constant for target organics
k	Corrected pseudo-first-order rate constant by partitioning factor
k_1	First-order-rate constant for dechlorination of 1,1,1-TCA to 1,1,1-DCA
$k_{1,p}$	First-order-rate constant for dechlorination of 1,1,1-TCA to 1,1-DCA in parallel reaction
$k_{2,p}$	First-order-rate constant for dechlorination of 1,1,1-TCA to ethane in parallel reaction
$k_{1,c}$	First-order-rate constant for dechlorination of 1,1,1-TCA to 1,1-DCA in consecutive reaction
$k_{1,c}$	First-order-rate constant for dechlorination of 1,1-DCA to CA in consecutive reaction
$k_{2,c}$	First-order-rate constant for dechlorination of CA to ethane in consecutive reaction
k_{max}	the maximum pseudo-first-order rate constant
k_{obs}	Pseudo-first-order rate constant
k_{obs}'	Corrected pseudo-first-order rate constant by the control
$k_{obs,\ control}$	Pseudo-first-order rate constant for the control
$k_{obs,Fe(II)}$	Pseudo-first-order rate constant normalized by Fe(II) dose
K_s	Solid phase partition coefficient for the target organic
K_{TCA}	Half-saturation constant for 1,1,1-TCA
K_{TCE}	Half-saturation constant for TCE*
$M_{CA,t}$	Total mass of target organics
M_{solid}	Mass of target organics in solid phase
p	Partitioning factor
r	Initial degradation rates
r_{max}	Maximum initial degradation rate calculated by a saturation model
V_g	Volume of gas phase
V_l	Volume of aqueous phase

APPENDIX B

B.1 COMPUTER PROGRAM (MATLAB®) TO PREDICT PSEUDO FIRST-

ORDER RATE CONSTANT FOR CAHs DECHLORINATION

disp('Nonlinear Regression Computation of Fe(II) Dose Effect')

%Calculation of rate constant and 95% confidence limits at Fe(II)4.9mM by a first-order rate model

data=load('reactor_4.9.txt'); %dataname of TCA, C0=0.247mM, Fe(II)=4.9mM
tmeas=data(:,1); %measured values of time(hr)
cmeas=data(:,2); %measured values of 1,1,1-tca(mM) in aqueous phase in the reactor with Fe(II)

plot(tmeas, cmeas, 'o')
hold on

beta0=[0.01 0.02];
[beta,r,J]=nlinfit(tmeas,cmeas,'Nlin_Model',beta0); %nonlinear least-square data fitting
ci=nlparci(beta,r,J); %The calling statement for nlparci
beta
ci=ci'
sum_of_square=sum(r.^2)
variance_C0 = (abs(beta(1,1)-ci(1,1))/beta(1,1))*100
variance_k1 = (abs(beta(2,1)-ci(1,2))/beta(2,1))*100

dt=(max(tmeas)-min(tmeas))/100;
tp=min(tmeas):dt:max(tmeas);
for i=1:size(tp,2)
  Cestp(i)=beta(1)*exp(-beta(2)*tp(i));
end

plot(tp,Cestp)

....

function Cest=Nlin_model(beta,t)

Cest=beta(1)*exp(-beta(2)*t);

B.2 COMPUTER PROGRAM (MATLAB[®]) TO PREDICT RATE CONSTANTS

BY THE DUAL CONCENTRATION SECOND-ORDER RATE MODEL

```
disp('the Dual concentration second-order rate model')
%Calculation of rate constant and 95% confidence limits at Fe(II)1.96mM by
%a dual concentration second-order rate model.


data=load('fe196.txt');  % data of experiment 6. when Fe(II) 1.96mM
t=data(:,1);   % measured values of time (hr)
c=data(:,2);   % measured values of tca in aqueous phase (mM)

%beta(1)=k, k is the rate constant (1/hr)
%beta(2)=crc0, crc0 is the initial reductant capacity (mM)

beta0=[0.01 2];
[beta,r,j]=nlinfit(t,c,@calcc,beta0); % call function to do least-squares regression
ci=nlparci(beta,r,j);   %  call function to calculate confidence intervals
beta
ci=ci'
sum_of_square=sum(r.^2)
variance_k = abs(beta(1,1)-betaci(1,1))/beta(1,1)*100
variance_crc0 = abs(beta(2,1)-betaci(1,2))/beta(2,1)*100

plot(t,c,'o')
```

```
function  cmod=calcc(beta,t)

% function to calculate concentrations at time t from model
% tmod: time calculated from a model
% cmod: concentration calculated from a model

ctca0=0.245; %define the initial concentration of 1,1,1-tca
options=[];
[tmod,cmod]=ode45(@rateeqn,t, ctca0, options, beta);
```

```
function  dcdt=rateeqn(t,c,beta)

k=beta(1); % define rate constant
crc0 = beta(2); % define initial reductive capacity
ctca0 = 0.245; % define initial concentration of 1,1,1-TCA
p=1.07; % define value of partition coefficient of 1,1,1-TCA onto the solid phase

dcdt=-(k)*(crc0-p*(ctca0-c))*c;
```

B.3 COMPUTER PROGRAM (MATLAB®) TO PREDICT RATE CONSTANTS

BY THE SECOND-ORDER RATE MODEL

```
disp('Nonlinear Regression Computation of effect of initial target organic concentration')
% calculation of rate constants and 95% confidence interval for parameters
% When Fe(II)dose is 4.9mM, and C0=1mM, dc/dt=-kc^2, c=(c0)/(1+k*c0*t)


data=load('fe_1.txt'); %dataname of TCA, C0=1mM, Fe(II)=4.9mM
tmeas=data(:,1); %measured values of time(hr)
cmeas=data(:,2); %measured values of tca(mM)in the reactor with Fe(II)

plot(tmeas, cmeas, 'o')
hold on

beta0=[0.01 0.02];
[beta,r,J]=nlinfit(tmeas,cmeas,'Nlin_Model2',beta0); %nonlinear least-square data fitting
ci=nlparci(beta,r,J); %The calling statement for nlparci
beta
ci=ci'
sum_of_square=sum(r.^2)
variance_C0 = (abs(beta(1,1)-ci(1,1))/beta(1,1))*100
variance_k = (abs(beta(2,1)-ci(1,2))/beta(2,1))*100


dt=(max(tmeas)-min(tmeas))/100;
tp=min(tmeas):dt:max(tmeas);
for i=1:size(tp,2)
  Cestp(i)=beta(1)./(1+beta(1)*beta(2)*tp(i));
end

plot(tp,Cestp)
```

```
function Cest=Nlin_model2(beta,t)
Cest=beta(1)./(1+beta(1)*beta(2)*t);
```

B.4 COMPUTER PROGRAM (MATLAB®) TO PREDICT PARAMETERS BY

SATURATION MODEL

disp('Calculation of parameters of saturation model')

% calculation parameters of saturation model, R=(rm*C0)/(K+C0)
% R is the initial degradation rate(kobs*C0), Each R was obtained :
% kobs(at C0=0.01)*0.01, kobs(at C0=0.1)*0.1, kobs(at C0=1)*1
% rm is the maximum 1,1,1-TCA degradation rate, K is the half saturation constant.

C=[0.01 0.1 1]; % C is initial concentration of target compound
k_obs=[0.1658 0.1443 0.0670]; % kobs is the first-order rate constant obtained at each initial conc. degradation exp.

R=C.*k_obs; %R is initial rate

[beta r,j]=nlinfit(C,R,@Rmodel,[0.1 0.2]);
disp('parameters of saturation model, rm and K') % rm is the maximum 1,1,1-TCA degradation rate, K is the half saturation constant.
beta
ci=nlparci(beta,r,j);
disp('95% confidence intervals of parameters, rm and K')
ci=ci'
sum_of_square=sum(r.^2)
variance_rm = abs(beta(1,1)-ci(1,1))/beta(1,1)*100
variance_K = abs(beta(2,1)-ci(1,2))/beta(2,1)*100

Cp=[0.01:0.001:3];
for i=1:size(Cp,2)
ESTRCp(i)=(beta(1)*Cp(i))./(beta(2)+Cp(i));
end

plot(C,R,'kd',Cp,ESTRCp,'k-')
xlabel('Initial Conc.(mM)');
ylabel('Initial Rate(r,(mM/hour))');

----

function ESTR=Rmodel(beta,C)
ESTR=(beta(1)*C)./(beta(2)+C);

B.5 COMPUTER PROGRAM (MATLAB®) TO PREDICT RATE CONSTANTS

IN DECHLORINATION FROM 1,1,1-TCA TO 1,1-DCA

```
disp('obtain ca0, k_obs, and 95% confidence interval in TCA->DCA reaction')

% assume the first-order rate law
% assume the irreversible reaction
% r1=k1*[TCA]
%d[TCA]/dt=-r1=-k1*[TCA]
%d[DCA]/dt=r1=k1*[TCA]


data=load('fe49.txt');
tmeas=data(:,1);
cmeas=data(:,2);
plot(tmeas,cmeas, 'x')
hold on

[beta,r,J]=nlinfit(tmeas,cmeas,@rateeqn_fe49, [0.25 0.1] );
ci=nlparci(beta,r,J); %The calling statement for nlparci
beta
ci=ci'
sum_of_square=sum(r.^2)
variance_C0 = (abs(beta(1,1)-ci(1,1))/beta(1,1))*100
variance_k1 = (abs(beta(2,1)-ci(1,2))/beta(2,1))*100

dt=(max(tmeas)-min(tmeas))/100;
tp=min(tmeas):dt:max(tmeas);
for i=1:size(tp,2)
   ca0=beta(1);
   k1=beta(2);
   camodeltp(i)=ca0*exp(-k1*tp(i));
   cbmodeltp(i)=ca0*(1-exp(-k1*tp(i)));
end
tp=tp';
camodeltp=camodeltp';
cbmodeltp=cbmodeltp';

plot(tp,camodeltp,tp,cbmodeltp)
  hold off
```

```
function  cmodel=rateeqn_fe49(beta, t)

data=load('fe49.txt');
t=data(:,1);
ca0=beta(1);
k1=beta(2);

for i=1:11
   camodel(i)=ca0*exp(-k1*t(i));
end
camodel=camodel';

for i=12:22
   camodel(i)=ca0*exp(-k1*t(i));
   cbmodel(i)=ca0*(1-exp(-k1*t(i)));
end

cbmodel=cbmodel';
cmodel=[camodel(1:11);cbmodel(12:22)];
```

B.6 COMPUTER PROGRAM (MATLAB®) TO PREDICT RATE CONSTANTS

BY PARALLEL REACTION MODEL FOR 1,1,1-TCA TRANSFORMATION

```
disp('calculate kinetic parameters for TCA dechlorination in parallel reaction')

% obtain ca0, rate constants, and 95% confidence interval
% assumption A->B, A->C, first-order-rate law, r1=k1[A], r2=k2[A],
% [A]=1,1,1-TCA,[B]=1,1-DCA, [C]=Ethane
% irreversible reactions
% assumption that B0=0, C0=0
%d[A]/dt=-r1-r2, d[B]/dt=r1, d[C]/dt=r2

data=load('fe196_3.txt'); % data of exp.21 when Fe(II)=19.6mM, C0=0.245mM
t=data(:,1); %measured time (min)
c=data(:,2);

plot(t, c, 'x')
hold on

[beta,r,j]=nlinfit(t, c,@rateeqn_pall, [0.25 0.1 0.1] );
ci=nlparci(beta,r,j); %The calling statement for nlparci
beta
ci=ci'
variance_C0 = abs(beta(1,1)-ci(1,1))/beta(1,1)*100
variance_k1 = abs(beta(2,1)-ci(1,2))/beta(2,1)*100
variance_k2 = abs(beta(3,1)-ci(1,3))/beta(3,1)*100

sum_of_square=sum(r.^2)

dt=(max(t)-min(t))/100;
tp=min(t):dt:max(t);
for i=1:size(tp,2)
   ca0=beta(1);
   k1=beta(2);
   k2=beta(3);
   camodeltp(i)=ca0*exp(-(k1+k2)*tp(i));
   cbmodeltp(i)=((k1*ca0)/(k1+k2))*(1-exp(-(k1+k2)*tp(i)));
   ccmodeltp(i)=((k2*ca0)/(k1+k2))*(1-exp(-(k1+k2)*tp(i)));
end
tp=tp';
camodeltp=camodeltp';
cbmodeltp=cbmodeltp';
ccmodeltp=ccmodeltp';
plot(tp,camodeltp,tp,cbmodeltp,tp,ccmodeltp)
   hold off
```

```
function  cmodel=rateeqn_pall(beta, t)

data=load('fe196_3.txt');
t=data(:,1);
ca0=beta(1);
k1=beta(2);
k2=beta(3);

for i=1:8
   camodel(i)=ca0*exp(-(k1+k2)*t(i));
end
camodel=camodel';
 for i=9:16
   camodel(i)=ca0*exp(-(k1+k2)*t(i));
   cbmodel(i)=((k1*ca0)/(k1+k2))*(1-exp(-(k1+k2)*t(i)));
   ccmodel(i)=((k2*ca0)/(k1+k2))*(1-exp(-(k1+k2)*t(i)));
end
cbmodel=cbmodel';
for i=17:24
   camodel(i)=ca0*exp(-(k1+k2)*t(i));
   cbmodel(i)=((k1*ca0)/(k1+k2))*(1-exp(-(k1+k2)*t(i)));
   ccmodel(i)=((k2*ca0)/(k1+k2))*(1-exp(-(k1+k2)*t(i)));
 end
ccmodel=ccmodel';
cmodel=[camodel(1:8);cbmodel(9:16);ccmodel(17:24)];
```

B.7 COMPUTER PROGRAM (MATLAB®) TO PREDICT RATE CONSTANTS

BY CONSECUTIVE REACTION MODEL FOR 1,1,1-TCA TRANSFORMATION

```
disp('Calculate Kinetic Parameters for 1,1,1-TCA dechlorination in consecutive reaction')

% obtain ca0, rate constant, and 95% confidence interval
% assumption A->B->C->D first-order-rate law,
% r1=k1[A],r2=k2[B],r3=k3[C]
% [A]=1,1,1-TCA,[B]=1,1-DCA,[C]=CA, [D]=Ethane
% irreversible reactions
% B0=0, C0=0 and D0=0
%d[A]/dt=-r1, d[B]/dt=r1-r2, d[C]/dt=r2-r3, d[D]/dt=r3


data=load('fe196_3.txt');
t=data(:,1);
c=data(:,2);

plot(t, c,'o')
hold on

[beta,r,j]=nlinfit(t,c,@rateeqn_series,[0.25 0.1 0.01 0.2]);
ci=nlparci(beta,r,j); %The calling statement for nlparci
beta
ci=ci'
variance_ca0 = abs(beta(1,1)-ci(1,1))/beta(1,1)*100
variance_k1 = abs(beta(2,1)-ci(1,2))/beta(2,1)*100
variance_k2 = abs(beta(3,1)-ci(1,3))/beta(3,1)*100
variance_k3= abs(beta(4,1)-ci(1,4))/beta(4,1)*100
sum_of_square=sum(r.^2)

dt=(max(t)-min(t))/100;
tp=min(t):dt:max(t);
for i=1:size(tp,2)
   ca0=beta(1);
   k1=beta(2);
   k2=beta(3);
   k3=beta(4);

   camodeltp(i)=ca0*exp(-k1*tp(i));
   cbmodeltp(i)=((k1*ca0)/(k2-k1))*(exp(-k1*tp(i))-exp(-k2*tp(i)));
   ccmodeltp(i)=((k1*k2*ca0)/((k2-k1)*(k3-k1)))*exp(-k1*tp(i))+((k1*k2*ca0)/((k1-k2)*(k3-
k2)))*exp(-k2*tp(i))+((k1*k2*ca0)/((k1-k3)*(k2-k3)))*exp(-k3*tp(i));
   cdmodeltp(i)=ca0-camodeltp(i)-cbmodeltp(i)-ccmodeltp(i);
end
```

```
tp=tp';
camodeltp=camodeltp';
cbmodeltp=cbmodeltp';
ccmodeltp=ccmodeltp;
cdmodeltp=cdmodeltp';
plot(tp,camodeltp,tp,cbmodeltp,tp,cdmodeltp)
   hold off
```

```
function  cmodel=rateeqn_series(beta,t)

data=load('fe196_3.txt');
t=data(:,1);
ca0=beta(1);
k1=beta(2);
k2=beta(3);
k3=beta(4);

for i=1:8
    camodel(i)=ca0*exp(-k1*t(i));
end
camodel=camodel';


for i=9:16
   camodel(i)=ca0*exp(-k1*t(i));
   cbmodel(i)=((k1*ca0)./(k2-k1))*(exp(-k1*t(i))-exp(-k2*t(i)));
   ccmodel(i)=((k1*k2*ca0)/((k2-k1)*(k3-k1)))*exp(-k1*t(i))+((k1*k2*ca0)/((k1-k2)*(k3-
k2)))*exp(-k2*t(i))+((k1*k2*ca0)/((k1-k3)*(k2-k3)))*exp(-k3*t(i));
   cdmodel(i)=ca0-camodel(i)-cbmodel(i)-ccmodel(i);
end
cbmodel=cbmodel';

for i=17:24
    camodel(i)=ca0*exp(-k1*t(i));
   cbmodel(i)=((k1*ca0)./(k2-k1))*(exp(-k1*t(i))-exp(-k2*t(i)));
   ccmodel(i)=((k1*k2*ca0)./((k2-k1)*(k3-k1)))*exp(-k1*t(i))+((k1*k2*ca0)./((k1-k2)*(k3-
k2)))*exp(-k2*t(i))+((k1*k2*ca0)./((k1-k3)*(k2-k3)))*exp(-k3*t(i));
   cdmodel(i)=ca0-camodel(i)-cbmodel(i)-ccmodel(i);
end
cdmodel=cdmodel';

cmodel=[camodel(1:8);cbmodel(9:16);cdmodel(17:24)];
```

APPENDIX C

CALCULATION PROCEDURE FOR ONE-ELECTRON REDUCTION

POTENTIAL

The procedure of calculations for reduction potentials of chlorinated hydrocarbons has been demonstrated in many researches (35, 67, 90-92, 94).

One-electron reduction reaction can be written as

$$RX(aq) + e^- \rightarrow R\bullet(aq) + X^-(aq) \tag{C-1}$$

Reduction potentials were obtained from the Nernst relationship (93):

$$E^\circ = \frac{-\Delta G^\circ}{nF} = \frac{2.3RT}{F} pe^\circ \tag{C-2}$$

E^o : standard reduction potential (V)

R : universal gas constant (8.314 J/mol K)

n: electron equivalents transferred

F : Faraday's constant (95.487 kJ/volt· equiv)

T: temperature (K)

ΔG^o : standard Gibbs free energy

The standard Gibbs free energy of reaction (C-1) from ref. (67) is written:

$$\Delta G^\circ_{(aq)} = \sum G^\circ_{f(aq)} \text{ for products} - \sum G^\circ_{f(aq)} \text{ for reactants} \tag{C-3}$$

$$\Delta G^\circ_{(aq)} = \Delta G^\circ_f(R\bullet)_{(aq)} + \Delta G^\circ_f(X^-)_{(aq)} - \Delta G^\circ_f(RX)_{(aq)} \tag{C-4}$$

The Gibbs free energy in aqueous phase was related to the Gibbs free energy formation in the gas phase from ref.(67, 92):

$$\Delta G_f (RX)_{(aq)} = \Delta G_f (RX)_{(g)} + RTLn(H_{RX}) \qquad \text{(C-5)}$$

$$\Delta G_f (R\bullet)_{(aq)} = \Delta G_f (R\bullet)_{(g)} + RTLn(H_{RH}) \qquad \text{(C-6)}$$

$$\Delta G_f (R\bullet)_{(g)} = \Delta H_f (R\bullet)_{(g)} - T\Delta S_f (R\bullet)_{(g)} \qquad \text{(C-7)}$$

$\Delta G_f(RX)$: the Gibbs free energy of formation of the alkyl halide

$\Delta G_f(R\bullet)$: the Gibbs free energy of formation of alkyl radicals

$\Delta G_f(X^-)$: the Gibbs free energy of formation of halide ion

$\Delta H_f(R\bullet)$: the enthalpy of formation of the alkyl radical

$\Delta S_f(R\bullet)$: the entropy of formation of the alkyl radical

$H_{RX:}$ Henry's constant for the alkyl halide

$H_{RH:}$ Henry's constant for the alkyl radical

$\Delta G_f(R\bullet)_{(g)}$ can be calculated from the Equation C-7 and values of H_{RX}, H_{RH}, $\Delta G_f(RX)_{(g),}$ $\Delta G_f(X^-)_{(aq),}$ $\Delta H_f(R\bullet)_{(g)}$ and $\Delta S_f(R\bullet)_{(g)}$ have been tabulated in many references. If Equation C-4 is rearranged by combining from Equations C-5 to C-7, it will be Equation C-8.

$$\Delta G^\circ = \Delta H_f (R\bullet)_{(g)} - T\Delta S_f (R\bullet)_{(g)} + \Delta G_f (X^-)_{(aq)} - \Delta G_f (RX)_{(g)} + RT \ln \frac{H_{RH}}{H_{RX}} \qquad \text{(C-8)}$$

In this study, D_{R-X} were used from ref.(35), E°_1 from ref.(90) and E_2° from ref. (67). Also the D_{R-X} can be calculated by Equation C-9.

$$D_{R-X} = \Delta H_f(RX)_{(g)} - \Delta H_f(R\bullet)_{(g)} - \Delta H_f(X\bullet)_{(g)} \qquad \text{(C-9)}$$

$\Delta H_f(RX)$: the enthalpy of formation of alkyl halide

$\Delta H_f(R\bullet)$: the enthalpy of formation of alkyl radical

$\Delta H_f(X\bullet)$: the enthalpy of formation of halide

APPENDIX D

TABULATED DATA

1. Characterization experiments for 1,1,1-TCA in cement slurries

Exp.1				Exp.2		
time(hr)	TCA(mM)	STDEV		time(hr)	TCA(mM)	STDEV
0	0.245			0	0.245	
1	0.127	0.0022		1	0.209	0.0035
2	0.071	0.0028		2	0.194	0.0016
3	0.050	0.0049		3	0.191	0.0042
5	0.021	0.0050		5	0.190	0.0173
24	0.000	0.0000		15	0.073	0.0185
				24	0.038	0.0187
				28.8	0.011	0.0103

Exp.3				Exp.4		
time(hr)	TCA(mM)	STDEV		time(hr)	TCA(mM)	STDEV
0	0.245			0	0.243	
0.5	0.180	0.0022		0.5	0.152	0.0086
1	0.158	0.0007		1	0.131	0.0037
2	0.093	0.0053		2	0.097	0.0037
3	0.071	0.0139		3	0.075	0.0035
5	0.031	0.0081		5	0.026	0.0053

Exp.5				Exp.6		
time(day)	TCA(mM)	STDEV		time(hr)	TCA(mM)	STDEV
0	0.248			0	0.247	
0.1	0.243			2	0.213	0.0033
0.2	0.237	0.0265		3	0.208	0.0006
0.3	0.253	0.0041		12	0.177	0.0050
4	0.193	0.0097		14	0.167	0.0039
12	0.058	0.0064		19	0.147	0.0172
				24	0.157	0.0091
				48	0.143	0.0230
				72	0.135	0.0386
				120	0.134	0.0490

	Exp.7				Exp.8	
time(hr)	TCA(mM)	STDEV		time(hr)	TCA(mM)	STDEV
0	0.247			0	0.245	
2	0.158	0.0083		2	0.102	0.0039
3	0.148	0.0042		3	0.070	0.0145
12	0.044	0.0044		5	0.037	0.0144
14	0.033	0.0026				
19	0.014	0.0027				
24	0.008	0.0024				

	Exp.9				Exp.10	
time(hr)	TCA(mM)	STDEV		time(hr)	TCA(mM)	STDEV
0	0.243			0	0.247	
2	0.043	0.0088		1	0.036	0.0023
3	0.016	0.0053				
4	0.013	0.0128				

	Exp.11				Exp.12	
time(hr)	TCA(mM)	STDEV		time(hr)	TCA(mM)	STDEV
0	0.246			0	0.246	
2	0.235	0.0039		2	0.238	0.0018
3	0.229	0.0055		3	0.210	0.0270
5	0.230	0.0066		4	0.226	0.0026
7	0.228	0.0015		7	0.205	0.0089
17	0.218	0.0089		17	0.166	0.0025
24	0.223	0.0047		24	0.169	0.0058
28.8	0.219	0.0038		28.8	0.138	0.0135
72	0.203	0.0073		72	0.013	0.0086
96	0.157	0.0177		96	0.002	0.0029

	Exp.13				Exp.14	
time(hr)	TCA(mM)	STDEV		time(hr)	TCA(mM)	STDEV
0	0.246			0	0.245	
2	0.235	0.0051		2	0.103	0.0104
3	0.225	0.0068		3	0.065	0.0183
5	0.217	0.0028		5	0.029	0.0061
7	0.204	0.0026		7	0.020	0.0027
17	0.126	0.0090				
24	0.072	0.0014				
28.8	0.048	0.0020				

Exp.15			Exp.16		
time(hr)	TCA(mM)	STDEV	time(hr)	TCA(mM)	STDEV
0	0.245		0	0.010	
2	0.148	0.0144	3	0.006	0.0001
3	0.132	0.0092	4	0.006	0.0003
5	0.090	0.0113	5	0.004	0.0008
7	0.082	0.0079	6	0.004	0.0002
17	0.020	0.0002	7	0.003	0.0002
24	0.003	0.0029	8	0.002	0.0003
			24	0.000	0.0001

Exp.17			Exp.18		
time(hr)	TCA(mM)	STDEV	time(hr)	TCA(mM)	STDEV
0	0.100		0	1.000	
1	0.083	0.0006	1	0.799	0.0096
3	0.070	0.0044	5	0.566	0.0371
5	0.052	0.0019	9	0.490	0.0041
7	0.035	0.0055	21	0.230	0.0073
17	0.004	0.0007	24	0.197	0.0254
24	0.000	0.0000	48	0.155	0.0373
48	0.000	0.0000	96	0.093	0.0291
72	0.000	0.0000	144	0.076	0.0376

Exp.19			Exp.19		
Time(min)	TCA(mM)	STDEV	Time(min)	DCA(mM)	STDEV
0	0.240		0	0.000	
40	0.205	0.0005	40	0.036	0.0004
90	0.176	0.0027	90	0.061	0.0001
180	0.147	0.0007	180	0.089	0.0025
230	0.134	0.0019	230	0.088	0.0111
330	0.103	0.0002	330	0.115	0.0078
380	0.090	0.0028	380	0.119	0.0041
520	0.057	0.0062	520	0.171	0.0025
670	0.047	0.0012	670	0.176	0.0027
1320	0.005	0.0002	1320	0.232	0.0459
1440	0.002	0.0003	1440	0.235	0.0132

Exp.20				Exp.20		
time(min)	TCA(mM)	STDEV		time(min)	DCA(mM)	STDEV
0	0.245			0	0.000	
30	0.191	0.0073		30	0.061	0.0152
60	0.169	0.0090		60	0.071	0.0069
120	0.124	0.0045		120	0.127	0.0051
180	0.083	0.0048		180	0.156	0.0046
240	0.054	0.0020		240	0.177	0.0004
300	0.036	0.0060		300	0.196	
420	0.030	0.0048		420	0.186	0.0079
480	0.017	0.0056		480	0.220	
				600	0.240	
				720	0.233	0.0122

Exp.21				Exp.21		
time(min)	TCA(mM)	STDEV		time(min)	DCA(mM)	STDEV
0	0.244			0	0.000	
20	0.128	0.0055		20	0.094	0.0021
50	0.086	0.0009		50	0.138	
80	0.061	0.0019		80	0.181	0.0002
110	0.044	0.0020		110	0.195	0.0004
140	0.018	0.0077		140	0.212	
180	0.004	0.0013		180	0.234	
				240	0.231	
				580	0.211	0.0139
				750	0.237	0.0037
				1110	0.252	0.0154
				2250	0.224	0.0121
				3690	0.244	0.0043
				9450	0.226	0.0051

Exp.21		
time(min)	ethane(mM)	STDEV
0	0.000	
20	0.005	0.0008
50	0.007	
80	0.010	0.0012
110	0.010	
140	0.013	0.0010
180	0.013	
240	0.014	0.0002
580	0.014	0.0001
750	0.017	0.0030
1110	0.016	0.0033

Exp.22			Exp.22		
Time(min)	TCA(mM)	STDEV	Time(min)	DCA(mM)	STDEV
0	0.245		0	0.000	
10	0.117	0.0130	10	0.141	0.0109
30	0.070	0.0003	30	0.186	0.0058
50	0.045	0.0023	50	0.221	0.0098
70	0.026	0.0047	90	0.225	0.0007
90	0.031	0.0013	110	0.234	0.0096
110	0.021	0.0007	130	0.250	0.0067
130	0.014	0.0013	150	0.254	0.0036
150	0.006	0.0019	170	0.257	0.0031
170	0.005	0.0005	240	0.258	
190	0.002	0.0001	600	0.253	0.0034
			1440	0.242	0.0043
			4320	0.238	0.0190
			11520	0.252	

2. Characterization experiments for TCE*

Exp.23			Exp.24		
time(day)	TCE*(mM)	STDEV	time(day)	TCE*(mM)	STDEV
0	0.245		0	0.245	
0.2	0.243	0.0040	0.2	0.215	0.0168
10	0.211	0.0039	4	0.187	0.0342
21	0.185	0.0028	8	0.190	0.0025
35	0.147	0.0079	14	0.140	0.0203
48	0.143	0.0067	19	0.098	0.0031
88	0.141	0.0003	26	0.057	0.0148
102	0.108	0.0205	35	0.040	0.0345
123	0.125	0.0070	46	0.024	0.0132
			61	0.013	0.0229
			87	0.002	0.0032

Exp.25			Exp.26		
time(day)	TCE*(mM)	STDEV	time(day)	TCE*(mM)	STDEV
0	0.245		0	0.248	
0.2	0.231	0.0034	1	0.194	0.0169
2	0.198	0.0046	6	0.200	0.0066
4	0.150	0.0207	9	0.201	0.0024
6	0.162	0.0044	13	0.186	0.0116
9	0.133	0.0080	16	0.178	0.0000
13	0.099	0.0125	21	0.177	0.0108
17	0.044	0.0201	26	0.178	0.0096

Exp.27			Exp.28		
time(day)	TCE*(mM)	STDEV	time(day)	TCE*(mM)	STDEV
0	0.248		0	0.244	
0.2	0.221	0.0000	0.2	0.224	0.0032
1	0.208	0.0037	1	0.217	0.0030
6	0.209	0.0076	10	0.149	0.0000
9	0.165	0.0010	14	0.135	0.0129
13	0.198	0.0047	17	0.120	0.0179
16	0.196	0.0029	22	0.091	0.0056
21	0.189	0.0074	27	0.057	0.0118
26	0.187	0.0031			

Exp.29			Exp.30		
time(day)	TCE* (mM)	STDEV	time(day)	TCE* (mM)	STDEV
0	0.244		0	0.248	
0.2	0.226	0.0063	0.2	0.223	0.0023
1	0.219	0.0019	1	0.217	0.0017
5	0.207	0.0054	6	0.210	0.0055
10	0.184	0.0033	9	0.206	0.0029
14	0.174	0.0053	13	0.184	0.0075
17	0.163	0.0152	16	0.174	0.0016
22	0.144	0.0112	21	0.166	0.0099
27	0.148	0.0118	26	0.153	0.0107

Exp.31			Exp.32		
time(day)	TCE*(mM)	STDEV	time(day)	TCE*(mM)	STDEV
0	0.010		0	0.100	
0.2	0.009	0.0004	0.25	0.091	0.0007
0.71	0.008	0.0009	1	0.089	0.0008
1	0.008	0.0004	3	0.066	0.0100
1.66	0.007	0.0013	5	0.043	0.0063
2	0.004	0.0002	7	0.028	0.0057
2.2	0.003	0.0003	10	0.009	0.0148
			13	0.001	0.0016

Exp.33			Exp.33 (continued)		
time(day)	TCE*(mM)	STDEV	time(day)	TCE*(mM)	STDEV
0	1.000		14	0.760	0.0305
0.2	0.924	0.0164	20	0.665	0.0152
2	0.945	0.0065	27	0.576	0.1351
3	0.934	0.0172			
5	0.858	0.0620			
7	0.871	0.0108			

3. Characterization experiments for 1,1,1-TCA in the presence of soil minerals

Exp.34				Exp.35		
time(hr)	TCA(mM)	STDEV		time(hr)	TCA(mM)	STDEV
0.00	0.347			0.00	0.347	
0.50	0.290	0.0030		0.25	0.357	0.0203
0.83	0.259	0.0098		0.50	0.323	0.0039
1.50	0.234	0.0009		0.83	0.288	0.0048
2.25	0.182	0.0279		1.33	0.263	0.0172
3.00	0.191	0.0007		1.83	0.221	0.0156
4.00	0.172	0.0008		2.66	0.156	0.0128
4.83	0.162	0.0265		3.33	0.138	0.0063
20.00	0.040	0.0286		4.50	0.102	0.0049
33.75	0.002	0.0015		5.92	0.089	0.0115
				9.00	0.031	0.0026
				27.50	0.012	

Exp.36				Exp.37		
time(hr)	TCA(mM)	STDEV		time(hr)	TCA(mM)	STDEV
0.00	0.347			0.00	0.347	
0.16	0.268	0.0006		0.50	0.271	0.0022
0.33	0.241	0.0008		1.17	0.236	0.0054
0.50	0.231	0.0018		1.83	0.200	0.0085
0.75	0.198	0.0066		2.83	0.156	0.0291
1.00	0.251	0.1111		3.83	0.142	
1.33	0.157	0.0015		4.58	0.120	0.0183
1.83	0.142	0.0048		7.75	0.073	0.0000
2.33	0.135	0.0013		8.67	0.064	0.0071
3.50	0.111	0.0350		26.00	0.008	0.0055
4.53	0.066					
16.45	0.032	0.0001				

Exp.38				Exp.39		
time(hr)	TCA(mM)	STDEV		time(hr)	TCA(mM)	STDEV
0.00	0.347			0.00	0.346	
0.17	0.294	0.0027		0.50	0.292	0.0096
0.42	0.271	0.0080		1.50	0.251	0.0085
0.67	0.248			2.33	0.192	0.0022
0.92	0.221			5.83	0.135	0.0018
1.33	0.217	0.0021		7.50	0.136	0.0040
1.67	0.204	0.0022		8.67	0.084	0.0071
2.17	0.179			23.00	0.029	0.0004
2.83	0.141	0.0069				
3.25	0.084	0.0022				
7.33	0.032	0.0191				

	Exp.40				exp.41	
time(hr)	TCA(mM)	STDEV		time(hr)	TCA(mM)	STDEV
0.00	0.363			0.00	0.346	
0.33	0.286	0.0235		0.17	0.227	0.0053
1.00	0.267	0.0241		0.42	0.197	0.0275
1.50	0.201	0.0383		0.67	0.192	0.0135
2.00	0.192	0.0143		1.00	0.170	0.0162
2.50	0.166	0.0028		1.33	0.153	0.0058
3.00	0.150	0.0165		1.67	0.136	0.0077
4.00	0.116	0.0049		2.17	0.125	0.0197
5.00	0.061	0.0054		2.83	0.068	0.0076
7.00	0.053	0.0191		4.00	0.037	0.0124
9.00	0.042	0.0150		6.00	0.033	0.0214

	Exp.42				Exp.43	
time(hr)	TCA(mM)	STDEV		time(hr)	TCA(mM)	STDEV
0.00	0.348			0.00	0.350	
0.50	0.282	0.0240		0.17	0.315	0.0005
1.17	0.275	0.0183		0.33	0.307	0.0055
2.00	0.241	0.0008		0.58	0.301	0.0147
2.83	0.221	0.0321		0.83	0.274	0.0249
3.83	0.242	0.0049		1.33	0.258	0.0155
7.08	0.184	0.0019		1.67	0.244	0.0093
8.67	0.178	0.0147		2.00	0.232	0.0040
21.08	0.106	0.0116		3.83	0.142	0.0077
27.08	0.092	0.0242				

	Exp.44				Exp.45	
time(hr)	TCA(mM)	STDEV		time(hr)	TCA(mM)	STDEV
0.00	0.347			0.00	0.347	
2.33	0.326	0.0012		1.50	0.301	0.0061
6.00	0.314	0.0089		3.00	0.292	0.0005
7.92	0.314	0.0187		4.75	0.280	0.0083
9.25	0.315	0.0036		7.08	0.283	0.0026
18.92	0.271	0.0195		8.42	0.261	0.0065
21.67	0.277	0.0231		18.08	0.215	0.0270
23.17	0.293	0.0018		20.83	0.241	0.0061
25.67	0.261	0.0124		22.33	0.215	0.0147
31.67	0.266	0.0440		24.83	0.219	0.0056
43.83	0.237	0.0061		30.83	0.222	0.0159
47.25	0.203	0.0317		46.42	0.191	0.0167
53.58	0.255	0.0494		53.58	0.192	0.0188
79.58	0.250	0.0001		78.75	0.133	0.0103

Exp.46				Exp.47		
time(hr)	TCA(mM)	STDEV		time(hr)	TCA(mM)	STDEV
0.00	0.347			0.00	0.347	
0.67	0.308			2.50	0.321	0.0063
1.50	0.280	0.0013		5.75	0.318	0.0051
2.50	0.291	0.0097		6.75	0.322	0.0073
3.50	0.261	0.0042		18.92	0.311	0.0041
4.58	0.256			22.33	0.297	0.0081
6.25	0.244	0.0016		26.58	0.310	0.0003
7.58	0.224	0.0000		28.67	0.311	0.0092
17.25	0.135	0.0352		42.83	0.300	0.0116
24.00	0.142	0.0104		46.50	0.299	0.0188
30.00	0.124			54.08	0.306	0.0050
45.58	0.099	0.0054		70.50	0.300	0.0013
52.75	0.084	0.0043				
77.92	0.062					
432.00	0.020	0.0016				

exp.48		
time(hr)	TCA(mM)	STDEV
0.00	0.347	
0.83	0.303	0.0059
1.67	0.296	0.0014
4.50	0.248	0.0124
6.00	0.199	0.0140
7.42	0.217	
20.75	0.099	0.0122
24.08	0.089	0.0045
26.92	0.079	0.0053
32.58	0.062	0.0005
48.42	0.041	0.0064

VITA

Bahng Mi Jung was born in Masan, Korea. She completed her Bachelor of Science degree in Chemical Engineering at Chung-Ang University, Korea in 1998. In 2000, she received her Master of Science degree in Civil Engineering from Chung-Ang University, Korea. She received her Ph.D. degree in Civil Engineering from Texas A&M University, College Station, Texas in December 2005. Her research activities at Texas A&M University have focused on remediation of soils contaminated with chlorinated organics using reductive processes. Her research interests include reductive dechlorination, soil remediation, solidification/stabilization, chemical treatment of hazardous materials, and chlorinated aliphatic hydrocarbons. Her permanent address is 108-605 Daedong APT. Banji-Dong, Changwon, Korea. Her email address is jung.bahngmi@gmail.com.